ASSESSMENT OF STABILITY OF SLOPES SUBJECTED TO BLASTING VIBRATION

GEO REPORT No. 15

H.N. Wong & P.L.R. Pang

GEOTECHNICAL ENGINEERING OFFICE
CIVIL ENGINEERING DEPARTMENT
THE GOVERNMENT OF THE HONG KONG
SPECIAL ADMINISTRATIVE REGION

ASSESSMENT OF STABILITY OF SLOPES SUBJECTED TO BLASTING VIBRATION

GEO REPORT No. 15

H.N. Wong & P.L.R. Pang

© The Government of the Hong Kong Special Administrative Region

First published, September 1992
Reprinted, April 1995
Reprinted, August 2000

Prepared by:

Geotechnical Engineering Office,
Civil Engineering Department,
Civil Engineering Building,
101 Princess Margaret Road,
Homantin, Kowloon,
Hong Kong.

This publication is available from:

Government Publications Centre,
Ground Floor, Low Block,
Queensway Government Offices,
66 Queensway,
Hong Kong.

Overseas orders should be placed with:

Publications Sales Section,
Information Services Department,
Room 402, 4th Floor, Murray Building,
Garden Road, Central,
Hong Kong.

Price in Hong Kong: HK$56
Price overseas: US$10.5 (including surface postage)

An additional bank charge of **HK$50** or **US$6.50** is required per cheque made in currencies other than Hong Kong dollars.

Cheques, bank drafts or money orders must be made payable to
The Government of the Hong Kong Special Administrative Region.

PREFACE

In keeping with our policy of releasing information of general technical interest, we make available some of our internal reports in a series of publications termed the GEO Report series. The reports in this series, of which this is one, are selected from a wide range of reports produced by the staff of the Office and our consultants.

Copies of GEO Reports have previously been made available free of charge in limited numbers. The demand for the reports in this series has increased greatly, necessitating new arrangements for supply. In future a charge will be made to cover the cost of printing.

The Geotechnical Engineering Office also publishes guidance documents and presents the results of research work of general interest in GEO Publications. These publications and the GEO Reports are disseminated through the Government's Information Services Department. Information on how to purchase them is given on the last page of this report.

A. W. Malone
Principal Government Geotechnical Engineer
April 1995

EXPLANATORY NOTE

This GEO Report consists of two Special Project Reports on the assessment of stability of soil and rock slopes subjected to blasting vibration.

They are presented in two separate sections in this Report. Their titles are as follows :

Section	Title	Page No.
1	An Energy Approach for the Assessment of Stability of Rock Slopes Subjected to Blasting Vibration H.N. Wong & P.L.R. Pang (1991)	5
2	Pseudo-static Assessment of Stability of Soil Slopes Subjected to Blasting Vibration H.N. Wong (1992)	33

SECTION 1 :
AN ENERGY APPROACH FOR THE ASSESSMENT OF STABILITY OF ROCK SLOPES SUBJECTED TO BLASTING VIBRATION

H.N. Wong & P.L.R. Pang

This report was originally produced as GEO Special Project Report No. SPR 7/91

FOREWORD

Following the 28.2.1991 rock slide at Shau Kei Wan, a Working Group was set up in the Geotechnical Engineering Office under the chairmanship of Chief Geotechnical Engineer/Advisory (Mr R.K.S. Chan) to review the methods and draw up guidelines for assessing and limiting the adverse effects of blasting on the stability of existing slopes. The Working Group has identified, inter-alia, the need for a rational method for assessing the stability of rock slopes subjected to blasting vibration. This report, which documents the formulation of an energy approach developed in the Special Projects Division for carrying out such assessments, forms part of this Division's contribution to the Working Group. Based on the principle of conservation of energy, the proposed Energy Approach has been found to be simple to apply and gives consistent and realistic results.

This report was prepared by Mr H.N. Wong, who is the Special Projects Division's representative to the Working Group, under the supervision of Dr. P. L. R. Pang. The Working Group has reviewed the report and accepted the proposed Approach as one of its recommended methods for assessing and limiting the adverse effects of blasting vibrations on the stability of rock slopes.

(Y.C. Chan)
Chief Geotechnical Engineer/Special Projects

CONTENTS

Page No.

Title Page 5

FOREWORD 6

CONTENTS 7

1. INTRODUCTION 8

2. THE ENERGY APPROACH 9

2.1 Energy Equation 9

2.2 Peak Resultant Velocity of a Rock Block Subjected to Uni-directional Vibrations 10

2.3 Peak Resultant Velocity of a Rock Block Subjected to Multi-directional Vibrations 10

3. ENERGY DISSIPATION AT THE ROCK JOINT 11

3.1 General 11

3.2 Rigid Plastic Model 11

3.3 Linear Shear Displacement Model 12

3.4 Combined Model 13

4. DISCUSSION 15

5. SUGGESTED PROCEDURE FOR BLAST CONTROL 17

6. CONCLUSIONS 17

7. REFERENCES 18

LIST OF TABLES 19

LIST OF FIGURES 24

1. INTRODUCTION

A number of approaches may be used to assess the stability of rock slopes subjected to blasting vibration. These include the Pseudo-static Approach, Dynamic Analysis, the Empirical Approach and the Energy Approach. Table 1 summarises the advantages and limitations of these approaches.

At present, there are many limitations in the use of the Empirical Approach and Dynamic Analysis for routine assessment of rock slope stability in Hong Kong. These approaches are not discussed further in this report.

Analyses by the Pseudo-static Approach, in which an equivalent static driving force based on the peak ground acceleration is applied, derive the solutions from a consideration of force (and sometimes moment) equilibrium. While the Pseudo-static Approach has been widely accepted for use in the analysis of seismic slope stability, its validity has not been proved for blasting vibration analysis. Unlike earthquake ground motions, blasting vibration is characterised by short duration high frequency pulses, which according to Mines Division's records have a frequency content ranging typically from 30 to 100 Hz. Large ground accelerations are often induced in blasting (e.g. peak particle accelerations PPA of 1 g or higher have been recorded). However, despite the large PPA's, blasting pulses often possess relatively low vibration energy. The use of a large pseudo-static inertia force derived from the measured PPA's in the analyses has been found to give dynamic factors of safety less than unity (i.e. failures), even for slopes with reasonably high static factors of safety. These results are in spite of the low level of vibration energy transmitted to the potential failure wedge on the slope. Because of the unrealistic results obtained, it is generally believed that using the Pseudo-static Approach to analyse problems of blasting vibrations characterised by high frequency pulses is very conservative.

The proposed Energy Approach tackles the problem by a consideration of the blasting vibration energy transmitted to the potential failure wedge (modelled as a rock block) resting on the rock slope, as well as the energy dissipation at the rock joint. The stability and the downslope displacement of the rock block are assessed using equations based on the principle of conservation of energy. Different rock joint models may be incorporated in the analysis to calculate the energy dissipated at the joint. In the present study, an evaluation has been made by applying the Energy Approach to a range of situations. The empirical formulae developed by Barton (1990) correlating the shear strength and stiffness of rock joints with various joint characteristics have been used in the analysis.

The peak particle velocity PPV of the rock block is a key parameter in the Energy Approach. PPV is widely adopted in control criteria to prevent buildings from being damaged by blasting vibration. It is a good measure of the vibration energy induced by blasting. Therefore, application of PPV values in the analysis is likely to give more realistic predictions than the use of PPA's.

2. THE ENERGY APPROACH

2.1 Energy Equation

Consider a rock block resting on an inclined plane subjected to blasting vibration, as shown in Figure 1(a). The total energy of this rock block system which models the rock slope subjected to blasting vibration consists of two parts :

(a) Potential energy of the rock block, E_p, which can be expressed as :

$$E_p = M\ g\ h = W\ h \qquad \ldots\ldots\ldots \quad (1)$$

where M = mass of rock block
g = acceleration due to gravity = 9.81 m/s^2
h = height of the centre of gravity (C.G.) of the rock block above a reference datum
W = weight of the block = Mg

(b) Kinetic energy or vibration energy, E_k, which can be expressed as :

$$E_k = \tfrac{1}{2}\ M\ V_p^2 = \tfrac{1}{2}\ \frac{W}{g}\ V_p^2 \qquad \ldots\ldots\ldots \quad (2)$$

where V_p = peak resultant velocity of rock block at its C.G. For a rigid rock block with translational motion as being the predominant mode of motion, the velocity at the surface of the block may be assumed to be the same as that at the C.G. of the block (see Sections 2.2. and 2.3).

As shown in Figure 1(b), at its initial position, the rock block is forced by the blast-induced energy waves to vibrate with a peak resultant velocity V_p. The block comes to rest (i.e. with final velocity = 0) after it has moved downslope by an amount u_f. By considering the principle of conservation of energy, the following equation can be written :

$$\begin{pmatrix}\text{Total Energy of}\\ \\ \text{Rock Block System}\end{pmatrix}_i = \begin{pmatrix}\text{Total Energy of}\\ \\ \text{Rock Block System}\end{pmatrix}_f + \begin{matrix}\text{Energy Loss}\\ \text{at the}\\ \text{Boundaries}\end{matrix} \qquad \ldots \quad (3)$$

The subscripts i and f above denote the initial and final condition respectively.

Substituting equations (1) and (2) into (3), we have :

$$(E_p + E_k)_i = (E_p + E_k)_f + \text{Energy Loss}$$

$$\text{i.e. Energy Loss} = \tfrac{1}{2}\ \frac{W}{g}\ (V_p)^2 + W\ u_f\ \sin\beta \qquad \ldots\ldots\ldots \quad (4)$$

If the energy loss due to rock material damping and radiation damping is neglected, the term in the left hand side of the above equation is just that due to energy dissipated at the rock joint as a result of downslope movement of the rock block. Equation (4) may therefore be written as :

$$\int_{0}^{u_f} \tau \, A_b \, d\delta = \tfrac{1}{2} \, \frac{W}{g} \, (V_p)^2 + W \, u_f \sin \beta \qquad \ldots\ldots\ldots \quad (5)$$

where A_b = base area of the rock block
τ = shear stress acting along the rock joint

Equation (5) is the fundamental energy equation from which the downslope displacement u_f can be calculated if values of the other parameters in the equation are known.

2.2 Peak Resultant Velocity of a Rock Block Subjected to Uni-directional Vibrations

Consider a rock block subjected to uni-directional vibration along the dip direction of the joint plane only. The velocity of the rock block (hence its kinetic energy) will change with time. This is the result of interaction between the vibration energy transmitted to the rock block system (from the in-coming energy waves) and the energy loss due to material damping and radiation damping. If there is no relative movement between the rock block and the rock slope when V_p is reached, V_p in equation (5) can be taken to be the peak particle velocity (PPV) of the block, which is assumed to be acting in the downslope direction.

If the rock block slides along the joint, the PPV at A (Figure 1(a)) will be smaller than the PPV at B because of energy loss at the rock joint. Part of the input vibration energy will have been dissipated prior to the attainment of PPV at B. To avoid duplicating the term of energy loss at the rock joint in equation (5) and the possibility of obtaining an unsafe solution, V_p in equation (5) should be taken as the PPV at B and not the PPV at A.

2.3 Peak Resultant Velocity of a Rock Block Subjected to Multi-directional Vibrations

Supposing $\vec{V}_x(t)$, $\vec{V}_y(t)$ and $\vec{V}_z(t)$ are the velocities expressed as a function of time in any 3 orthogonal directions x, y and z, respectively of a rock block subjected to multi-directional vibration. The resultant velocity V(t) is given by taking the vector sum :

$$\vec{V}(t) = \vec{V}_x(t) + \vec{V}_y(t) + \vec{V}_z(t) \qquad \ldots\ldots\ldots \quad (6)$$

A conservative value of V_p to be used in equation (5) may be taken as the maximum value of $\vec{V}(t)$, i.e. :

$$V_p = \left| \vec{V}_x(t) + \vec{V}_y(t) + \vec{V}_z(t) \right|_{\text{maximum}}$$

$$\leq \sqrt{(PPV_x)^2 + (PPV_y)^2 + (PPV_z)^2}$$

$$\leq \sqrt{3} \, PPV = 1.7 \, PPV$$

where PPV = maximum of PPV_x, PPV_y and PPV_z, and
PPV_x, PPV_y and PPV_z are the peak particle velocities in directions x, y and z, respectively.

The chance of having V_p close to 1.7 PPV is very remote as this requires the simultaneous occurrence of PPV_x, PPV_y and PPV_z. It also assumes that the conservatively assessed V_p acts in the dip direction of the joint plane. To avoid being overly conservative, the following assumption is made:

$$V_p = \frac{PPV + 1.7\ PPV}{2} = 1.35\ PPV \qquad \ldots\ldots\ldots \quad (7)$$

This value is still likely to be conservative, but it may be refined when a generalised relationship between V_p and PPV_x, PPV_y and PPV_z can be established. This may be achieved by studying the velocity time records obtained from blasting operations in Hong Kong. This is, however, a subject for development. As this report will show, equation (7) can permit reasonable predictions to be made on effects of blasting vibrations.

Substituting equation (7) into (5), the fundamental energy equation becomes :

$$\int_0^{u_f} \tau\ A_b\ d\delta = 0.91\ \frac{W}{g}\ (PPV)^2 + W\ u_f\ \sin\beta \qquad \ldots\ldots\ldots \quad (8)$$

3. ENERGY DISSIPATION AT THE ROCK JOINT

3.1 General

The energy dissipation at the rock joint needs to be evaluated in order to solve the energy equation. This may be done using the shear-displacement curve of the joint, which may be obtained from laboratory shear tests, or more usually from an idealised rock joint model. The energy dissipation corresponding to three different idealised rock joint models is examined in the following Sections. For simplicity, only the case of a clean, tight joint with no rock bridging (i.e. with c' = 0) is considered, although the relevant equations may be easily modified to cover the c' ≠ 0 cases.

3.2 Rigid Plastic Model

The Rigid Plastic Model shown in Figure 2 assumes that no displacement occurs when the initial shear stress at the rock joint is increased to reach the residual shear stress (i.e. an infinite elastic stiffness). Thereafter, τ_r is assumed to remain constant for any subsequent displacement δ.

In this case, τ_r is given by :

$$\tau_r = \frac{W}{A_b} \cos\beta\ \tan\phi'_r \qquad \ldots\ldots\ldots \quad (9)$$

where ϕ'_r = residual angle of shearing resistance of the rock joint

Substituting equation (9) into (8), and putting PPV = X and $u_f = u_x$ into the equation, the following is obtained :

$$u_x = \frac{0.91}{g} X^2 \Big/ [\cos\beta \tan\phi'_r - \sin\beta] \quad \ldots\ldots\ldots \quad (10)$$

For a rock block with a static factor of safety F_{rs}, the downslope movement u_x may be expressed as :

$$u_x = \frac{0.91}{g} X^2 \Big/ [\sin\beta\,(F_{rs} - 1)] \quad \ldots\ldots\ldots \quad (11)$$

where $F_{rs} = \dfrac{\tan\phi'_r}{\tan\beta}$

The calculated values of u_f (i.e. u_x) for various combinations of values of ϕ'_r, F_{rs} and X (i.e. PPV) are given in Table 2 and plotted in Figure 3.

It can be seen that for the same values of F_{rs} and X (i.e. PPV), u_x is not too sensitive to the assumed ϕ'_r value. However, u_x increases rapidly with increase of PPV and decrease of F_{rs}.

3.3 Linear Shear Displacement Model

The Linear Shear Displacement Model shown in Figure 4 assumes that the shear stress τ increases linearly with the joint displacement δ until it reaches a peak shear stress τ_p. A measure of the rock joint stiffness is given by K_s :

$$K_s = \frac{\tau_p}{\delta_p} \quad \ldots\ldots\ldots \quad (12)$$

where δ_p = joint displacement at $\tau = \tau_p$

For a clean, tight rock joint with shear strength parameters $c' = 0$ and $\phi' = \phi'_p$ (peak angle of shearing resistance) :

$$\tau_p = \frac{W}{A_b} \cos\beta \tan\phi'_p \quad \ldots\ldots\ldots \quad (13)$$

In this study, the following empirical formulae given by Barton (1990) have been used to calculate ϕ'_p and δ_p :

$$\phi'_p = \mathrm{JRC} \log\left[\frac{\mathrm{JCS}}{\sigma_n'}\right] + \phi'_r + i \quad \ldots\ldots\ldots \quad (14)$$

$$\delta_p = \frac{L}{500}\left[\frac{\mathrm{JRC}}{L}\right]^{0.33} \quad \ldots\ldots\ldots \quad (15)$$

where JCS = joint wall compressive strength
JRC = joint roughness coefficient
L = joint length
ϕ'_r = residual angle of shearing resistance
i = roughness component of shearing resistance expressed as an angle

Based on the Linear Shear Displacement Model, the energy dissipated at the rock joint as a result of joint displacement $u_f = \delta_p - \delta_i$ is given by:

$$\text{Energy loss} = \int_0^u \tau\, A_b\, du$$

$$= \int_{\delta_l}^{\delta_p} \tau\, A_b\, d\delta$$

$$= \frac{A_b}{2} \left[\frac{\delta_p}{\tau_p} \right] \left[\tau_p^2 - \tau_l^2 \right]$$

where τ_l = initial shear stress = $\frac{W}{A_b} \sin \beta$

The critical peak particle velocity PPV_c, at which the block will be driven to a state whereby peak shear stress τ_p is developed at the rock joint, can be shown to be given by:

$$PPV_c = \sqrt{\frac{g}{0.91} [\delta_p] [\sin \beta] \left[\frac{\tan \phi'_p}{2 \tan \beta} + \frac{\tan \beta}{2 \tan \phi'_p} - 1 \right]} \quad \ldots (16)$$

In terms of the initial static factor of safety $F_s = \frac{\tan \phi'_p}{\tan \beta}$:

$$PPV_c = \sqrt{\frac{g}{0.91} [\delta_p] [\sin \beta] \left[\frac{F_s}{2} + \frac{1}{2 F_s} - 1 \right]} \quad \ldots\ldots (17)$$

The calculated PPV_c values for various combinations of values of ϕ'_p, F_s and δ_p are given in Table 3 and plotted in Figure 5.

It can be seen that for the same values of F_s and δ_p (which is related to L and JRC through equation (15)), PPV_c is not too sensitive to the ϕ'_p values. For small L and JRC values, δ_p and hence the energy dissipation capacity of the rock joint are both small. Therefore, the calculated PPV_c values are also small. This suggests that smaller blocks tend to slide more easily than larger ones under blasting vibration.

3.4 Combined Model

Figure 6 shows a more realistic rock joint model which combines the characteristics of the two models described in Sections 3.2 and 3.3. In this model, the pre-peak behaviour of the rock joint is represented by the Linear Shear Displacement Model and the post-peak behaviour of the rock joint is modelled as Rigid Plastic, with an abrupt change in shear stress at peak. The more gradual reduction in shear stress as the rock joint displaces beyond peak, as observed in real shear tests, is not modelled for the sake of simplicity.

For this model, the downslope displacement u_f of the rock block subjected to blasting vibration consists of two components : a pre-peak (linear) displacement u_l and a post-peak (residual) displacement u_r. Three cases are possible and these are considered below :

(a) Case 1 : PPV $\leq$ PPV$_c$

In this case, post-peak displacement u_r is zero. The maximum downslope displacement u_f is less than or equal to $\delta_p - \delta_i$.

Take for example, $\phi'_p = 40°$, $\beta = 30.9°$ (i.e. $F_s = 1.4$) and $\delta_p = 5$ mm,

$$\delta_i = \delta_p \left(\frac{\tau_i}{\tau_p}\right) = 5 \times \frac{1}{1.4} = 3.6 \text{ mm}$$

$$u_f \leq \delta_p - \delta_i = 1.4 \text{ mm}$$

In this case, δ_i (3.6 mm) is assumed to have occurred at the joint in the process of formation of the rock slope. Blasting under control with PPV $\leq$ PPV$_c$ will result in only a fairly small additional downslope displacement ($\leq$ 1.4 mm) at the joint. If the rock behaves in a perfectly elastic manner in the pre-peak state, any pre-peak displacement will be recovered after the cessation of blasting with the initial shear stress re-set at τ_i. However, if there is an irrecoverable component in the joint displacement, there will be a permanent set even after the shear stress has returned to τ_i. As long as the rock joint remains in the pre-peak state, the net displacement will be small.

(b) Case 2 : PPV > PPV$_c$ and $\tau_r > \tau_i$

In the case of PPV > PPV$_c$, post-peak displacement will occur. However, as the residual shear strength τ_r of the joint is greater than the initial shear stress τ_i, the residual static factor of safety F_{rs} will be greater than unity and the rock block will not continue to slide down the slope when blasting ceases.

The total downslope displacement u_f is given by :

$$u_f = u_i + u_r \qquad \text{. . . . . . . (18)}$$

where u_i = pre-peak displacement

$$= \delta_p - \delta_i = \delta_p \left(1 - \frac{1}{F_s}\right)$$

u_r = post-peak displacement

$$= \frac{0.91}{g} (\text{PPV}^2 - \text{PPV}_c^2) \left[\frac{1}{\sin\beta\,[F_{rs} - 1]} \right] \qquad \text{. . . . . . . (19)}$$

Values of u_r and u_f for the case of $\phi'_r = 30°$ and $\delta_p = 5$ mm for various combinations of ϕ'_p, F_s and PPV are given in Table 4.

It can be seen that if ϕ'_r is much larger than β (i.e. a large F_{rs}), u_r (and hence u_f) will remain relatively small even if PPV greatly exceeds PPV$_c$. However, if ϕ'_r is close to β (i.e. a small F_{rs}), u_r (and hence u_f) will be quite large in the case where PPV exceeds PPV$_c$. This demonstrates the importance of the residual static stability of the rock slope in blasting vibration analyses.

(c) Case 3 : $PPV > PPV_c$ and $\tau_r \leq \tau_i$

As the residual shear strength τ_r of the rock joint is smaller than the initial static shear stress τ_i, infinite downslope displacement, i.e. complete failure, will occur if PPV exceeds PPV_c.

4. DISCUSSION

While the proposed Energy Approach is considered to be better than the other approaches for assessing the stability of rock slopes subjected to blasting vibration, there are several points which deserve discussion:

(a) Energy Dissipation

For vibrations with predominantly 'low' frequency, small acceleration pulses (such as those from seismic vibrations with frequencies typically from 1 to 10 Hz), energy dissipation is mainly through hysteretic damping (of the rock material and joints) and radiation damping. Therefore, to neglect such forms of damping in the analysis will yield very conservative results. For blasting vibrations comprising 'high' frequency, large acceleration pulses, energy dissipation by virtue of joint sliding becomes significant and the contribution from hysteretic damping and radiation damping is relatively smaller. Therefore, to neglect these damping factors in such case would not be too unrealistic.

(b) Rock Joint Model

The presence of any bridges (i.e. impersistence) in the rock joint is neglected in the proposed Energy Approach. This would give conservative estimates of PPV_c. In principle, the energy dissipation capacity of rock bridges can be considered by incorporating the relevant term in the governing energy equation (8). However, it is very difficult to assess the degree of joint impersistence and to quantify its energy dissipation capacity, in particular under repeated blasts. It is worth noting that even in assessing the static stability of a rock slope, the strength of rock bridges is usually disregarded.

Little information on the assessment of 'dynamic' values of ϕ'_p and ϕ'_r of typical Hong Kong rock joints is available. However, it has been found that the friction angle for the initiation of sliding under a fast rate of loading (i.e. the 'dynamic' ϕ'_p) is higher than the equivalent 'static' friction angle (i.e. the 'static' ϕ'_p), and also the 'dynamic' ϕ'_p values are higher for higher rates of loading (e.g. Hencher, 1981). Use of the 'static' ϕ'_p value assessed from conventional laboratory tests or from empirical formulae such as those by Barton (1990), would therefore give conservative PPV_c values.

In the proposed Energy Approach, it is assumed that the PPV_c value does not change with repeated blasts provided that the joint remains in the pre-peak state in previous blasts, i.e. the energy dissipation capacity of the joint is 'recoverable' after a certain period. However, there is no data on this. Because of uncertainty in the joint behaviour, movement monitoring at critical rock wedges is recommended as a precautionary measure.

(c) Vibration Perpendicular to the Joint Plane

The effect of the component of vibration perpendicular to the joint plane has not been allowed for in the assessment of the energy dissipation capacity of the rock joint. Since blasting vibration is composed of high frequency pulses, rapid increase and decrease of the normal stress over the static (i.e. mean) value at the rock joint would tend to balance each another out. Hence, it is a reasonable approximation to calculate the energy dissipation capacity of the rock joint based on the static normal stress.

(d) Dynamic Excess Water Pressure

The case of a water-filled rock joint deserves detailed consideration. Positive excess water pressure will not be induced in the joint under blasting vibration if the joint is tight, as such a joint will dilate upon shearing. Therefore, the joint energy dissipation terms and the fundamental energy equations in Section 3 of this report will need no modification to deal with dynamic excess water pressure. However, the terms for the various static factors of safety and the energy dissipation terms will need to be changed to incorporate the effects of the relevant joint water pressure under static condition. This can be easily done and examples will not be given here. The effect of water pressure in the joint is that for given β, ϕ'_p and ϕ'_r, F_s and F_{rs} will be smaller than for the case of a dry joint condition (i.e. zero water pressure). The resulting PPV_c values will be smaller.

No generalisation can be made for in-filled joints as the joint shear and dilation behaviour will depend on the nature of the infill. If positive excess water pressure can be induced under blasting vibration, such pressure should be allowed for in the analysis. This is not covered in this report.

(e) Analyzing Non-planar Rock Wedges

Potentially unstable blocks with non-planar wedge-type failure can also be analyzed using the proposed Energy Approach by considering the energy dissipation at the relevant joint planes in contact with the block.

(f) Calibration of Results

Although there are good reasons to believe that the proposed Energy Approach can give more realistic performance predictions, there is no field data at present for calibrating the results obtained from the proposed Energy Approach. Therefore, the use of the proposed Energy Approach should be reviewed in future when relevant monitoring data are available. It is worth noting that the results of dynamic analysis reported by Dowding & Gilbert (1988) agree with the findings of the proposed Energy Approach: the shear displacement of a block resting on an inclined plane decreases substantially as the frequency of the vibration increases at a given peak acceleration. They have also found that pseudo-static methods of analysis are inappropriate for excitation with high frequencies.

5. SUGGESTED PROCEDURE FOR BLAST CONTROL

A suggested procedure for blast control using the results of the proposed Energy Approach to safeguard the stability of rock slopes is given in Figure 7.

In the case of $F_{rs} < 1$ (i.e. $\tau_r < \tau_l$), the need for stabilisation works should be considered. Account should be taken of the consequence of failure, as well as the reliability of blast control including monitoring.

In any blasting event, PPV should not be allowed to exceed PPV_c. This is to ensure that the rock joint remains in the 'pre-peak state'. Otherwise, loss of shear strength at the joint (i.e. the 'post-peak state') may result, in which case considerable irrecoverable downslope displacement of the rock wedge will occur. Post-peak joint displacements can reduce the energy absorption capacity of the rock joint which is required for counteracting the vibrations from subsequent blasts. The long term stability of the rock wedge will also be weakened.

On-site monitoring is recommended to check the actual level of vibration of the rock wedge caused by blasting and the displacement of the wedge. This would provide the data required for the improvement of blast design, as well as of methods for assessing rock slope stability.

The suggested procedure is relatively simple. It involves only routine techniques for blast control in Hong Kong, including the measurement of PPV, and the use of the available attenuation laws relating PPV with scale distance and site factors.

Sophisticated analysis is not required. Although the calculated PPV_c are considered conservative, they are by no means restrictive. For instance, the PPV_c for δ_p = 5 mm (say, JRC = 5 and L = 1.8 m) and δ_p = 20 mm (say, JRC = 5 and L = 14 m) are:

F_s		1.4	1.2	1.1	1.05
PPV_c (mm/s)	δ_p = 5 mm	40	23	12	6
	δ_p = 20 mm	80	45	25	13

6. CONCLUSIONS

The Energy Approach presented in this report is a simple and rational approach for assessing the stability of rock slopes subjected to blasting vibration. The proposed Approach is based on the principle of conservation of energy and different rock joint models can be incorporated. Analyses using the empirical rock joint formulae developed by Barton (1990) have been carried out for a range of situations. These have been found to give consistent and realistic results.

Practical guidelines for blast control using results of the proposed Energy Approach are given in Section 5 of this report.

There is also scope for further development and refinement of the proposed Approach when good quality on-site monitoring results, blast vibration records and data on dynamic rock joint behaviour are available.

7. REFERENCES

Barton, N. (1990). Scale effects or sampling bias. Proceedings of the First International Workshop on Scale Effects in Rock Masses, Loen, Norway, pp 31-55.

Dowding, C. H. & Gilbert, C. (1988). Dynamic stability of rock slopes and high frequency travelling waves. Journal of Geotechnical Engineering, American Society of Civil Engineers, vol. 114, pp 1069-1088.

Hencher, S. R. (1981). Friction parameters for the design of rock slopes to withstand earthquake loading. Proceedings of the Conference on Dams and Earthquake, London, pp 79-87.

Newmark, N.M. (1965). Effects of earthquakes on dams and embankments. Geotechnique, vol. 15, pp 139-160.

Sarma, S. K. (1975). Seismic stability of earth dams and embankments. Geotechnique, vol 25, pp 743-761.

LIST OF TABLES

Table No.		Page No.
1	Summary of Approaches for Assessing the Stability of Rock Slopes Subjected to Blasting Vibration	20
2	Calculated u_x Values Based on the Rigid Plastic Rock Joint Model	21
3	Calculated PPV_c Values Based on the Linear Shear Displacement Rock Joint Model	22
4	Calculated u_r and u_f Values for the Combined Rock Joint Model	23

Table 1 - Summary of Approaches for Assessing the Stability of Rock Slopes Subjected to Blasting Vibration

Approach	Main Features	Ability to model*			Ease of Analysis	Advantages	Limitations
		Disturbance due to blasting vibration	Resistance of potential sliding mass	Effects of blasting vibration			
PSEUDO-STATIC (a) Without Displacement Analysis	- Model the blasting vibration disturbance as a constant pseudo-static inertia force - Consider force and moment equilibrium of the potential slidign mass - Failure is assumed to have occurred if F_d+ < 1.0	P	F	P	Easy	- Simple analysis - compatible with conventional static stability analysis	- Not suitable for blasting vibration, which contains high frequency pulses and results in high peak particle acceleration (PPA) - Too conservative if PPA is adopted in analysis. (Very often F_d < 1.0 is obtained)
(b) With Displacement Analysis	- Same as above, except that the displacement of the sliding mass is calculated when F_d < 1.0 - Displacement may be estimated using the sliding block model (e.g. Newmark, 1965; Sarma, 1975)	F	F	F	Easy	- Same as above. - An order of displacement can be estimated based on simple sliding block model.	- The calculation displacement may be unrealistic because of : (a) unrealistic rigid plastic rock joint model assumed (b) uncertainties in post-peak behaviour of rock joint (c) uncertainties in the characterisation of the blasting vibration - Key controlling parameter is PPA, and not PPV which is commonly adopted for blasting control. - Difficult to quantify the acceptable displacement.
DYNAMIC ANALYSIS	- Consider the full time history of the blasting vibration - Assess the response of the potential sliding mass by numeral technique such as the 'distinct element method'.	G	G	G	Hard	- Theoretically can give the 'best' solution with consideration of the full time history of vibration and use of a realistic rock joint model. - Complex rock mass and joints pattern can be handled.	- Results may be doubtful because of : (a) uncertainties in the required input parameters (b) uncertainties in the boundary conditions - Complicated analysis, not suitable for routine application.
EMPIRICAL	- Assess the response of the potential sliding mass using empirical correlations derived from observations from previous blasts.	P	P	F	Easy	- Experience from previous blasts carried out locally and elsewhere is utilised. - Provide a simple guide to good practice and precautionary measures.	- Little empirical data available on effects of blasting vibration on rock slopes. - Experience elsewhere may not be relevant because of differences in blasting techniques, site geology and topograph, rock slope conditions, etc.
ENERGY	- Consider the potential and kinetic energy of the potential sliding mass and the energy absorption capacity of the rock joint. - Assess the effect of blasting vibration on the potential sliding mass from the principle of conservation of energy. - pre-peak and post-peak displacements are estimated.	F	G	G	Easy	- More realistic joint model incorporating empirical rock joint data (e.g. Barton, 1990) is adopted. - Key controlling parameter is ppv, which is commonly adopted for blasting control and is a good representation of the energy of the blasting disturbance. - Give less conservative result than the Pseudo-static Approach using PPA. - Simple analysis.	- Neglects damping of rock joints. Hence, gives conservative results. - Unable to model the effects of repeated blasts because of uncertainties in the material properties. This problem exists in other approaches as well.

NOTES : * Assume the required input parameters are available.
G denotes good, F denotes fair and P denotes poor.

+ F_d is the factor of safety under dynamic (vibration) condition.

Table 2 - Calculated U_x Values Based on the Rigid Plastic Rock Joint Model

Static FOS, F_{rs}	1.4	1.2	1.1	1.05
Joint inclination, β	26.6°	30.3°	32.5°	33.7°
U_{25} (mm)	0.3	0.6	1.1	2.1
U_{50} (mm)	1.3	2.3	4.3	8.4
U_{100} (mm)	20.7	36.8	69.1	133.8

(a) ϕ'_r =35°

Static FOS, F_{rs}	1.4	1.2	1.1	1.05
Joint inclination, β	22.4°	25.7°	27.7°	28.8°
U_{25} (mm)	0.4	0.7	1.2	2.4
U_{50} (mm)	1.5	2.7	5.0	9.6
U_{100} (mm)	24.3	42.8	79.8	154.0

(b) ϕ'_r =30°

Static FOS, F_{rs}	1.4	1.2	1.1	1.05
Joint inclination, β	18.4°	21.2°	23.0°	23.9°
U_{25} (mm)	0.5	0.8	1.5	2.9
U_{50} (mm)	1.8	3.2	5.9	11.4
U_{100} (mm)	29.4	51.2	95.1	182.8

(c) ϕ'_r =25°

Legend : U_X - downslope displacement u_r in mm corresponding to a PPV of X mm/s

Table 3 - Calculated PPV_c Values Based on the Linear Shear Displacement Rock Joint Model

Initial Static FOS, F_s		1.4	1.2	1.1	1.05
Joint Inclination, β		35.5°	39.8°	42.3°	43.6°
PPV_c (mm/s) for	δ_p = 5 mm^1	42.3°	24.0	12.8	6.7
	δ_p = 10 mm^2	59.8	33.9	18.2	9.4
	δ_p = 20 mm^3	84.6	48.0	25.7	13.3

(a) ϕ'_p = 45°

Initial Static FOS, F_s		1.4	1.2	1.1	1.05
Joint Inclination, β		30.9°	35.0°	37.3°	38.6°
PPV_c (mm/s) for	δ_p = 5 m^1	39.8°	22.7	12.2	6.3
	δ_p = 10 mm^2	56.3	32.1	17.2	9.0
	δ_p = 20 mm^3	79.6	45.4	24.4	12.7

(b) ϕ'_p = 40°

Initial Static FOS, F_s		1.4	1.2	1.1	1.05
Joint Inclination, β		26.6°	30.3°	32.5°	33.7°
PPV_c (mm/s) for	δ_p = 5 mm^1	37.1	21.3	11.5	6.0
	δ_p = 10 mm^2	52.5	30.1	16.2	8.4
	δ_p = 20 mm^3	74.2	42.6	22.9	11.9

(c) ϕ'_p = 35°

Notes :
1. Corresponds to JRC = 5 & L = 1.8 m
2. Corresponds to JRC = 5 & L = 5.0 m
3. Corresponds to JRC = 5 & L = 14.0 m

Table 4 - Calculated u_r and u_f Values for the Combined Rock Joint Model

Initial Static FOS, F_s		1.4	1.2	1.1
Joint inclination, β		30.9°	35.0°	37.3°
PPV_c (mm/s)		39.8	22.7	12.2
u_r (u_f) in mm	PPV = 200 mm/s	Complete Failure (F_{rs} < 1.0)		
	PPV = 50 mm/s			
	PPV = 25 mm/s	0 (< 1.4)		

(a) ϕ'_p = 40°, ϕ'_r = 30°, δ_p = 5 mm

Initial Static FOS, F_s		1.4	1.2	1.1
Joint inclination, β		26.6°	30.3°	32.5°
PPV_c (mm/s)		37.1	21.3	11.5
u_r (u_f) in mm	PPV = 200 mm/s	51.9 (53.3)	Complete Failure (F_{rs} < 1.0)	
	PPV = 50 mm/s	1.5 (2.9)		
	PPV = 25 mm/s	0 (< 1.4)		

(b) ϕ'_p = 35°, ϕ'_r = 30°, δ_p = 5 mm

Initial Static FOS, F_s		1.4	1.2	1.1
Joint inclination, β		24.9°	28.4°	30.6
PPV_c (mm/s)		36.0	20.6	11.2
u_r (u_f) in mm	PPV = 200 mm/s	34.9 (36.3)	115.4 (116.2)	Complete Failure (F_{rs} < 1.0)
	PPV = 50 mm/s	1.1 (2.5)	6.1 (6.9)	
	PPV = 25 mm/s	0 (<1.4)	0.6 (1.2)	

(c) ϕ'_s = 33°, ϕ'_r = 30°, δ_p = 5 mm

Legend : u_r = post-peak displacement
u_f = total displacement
F_{rs} = post-peak factor of safety based on residual shear strength of rock joint

LIST OF FIGURES

Figure No.		Page No.
1	Rock Block System Subjected to Blasting Vibration	25
2	Energy Dissipation Based on the Rigid Plastic Rock Joint Model	26
3	Plot of u_f vs F_{rs} for the Rigid Plastic Rock Joint Model	27
4	Energy Dissipation Based on the Linear Shear Displacement Rock Joint Model	28
5	Plot of PPV_c vs F_s for the Linear Shear Displacement Rock Joint Model	29
6	Energy Dissipation Based on the Combined Rock Joint Model	30
7	Suggested Procedure for Blast Control Based on Results of the Proposed Energy Approach	31

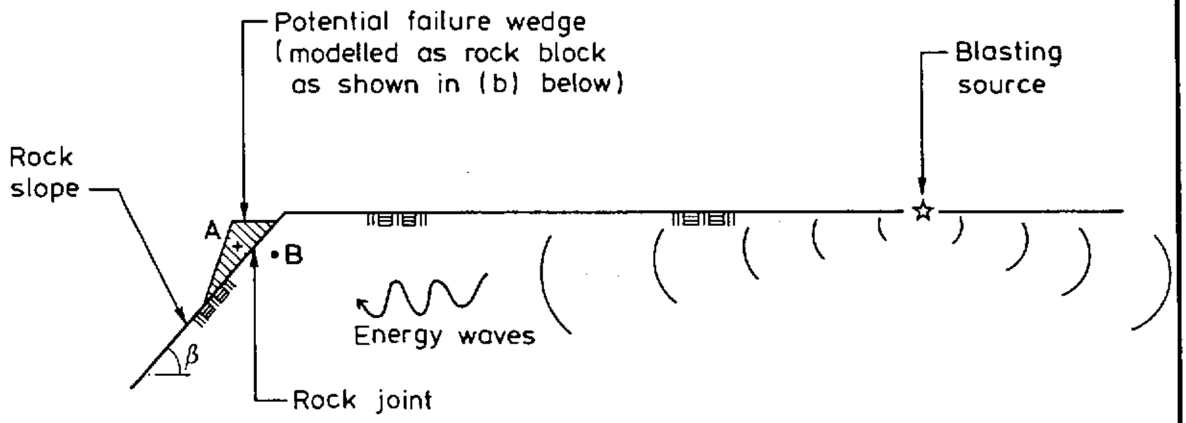
Potential failure wedge
(modelled as rock block
as shown in (b) below)
Blasting
source
Rock
slope
A
B
β
Energy waves
Rock joint

(a) Section through Blasting Source and Rock Slope

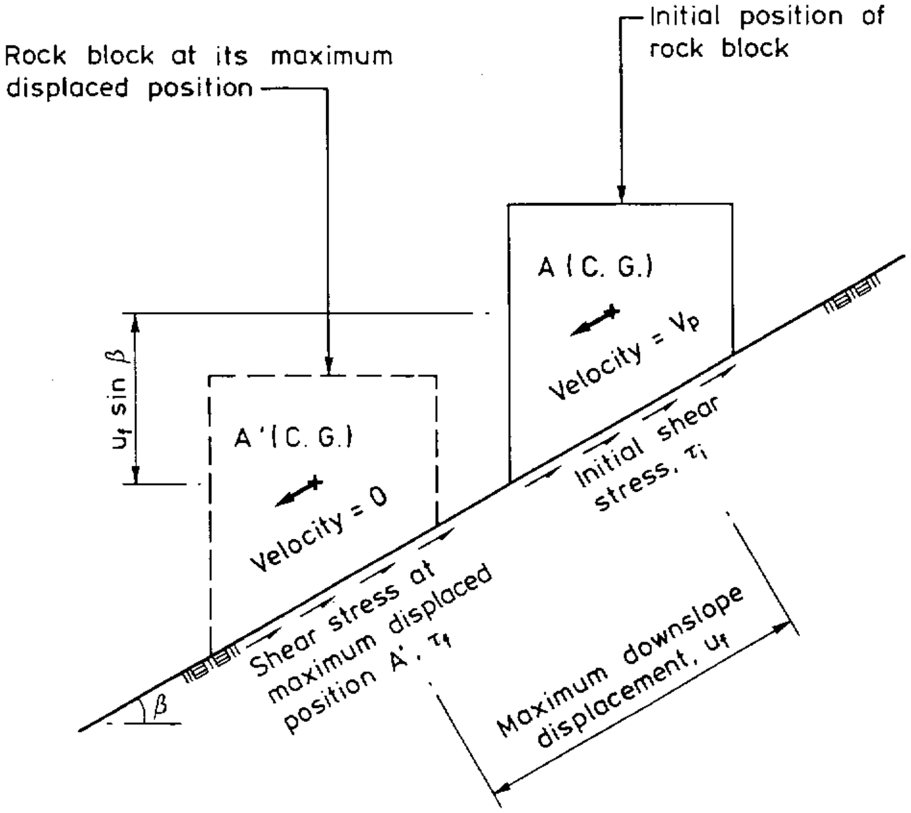
Initial position of
rock block
Rock block at its maximum
displaced position
A (C. G.)
Velocity = V_p
$u_f \sin \beta$
A' (C. G.)
Velocity = 0
Initial shear
stress, τ_i
Shear stress at
maximum displaced
position A', τ_f
Maximum downslope
displacement, u_f
β

(b) Displacement of Rock Block

Figure 1 - Rock Block System Subjected to Blasting Vibration

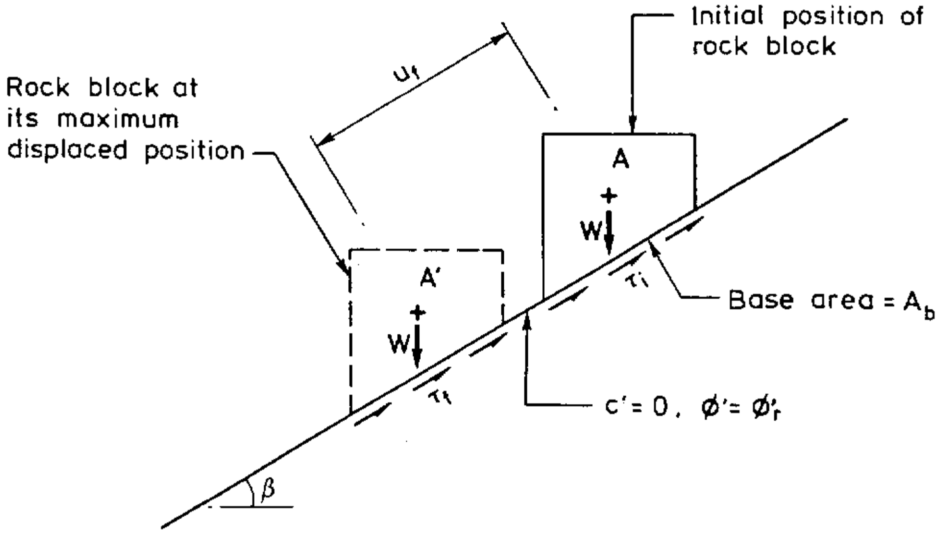
Rock block at its maximum displaced position
Initial position of rock block
u_f
A
W
A'
W
τ_i
τ_f
Base area = A_b
$c' = 0$, $\phi' = \phi'_r$
β

(a) Rock Block System

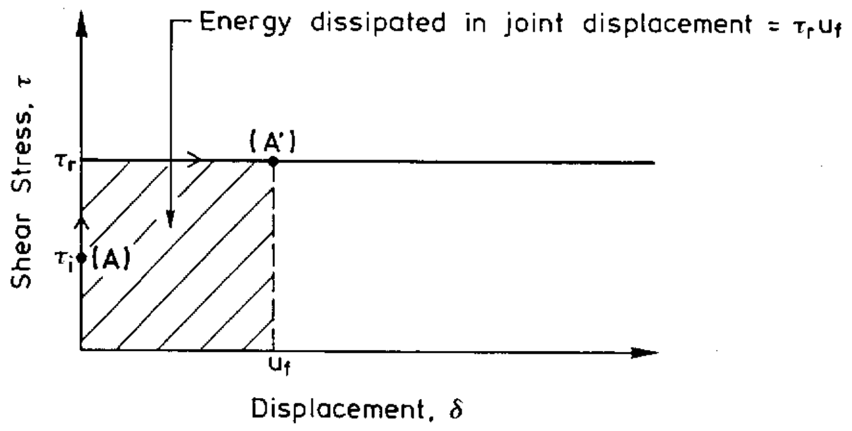

(b) $\tau - u$ Relationship for Rock Joint

Legend :

τ_i	Initial shear stress = $W \sin\beta / A_b$
τ_f	Shear stress at maximum displaced position A' = τ_r
τ_r	Residual shear strength = $W \cos\beta \tan\phi'_r / A_b$
c'	Effective cohesion of rock joint
ϕ'_r	Residual angle of shearing resistance of rock joint

Figure 2 - Energy Dissipation Based on the Rigid Plastic Rock Joint Model

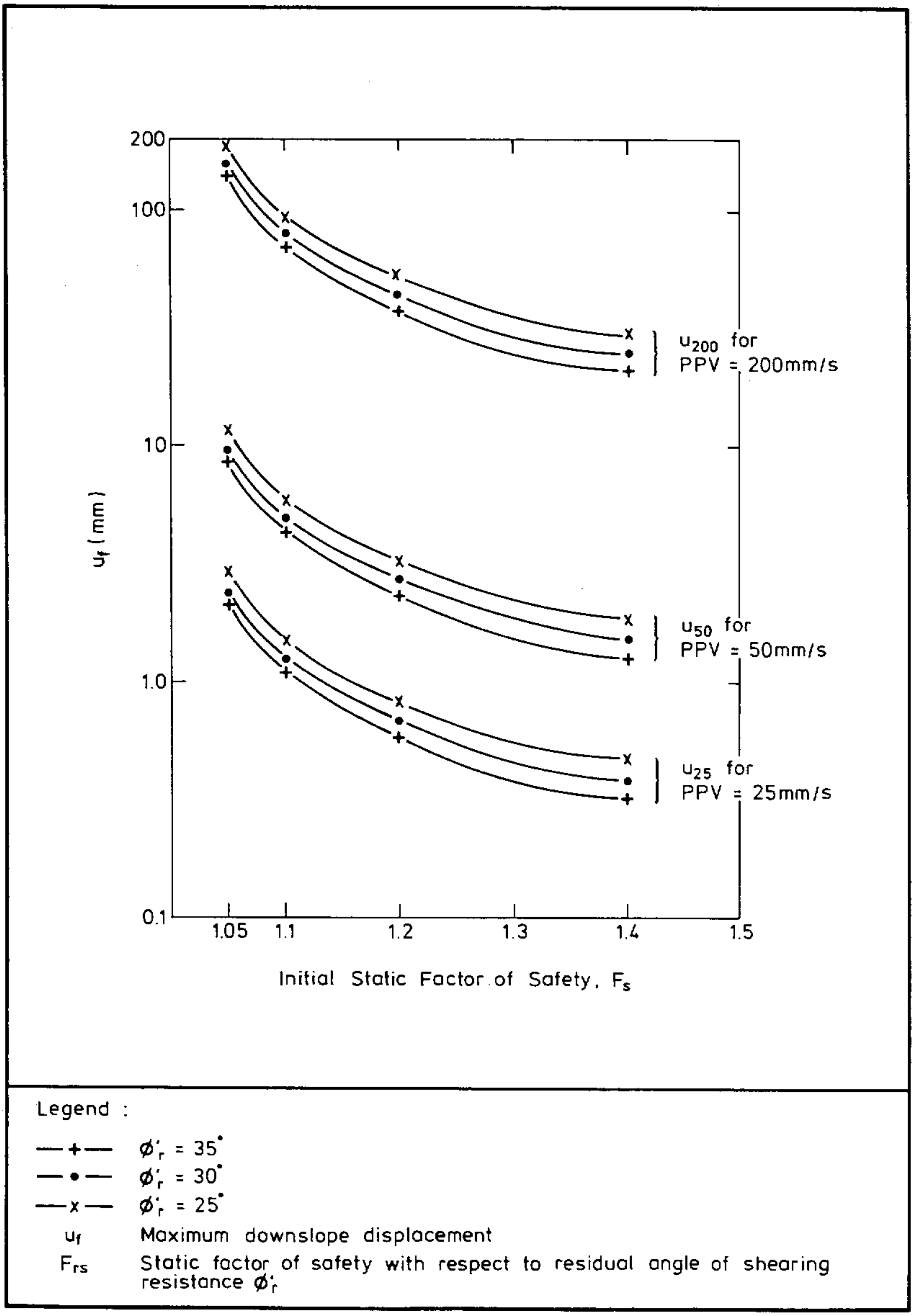

Figure 3 - Plot of u_f vs F_{rs} for the Rigid Plastic Rock Joint Model

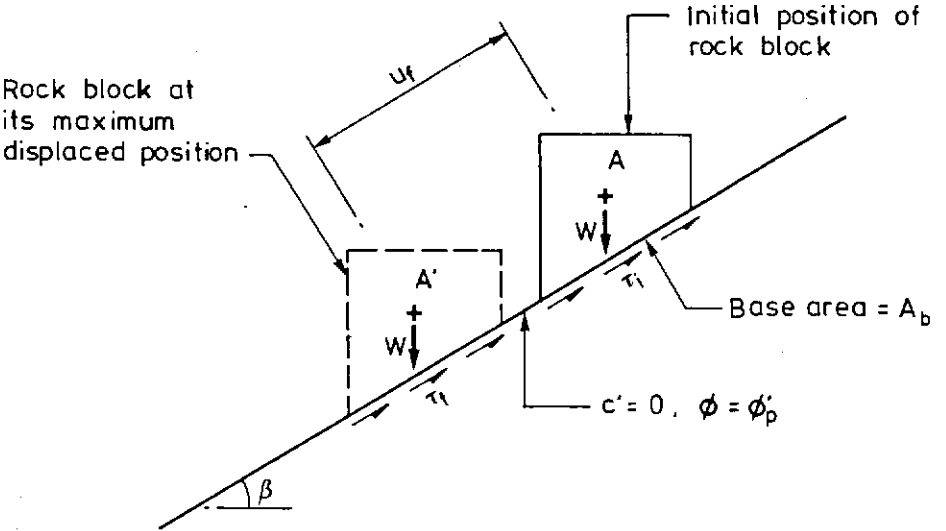
Initial position of rock block
Rock block at its maximum displaced position
u_f
A
W
A'
W
τ_i
τ_f
Base area = A_b
$c' = 0$, $\phi = \phi'_p$
β

(a) Rock Block System

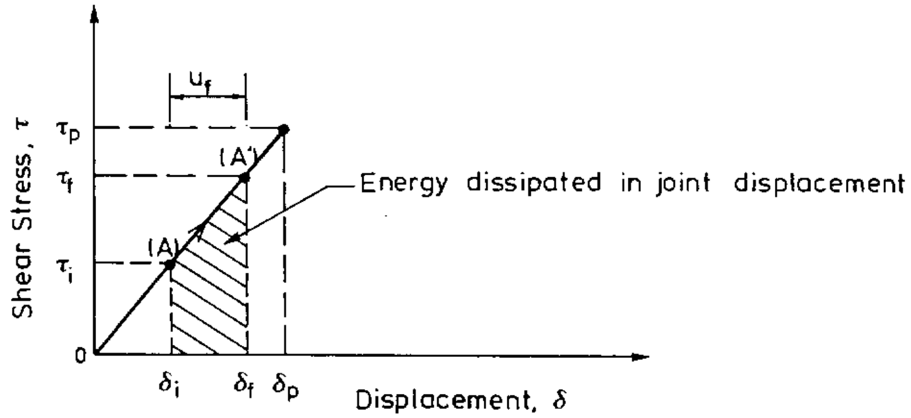

Energy (per unit joint area) dissipated in joint displacement

$$= \int_{\delta_i}^{\delta_f} \tau \, d\delta$$

$$= \frac{(\tau_f \delta_f - \tau_i \delta_i)}{2}$$

$$= \frac{\delta_p}{2\tau_p} \left[\tau_f^2 - \tau_i^2 \right]$$

(b) $\tau - u$ Relationship for Rock Joint

Legend:

τ_f	Shear stress at maximum displaced position A'
τ_p	Peak shear strength $= W \cos\beta \tan\phi'_p / A_b$
c'	Effective cohesion of rock joint
ϕ'_p	Peak angle of shearing resistance of rock joint
τ_i	Initial shear stress $= W \sin\beta / A_b$

Figure 4 - Energy Dissipation Based on the Linear Shear Displacement Rock Joint Model

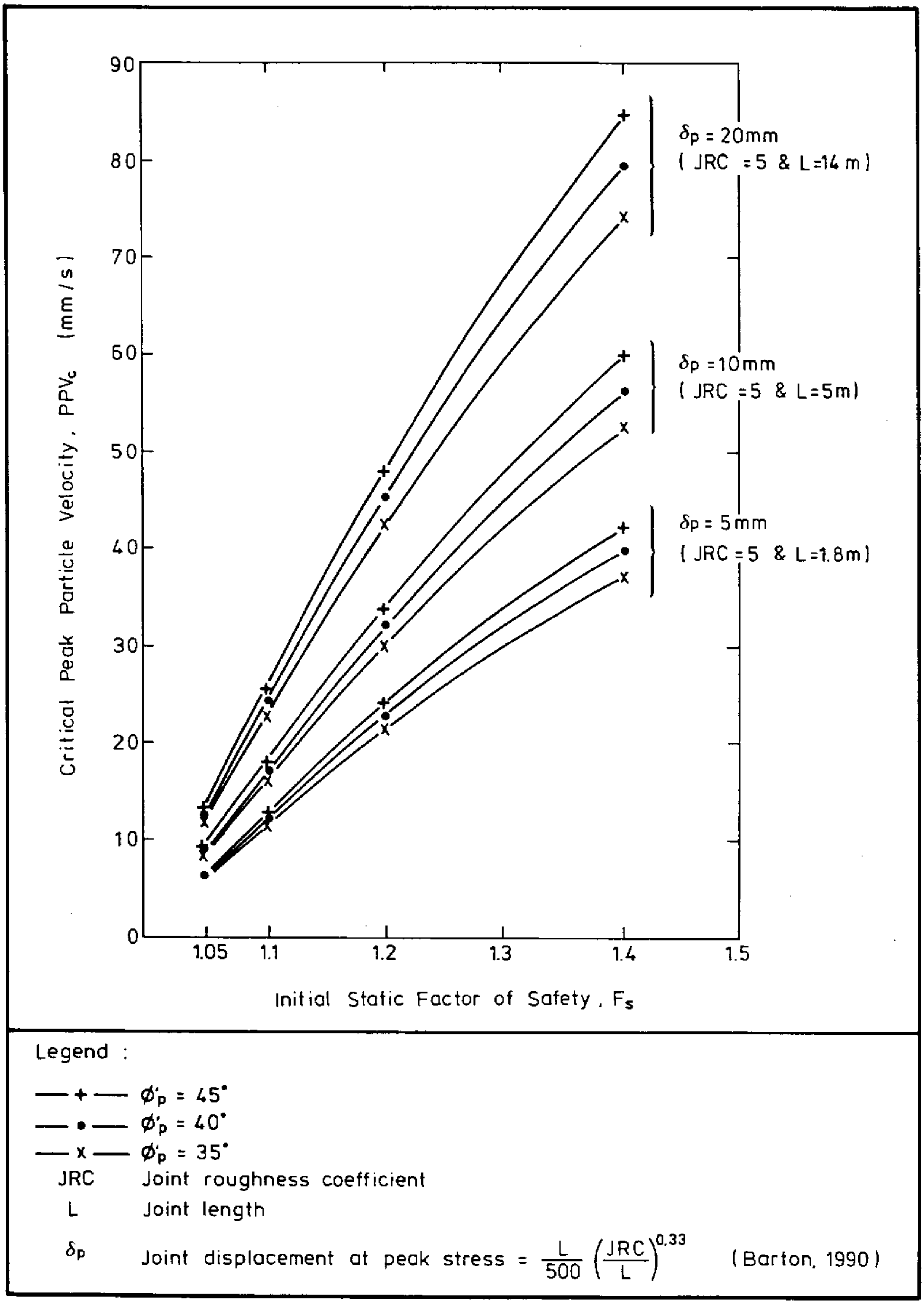

Figure 5 - Plot of PPV_c vs F_s for the Linear Shear Displacement Rock Joint Model

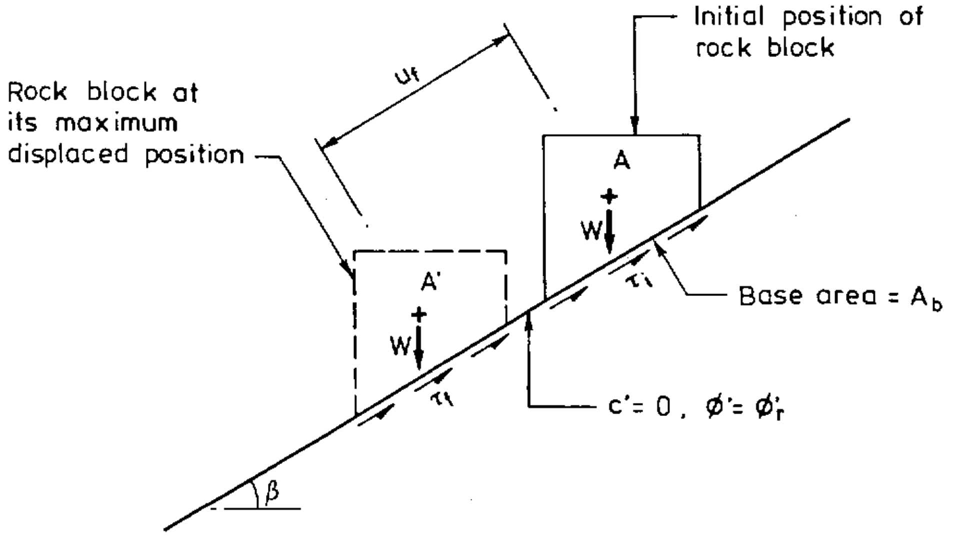
Initial position of rock block
Rock block at its maximum displaced position
u_f
A
W
A'
W
τ_i
Base area = A_b
$c' = 0$, $\phi' = \phi'_r$
β

(a) Rock Block System

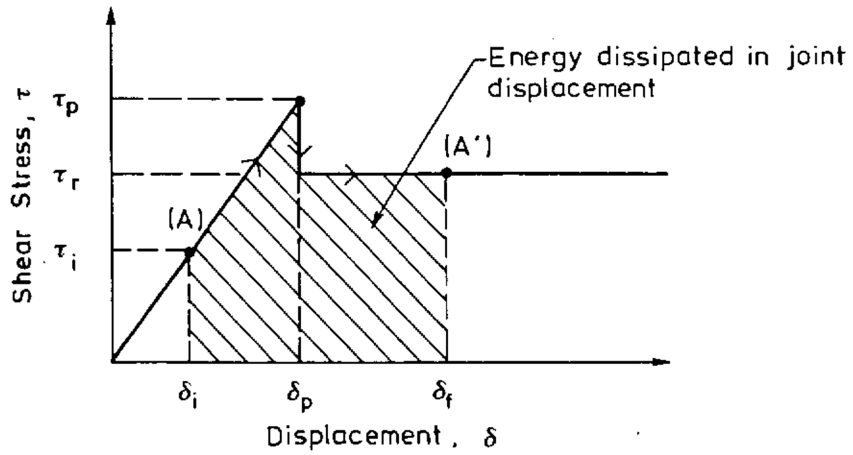

(b) τ - u Relationship for Rock Joint

Legend:

τ_i Initial shear stress = $W \sin\beta / A_b$
τ_f Shear stress at maximum displaced position A'
τ_p Peak shear strength = $W \cos\beta \ \tan\phi'_p / A_b$
τ_r Residual shear strength = $W \cos\beta \ \tan\phi'_r / A_b$
c' Effective cohesion of rock joint
ϕ'_p Peak angle of shearing resistance of rock joint
ϕ'_r Residual angle of shearing resistance of rock joint

Figure 6 - Energy Dissipation Based on the Combined Rock Joint Model

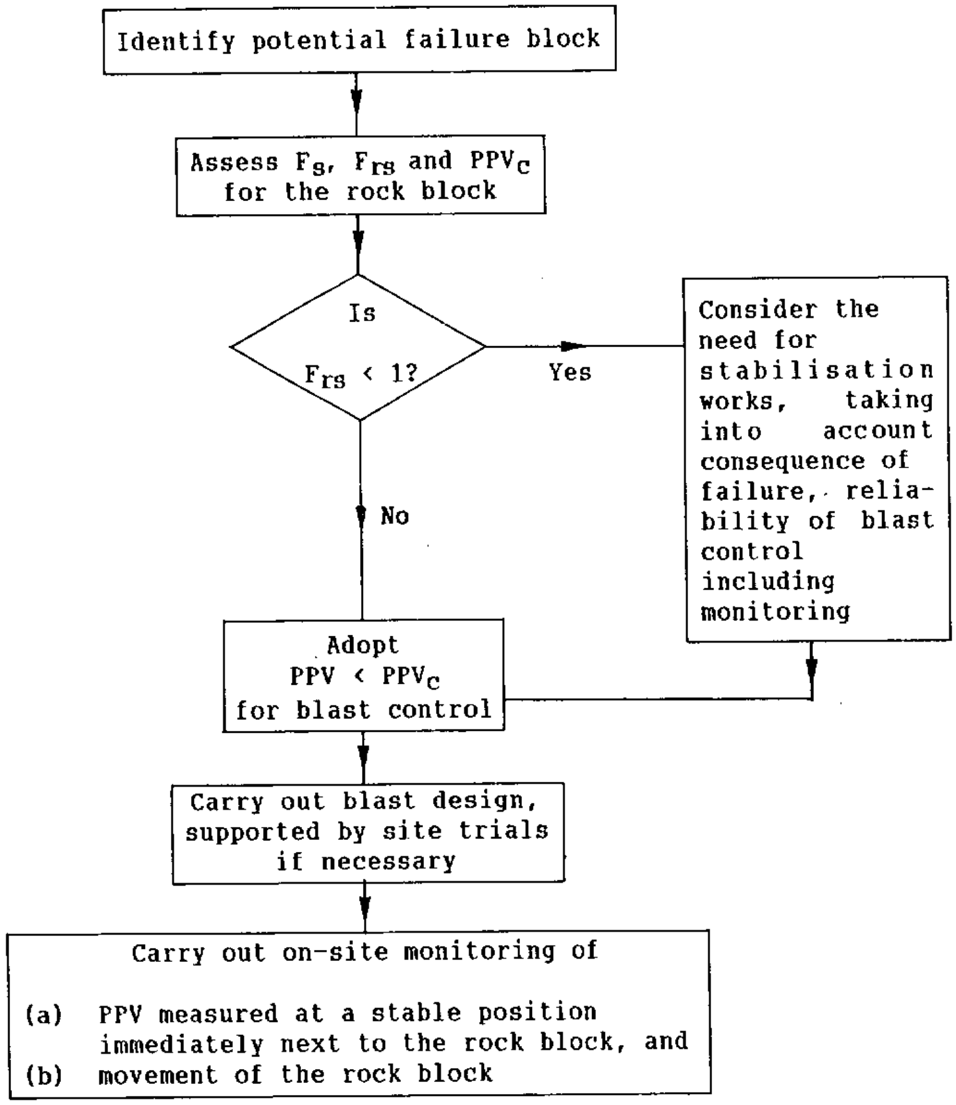
Identify potential failure block
Assess F_s, F_{rs} and PPV_c for the rock block
Is $F_{rs} < 1$?
Yes
No
Consider the need for stabilisation works, taking into account consequence of failure, reliability of blast control including monitoring
Adopt $PPV < PPV_c$ for blast control
Carry out blast design, supported by site trials if necessary
Carry out on-site monitoring of
(a) PPV measured at a stable position immediately next to the rock block, and
(b) movement of the rock block

Legend : F_s - initial static factor of safety
F_{rs} - post-peak factor of safety (based on residual shear strength of rock joint)
PPV - peak particle velocity
PPV_c - critical peak particle velocity calculated from the Energy Approach

Notes :

1. The suggested procedure is intended for application to sites where the consequence of rock slope instability induced by blasting vibration is of concern. Otherwise, less stringent requirements may be imposed.

2. Near-field effects of blasting, including the effects of delayed gas pressures, indiscriminate fracturing of the rock mass and fly rocks, need to be considered separately.

Figure 7 - Suggested Procedure for Blast Control Based on Results of the Proposed Energy Approach

SECTION 2 :

PSEUDO-STATIC ASSESSMENT OF STABILITY OF SOIL SLOPES SUBJECTED TO BLASTING VIBRATION

H.N. Wong

This report was originally produced as GEO Special Project Report No. SPR 7/92

FOREWORD

This report documents the formulation of an analytical method for routine assessment of the stability of soil slopes subjected to blasting vibration using the pseudo-static approach. The proposed method offers a major improvement to the ordinary pseudo-static method by taking the dynamic response of soil slopes and the generation of dynamic excess pore water pressure into account in the analysis. The proposed method has been found to be simple to apply. It gives conservative values of permissible peak particle velocity which are in general within achievable limits for application to blast design and control.

The study was initiated by the Working Group on the Effects of Blasting on Slopes under the chairmanship of Mr R.K.S. Chan (Chief Geotechnical Engineer/Advisory). It was undertaken by Mr H.N. Wong, who is the Special Projects Division's representative to the Working Group, under my general supervision. The members of the Working Group have reviewed a draft of the report and provided useful comments.

(Y.C. Chan)
Chief Geotechnical Engineer/Special Projects

CONTENTS

Page No.

Title Page 33

FOREWORD 34

CONTENTS 35

1. INTRODUCTION 37

2. MAIN FEATURES 37

3. SLOPES WITH HORIZONTAL BEDROCK UNDER SHEAR VIBRATION 39

3.1 Single-degree-freedom Model 39

3.1.1 Dynamic Response 39

3.1.2 PPV_c of Slopes Comprising Cohesionless Soils 40

3.1.3 PPV_c of Slopes Comprising $c' - \phi'$ Soils 41

3.2 Multi-degree-freedom Model 41

3.2.1 Dynamic Response 42

3.2.2 PPV_c of Slopes Comprising Cohesionless Soils 42

3.2.3 PPV_c of Slopes Comprising $c' - \phi'$ Soils 42

4. SLOPES WITH INCLINED BEDROCK UNDER COMPRESSION-RAREFACTION VIBRATION 42

5. DISCUSSION 43

5.1 Input Bedrock Motion 43

5.2 Single-degree-freedom Model vs Multi-degree-freedom Model 43

5.3 Multi-directional Vibration 43

5.4 Inclination of Pseudo-static Force 44

5.5 Dynamic Factor of Safety and Slope Displacement 44

5.6 Conservatism in the Analysis 45

5.7 Local Stability 45

5.8 Other Slope Geometry 46

5.9 Energy Approach 46

5.10 Further Studies 46

6. APPLICATION OF THE PROPOSED APPROACH TO BLAST CONTROL 47

7. CONCLUSIONS 47

8. REFERENCES 48

LIST OF FIGURES 50

APPENDIX A : A BRIEF SUMMARY OF THE METHOD OF PSEUDO-STATIC ANALYSIS 64

APPENDIX B : THE MAGNIFICATION FACTOR FOR A SINGLE-DEGREE-FREEDOM DAMPED FORCED VIBRATION SYSTEM 77

APPENDIX C : ONE-DIMENSIONAL SHEAR RESPONSE ANALYSIS FOR SLOPE WITH HORIZONTAL BEDROCK 82

APPENDIX D : ONE-DIMENSIONAL COMPRESSION-RAREFACTION RESPONSE ANALYSIS FOR SLOPE WITH INCLINED BEDROCK 96

APPENDIX E : WORKED EXAMPLES 104

1. INTRODUCTION

The stability of slopes subjected to vibration may be assessed by different approaches. The advantages and limitations of these approaches have been discussed by Wong (1992) and Wong & Pang (1991).

Amongst these approaches, the Pseudo-static Approach has been widely used for assessing the effects of earthquake vibration on slope stability. As discussed by Wong & Pang (1991), using this approach to analyse the stability of slopes subjected to blasting vibration characterised by high frequency pulses is expected to yield conservative results. In the case of rock slopes with simplified assumptions made on joint properties, such results may be so conservative as to make them impractical to apply. However, in the case of soil slopes, as this report will show, the Pseudo-static Approach may still give results which are generally within achievable limits for application to blast design and control.

A method to analyse the stability of soil slopes under blasting vibration using the Pseudo-static Approach is outlined in this report. Analysis of the dynamic response of soil slopes to the bedrock vibration, as well as calculation of the critical peak particle velocity PPV_c [1] are presented. Reference has also been made to the findings of Wong (1991 & 1992) on the classification of soils according to their undrained shear behaviour for dynamic stability analysis of soil slopes.

2. MAIN FEATURES

The following are the main features of the method presented in this report for assessing the stability of soil slopes subjected to blasting vibration :

(a) Adopt the Pseudo-static Approach

The disturbing effect of blasting vibration is modelled as an equivalent inertia force F, and :

$$F = W * K \quad \ldots\ldots\ldots\ldots\ldots\ldots\ldots\ldots (1)$$

where W = weight of soil mass above the potential slip surface
K = the response peak horizontal ground acceleration coefficient (in g) of the soil mass

Either the Simple Pseudo-static Approach or the Modified Pseudo-static Approach can be used, depending on the likely behaviour of the slope-forming materials involved. A brief summary of the two approaches is given in Appendix A.

(b) Model the Blasting Vibration as Simple Harmonic Motion

The blasting vibration at the bedrock is modelled, for simplicity, as a simple harmonic motion in the horizontal direction.

---

[1] PPV_c, as used in Wong & Pang (1991), is the peak particle velocity PPV of the bedrock vibration, under which the slope concerned will be just driven to the theoretical state of failure.

The general form of the equation of motion is :

$$\left.\begin{aligned} & & x &= \text{PPD}\sin(\omega t + \Theta) \\ \Rightarrow \frac{dx}{dt} &= & \dot{x} &= \text{PPV}\cos(\omega t + \Theta) \\ \Rightarrow \frac{d^2x}{dt^2} &= & \ddot{x} &= -\text{PPA}\sin(\omega t + \Theta) \end{aligned}\right\} \quad \ldots\ldots\ldots\ldots (2)$$

where x = displacement
$\dot{x}$ = velocity
$\ddot{x}$ = acceleration
ω = circular frequency of the ground motion
= 2π * frequency in Hz
Θ = phase shift
PPD = peak particle displacement
PPV = peak particle velocity = ω PPD
PPA = peak particle acceleration = ω PPV = ω^2PPD

According to Mines Division's records, the frequency content of blasting vibration in Hong Kong ranges typically from 30 to 100 Hz. Hence, values of ω from 60π to 200π are considered in this report.

(c) Consider the Dynamic Response of Soil Slopes

The response peak ground acceleration coefficient (i.e. K in equation (1)) at the soil mass is calculated from the input bedrock ground motion (i.e. equation (2)) and the dynamic response of the soil slope. K can be expressed as :

$$K = K_a \left(\frac{PPA}{g} \right) \quad \ldots\ldots\ldots\ldots\ldots (3)$$

where K_a = magnification factor determined from response analysis
g = acceleration due to gravity = 9.81 m/s^2

Values of K_a have been assessed in this report by modelling the slope as either a single-degree-freedom or a multi-degree-freedom system. A soil damping factor λ of 0.2 for the fundamental mode of vibration and 0.5 for the higher modes, and an infinite duration of input bedrock ground motion are assumed in the response analysis. Two alternative types of slope geometry, viz slopes with horizontal bedrock under shear vibration (Figure 1(a)) and slopes with inclined bedrock (i.e. an inclined soil layer) under compression-rarefaction vibration (Figure 1(b)) are considered.

(d) Adopt Limit Equilibrium Method of Slope Stability Analysis

The limit equilibrium method of slope stability analysis is adopted to calculate the initial static factors of safety F_s, the dynamic factors of safety F_d (i.e. under the action of pseudo-static inertia force), and the critical accelerations K_c [2] of the soil slopes.

The state of limiting equilibrium, i.e. F_d equal to unity, is taken as the onset of failure.

3. SLOPES WITH HORIZONTAL BEDROCK UNDER SHEAR VIBRATION

3.1 Single-degree-freedom Model

3.1.1 Dynamic Response

A simple but crude way to model the behaviour of a slope subjected to blasting vibration is to treat it as a single-degree-freedom system.

As shown in Appendix B, the magnification factor K_a for a damped single-degree-freedom system subjected to a simple harmonic forced vibration is :

$$K_a = \sqrt{\frac{1 + 4\lambda^2\alpha^2}{(1-\alpha^2)^2 + 4\lambda^2\alpha^2}}$$

$$= \sqrt{\frac{1 + 0.16\alpha^2}{(1-\alpha^2)^2 + 0.16\alpha^2}} \qquad \ldots\ldots\ldots\ldots\ldots (4)$$

where λ = damping factor = 0.2

$$\alpha = \frac{\text{Forcing (i.e. input vibration) Frequency}}{\text{Natural Frequency of Slope}}$$

$$= \frac{\omega T_1}{2\pi} \quad \text{or} \quad FT_1$$

$$F = \frac{\omega}{2\pi} = \text{Input vibration frequency in Hz at bedrock}$$

T_1 = fundamental period of slope (in second)

$$\approx \frac{3.3H}{S} \quad \text{(Wong, 1991)}$$

H = height of slope (in m)

---

[2] K_c (in g) is the response acceleration at the slope which will just drive the slope to the theoretical state of limiting equilibrium. It is a measure of the resistance of a slope to the action of pseudo-static inertia force.

S = velocity of the travelling wave (in m/s)

Values of K_a for different values of S/H and F are plotted in Figure 2.

From equations (2) and (3):

$$K = K_a \left(\frac{\omega \; PPV}{g} \right) \qquad \ldots\ldots\ldots\ldots\ldots (5)$$

At $K = K_c$, $PPV = PPV_c$,

$$K_c = \omega \; K_a \; PPV_c \; / \; g \qquad \ldots\ldots\ldots\ldots\ldots (6)$$

or

$$PPV_c = \left(\frac{K_c \; g}{\omega \; K_a} \right) \qquad \ldots\ldots\ldots\ldots\ldots (7)$$

Values of ωK_a for different values of S/H and F are plotted in Figure 3.

For a slope with a given K_c, the higher the value of ωK_a, the lower is the value of PPV_c and the more susceptible is the slope to instability induced by vibration. Within the typical ranges of values of F from 30 to 100 Hz and S/H less than 125 (e.g. S = 300 m/s and H > 2.4 m), an input vibration frequency of 30 Hz will result in the lowest PPV_c and hence the most critical situation. Therefore, the case of F equal to 30 Hz is considered in the following analyses for simplicity.

3.1.2 PPV_c of Slopes Comprising Cohesionless Soils

(a) Simple Pseudo-static Analysis

Figure 4 plots F_d vs K obtained from simple pseudo-static analysis for slopes with $c' = 0$ and $\phi' = 35°$ under 'dry' (i.e. Skempton's pore pressure coefficient B = 0) condition. Wong (1991) has shown that for the same F_s values, the relationship between F_d and K is not sensitive to the values of ϕ'.

By substituting values of K_c into equation (7), the corresponding PPV_c values for such slopes can be calculated. Figure 6 gives calculated values for S/H = 50, 30, 20 and 15 s-1, corresponding respectively to H = 6, 10, 15 and 20 m, for S = 300 m/s.

(b) Modified Pseudo-static Analysis

Figure 5 plots the values of K_c vs A_n for slopes with $c' = 0$ and $\phi' = 35°$ under 'saturated' (i.e. Skempton's Pore Pressure Coefficient B = 1.0) condition obtained from modified pseudo-static analysis (Wong, 1991). A_n is the dynamic pore pressure parameter (Sarma & Jennings, 1980). A brief discussion on the determination and use of A_n in modified pseudo-static analysis and the identification of 'degrading' soils in Hong Kong is given in

Appendix A. Soils with A_n greater than about 0.2 are denoted as 'degrading' soils, and reduction in soil shear strength under the undrained pseudo-static loading condition as compared with the drained condition would occur. If B is greater than zero, the higher the A_n value of the slope-forming material, the lower will be the resistance of the slope against instability induced by vibration.

Using equation (7), the PPV_c values for slopes with S/H = 50, 30, 20 and 15 s^{-1}, and A_n = 0.5 and 1.0 are plotted in Figures 6(b) and 6(c). The effect of 'degrading' materials in a slope in reducing its resistance against vibration is apparent.

3.1.3 PPV_c of Slopes Comprising c' - ϕ' Soils

Slopes comprising c' - ϕ' soils will have higher K_c than c' = 0 slopes having the same F_s. Hence, the values of PPV_c calculated in Section 3.1.2 are conservative for slopes with $c' \neq 0$.

The K_c values of slopes comprising c' - ϕ' soils cannot be generalised by charts. Where necessary, stability analysis can be carried out on individual slopes by limit equilibrium methods.

3.2. Multi-degree-freedom Model

3.2.1 Dynamic Response

More sophisticated multi-degree-freedom model may be used to analyse the slope response under shear vibration taking into consideration the contribution of higher vibration modes of the slope. Here, the one-dimensional shear response model has been adopted for this purpose. A similar model has been described by Ambraseys (1960) and adopted by Ambraseys & Sarma (1967) to analyse the dynamic response of earth dams subjected to real earthquake time-history vibration.

Details of the mathematics involved in the dynamic response analysis using the one-dimensional shear response slope model are summarised in Appendix C. A simple harmonic, 30 Hz frequency input blasting vibration at the bedrock is considered in the analysis.

The calculated values of the magnification factor K_a for F = 30 Hz and S/H = 50, 30, 20 and 15 s^{-1} are plotted in Figure 7. It can be seen that for overall slope failure (i.e. $y/H \approx 1.0$), K_a is much less than unity. However, for local slope failure at the upper portion of the slope (i.e. $y/H < 0.4$), K_a is large, implying that there would be considerable magnification of ground motion.

Figure 8 compares the difference in the K_a values calculated by using the multi-degree-freedom model (at y/H = 1.0) and the single-degree-freedom model. It can be seen that when values of S/H are smaller than 50 (i.e. $H \geq 6$ m for S = 300 m/s), the single-degree-freedom model would underestimate the response acceleration.

3.2.2 PPV_c of Slopes Comprising Cohesionless Soils

(a) Simple Pseudo-static Analysis

The PPV_c for 'dry' slopes comprising c' = 0 soils are plotted in Figure 9(a), by substituting the results of K_a from Figure 7 and K_c from Figure 4 to equation (7).

(b) Modified Pseudo-static Analysis

For 'saturated', c' = 0 slopes comprising 'degrading' soils (A_n = 0.5 and 1.0), the calculated PPV_c values are plotted in Figures 9(b) and (c). Again, the reduction in slope resistance against vibration due to the presence of 'degrading' soils is apparent.

3.2.3 PPV_c for Slopes Comprising c' - ϕ' Soils

The K_c values of such slopes may be calculated using methods of limit equilibrium slope stability analysis. The PPV_c values can then be evaluated from equation (7) using the values of K_a in Figure 7. This is illustrated in worked example No. 1 in Appendix E.

4. SLOPES WITH INCLINED BEDROCK UNDER COMPRESSION-RAREFACTION VIBRATION

Some steep slopes in Hong Kong are underlain by bedrock inclining approximately parallel to the slope surface. Provided that the height of the slope is large compared with the thickness D of soil (Figure 1(b)), the slope can be represented by an inclined soil layer on a rigid base. The dynamic response of such slopes would more appropriately be modelled by an inclined soil layer under one-dimensional compression-rarefaction vibration than by the one-dimensional shear response model described in Section 3 above.

By treating the inclined soil layer as a single-degree-freedom system, the calculated values of the magnification factor K_a for different values of S/D and F are plotted in Figure 10. The dynamic response analysis for such single-degree-freedom system is the same as that described in Section 3.1.1 except that the fundamental period T_1 of the soil layer is given by 4D/S.

An improved dynamic response analysis for the inclined soil layer has been carried out by modelling it as a multi-degree-freedom system under one-dimensional compression-rarefaction vibration. Details of the analysis are outlined in Appendix D. The analysis is very similar to that of the one-dimensional shear response model. Values of the magnification factor K_a calculated from the multi-degree-freedom one-dimensional compressional-rarefaction response analysis for the inclined soil layer are given in Figure 11.

Figure 12 compares the difference between the values of K_a calculated from the multi-degree-freedom model (at y/D = 1.0) and from the single-degree-freedom model. It can be seen that when S/D is less than 50 s^{-1}, the single-degree-freedom model would underestimate the response acceleration.

Results of the one-dimensional compression-rarefaction response analysis for the inclined soil layer can be applied in pseudo-static slope stability analysis in a way similar to those of the one-dimensional shear response analysis. This is illustrated in worked example No. 2 in Appendix E.

5. DISCUSSION

5.1 Input Bedrock Motion

It has been assumed in the above analyses that the input bedrock vibration is a simple harmonic motion with a frequency of 30 Hz. This value may be considered to represent the 'mode' of the spectral frequencies of the actual blasting vibration which comprises motion with a range of frequencies. In principle, the above analyses may be refined to consider the full range of the vibration frequencies using mathematical techniques such as Duhamel Integral or Fourier Transformation. Such refinement is, however, not warranted at this stage because detailed information on the spectrum of blasting vibrations in Hong Kong is not yet available. Considering typical blasting vibrations in Hong Kong with frequency ranges from 30 to 100 Hz, the simplified assumption of a singular frequency of 30 Hz as adopted in the analyses is conservative.

It should be noted that the frequency content of vibration tends to shift towards the lower frequency range with increasing distance from the source, since high frequency pulses would attenuate quicker than low frequency ones. Hence, consideration of a lower vibration frequency (e.g. 15 Hz) may be appropriate for slopes at large distance (say, of several hundreds of metres) from the blasting source. This can be done by changing the values of S_a adopted in the analyses in Appendices C and D.

5.2 Single-degree-freedom Model vs Multi-degree-freedom Model

The single-degree-freedom model is simple to use. However, as shown in Figures 8 and 12, such model could underestimate the response acceleration by more than 50% when S/H or S/D is smaller than 50 s^{-1} (i.e. H or D > 6 m for S = 300 m/s). This confirms that consideration of the higher modes of vibration is important if the fundamental period of the vibrating system is much longer than the predominant period of the exciting motion.

Whilst analyses using the single-degree-freedom model may be useful in giving engineers a quick and preliminary idea about the problem, it is suggested that solutions based on the multi-degree-freedom model should be adopted in detailed assessment and design.

5.3 Multi-directional Vibration

The effect of multi-directional vibration is generally not considered in pseudo-static analysis. This implies that the peak particle acceleration PPA adopted in the analysis is taken to be the maximum of the PPA's measured in any of the three orthogonal directions and not the maximum of the resultant acceleration. Hence, the PPV_c's calculated above also refer to the maximum of the PPV's in any of the three orthogonal directions.

Alternatively, if the resultant PPA was to be considered in design, this could be done by factoring the PPV_c calculated in this report by 1.35 (Wong & Pang, 1991). This is however not considered necessary in routine design to avoid being overly conservative.

5.4 Inclination of Pseudo-static Force

The values of K_c adopted for the calculation of PPV_c in Sections 3 and 4 are based on Wong (1991 & 1992), in which the inclination of the pseudo-static force is assumed to be acting in the horizontal direction. As discussed in Wong (1991), pseudo-static forces acting approximately in the horizontal direction will result in minimum K_c values.

In case a non-horizontal inertia force needs to be considered, the corresponding PPV_c may be assessed from equation (7) using the value of K_c calculated from slope stability analysis adopting an inclined pseudo-static force.

5.5 Dynamic Factor of Safety and Slope Displacement

It is considered in the calculation of PPV_c in this report that the dynamic slope factor of safety F_d is not allowed to drop below unity. This is to ensure that the slopes would not be stressed beyond the failure (i.e. peak soil shear strength) point. According to the rigid plastic soil model assumed for the Pseudo-static Approach, the net displacement of the slopes in such case will be zero.

In theory, the F_d of a slope subjected to blasting vibration may be allowed to drop below unity over a small time interval, without necessarily resulting in a complete slope failure. For some cohesionless slopes where the post-peak drop in shear strength is minimal (e.g. rock fill), a transient F_d value less than unity might only result in a very small slope displacement, and such condition could be acceptable. Depending on the allowable slope displacement, value of F_d less than unity and hence PPV_c higher than those given in Sections 3 and 4 might be acceptable for such slopes. Alternatively, the K_c and hence the PPV_c values calculated from $F_d = 1.0$ may be increased by a certain percentage. It can be shown by using Sarma (1975)'s sliding block method that the displacement of a slope subjected to a peak response acceleration of 1.1 to 1.2 K_c is small (about 1 mm for a 30 Hz, 1 second duration vibration) if there is negligible drop in the soil strength post-peak. It follows that for such slopes, an actual peak particle velocity of 1.1 to 1.2 PPV_c can be acceptable.

For slopes comprising soils for which the post-peak drop in shear strength may be considerable (e.g. saprolites), not allowing F_d to drop below unity is considered more appropriate in view that there is at present little understanding of the post-peak behaviour of these soils in Hong Kong under cyclic loading condition.

In case a dynamic factor of safety higher than unity is required to cater for, say, uncertainties in the soil shear strength parameters. The K_c values corresponding to the required F_d values may be calculated and substituted to equation (7) to assess the corresponding values of PPV_c.

5.6 Conservatism in the Analysis

Analysis using the method described in this report is expected to give conservative results. The main areas of conservatism are in:

(i) the assumption that the input bedrock vibration is a simple harmonic motion with a singular frequency of 30 Hz,

(ii) the S_a values adopted in the response analyses in Appendices C and D, assuming infinite duration of input motion, and

(iii) the use of Pseudo-static Approach adopting PPA and a minimum F_d of unity.

The assumption that the slopes vibrate in one-dimensional shear/compression-rarefaction together with the use of root-mean-square combination of the first four modes of vibration to calculate the K_a values may possibly be conservative, but this is not definite.

Modelling the slope as a wedge in the one-dimensional shear response analysis would also tend to overestimate the response acceleration near the crest of the slope.

5.7 Local Stability

Apart from checking against full-height slope instability (i.e. $y/H = 1.0$), the possibility of local instability involving part of a slope (i.e. $y/H < 1.0$) should also be considered in assessing the PPV_c of a slope. This is illustrated in the worked examples in Appendix E.

As shown in Figures 7 & 11, the K_a values for local slope failure can be well above 1.0 near the crest of the slope. This may result in low values of PPV_c for some slopes.

However, for a slope under elastic vibration, the maximum shear strain increment $\Delta\varepsilon_s$ induced by the vibration can be shown (e.g. see Wong, 1991) to be:

$$\Delta\varepsilon_s = \text{peak particle velocity at the slope} / S$$

$$= K_a \, PPV / S \qquad \ldots\ldots\ldots (8)$$

Consider PPV (at bedrock) = 30 mm/s, and a conservative $K_a = 2.0$. For $S = Smax$ = say, 300 m/s:

$$\Delta\varepsilon_s = 0.02\% \text{ , which is rather small.}$$

Hence, provided that the initial static factor of safety F_s of the slope is high (say, $F_s > 2.0$) such that the maximum shear strain at the slope is far less than the yield strain even with the addition of $\Delta\varepsilon_s$, the slope will remain in a state of elastic vibration (i.e. $S \approx Smax$). As such, slope instability will not occur, despite the possible large local PPA in the slope vibration and a low F_d calculated from the Pseudo-static Approach.

If the initial F_s of the slope is low and the initial shear strain of the slope is considerable, the shear stiffness of the slope may reduce significantly under vibration and S may drop to a value as low as 10% of Smax. Hence, for PPV = 30 mm/s, $K_a = 2.0$ and S = 30 m/s, $\Delta\varepsilon_s$ may reach 0.2% which is quite high. If the slope-forming material is relatively brittle, considerable irrecoverable cyclic shear strain and hence slope instability may be induced by the blasting vibration.

Further study in this area, particularly when data on the non-linear stiffness properties of the soils in Hong Kong is available, would be useful in improving our understanding of slope behaviour under dynamic loading.

5.8 Other Slope Geometry

The dynamic response of two sets of idealised slope geometry, i.e. slopes with horizontal bedrock and slopes with bedrock parallel to slope surface, was analysed and the results given in this report. There is unfortunately no simple mathematical solution for the dynamic response of slopes with other angles of bedrock inclination or slopes with more complicated geometry. Before more rigorous solutions from advanced dynamic analysis are available, the results of the dynamic response of the idealised slope geometry presented in this report may be used as an approximation. Amongst other uncertainties such as those related to the actual time-history of the blasting vibration and the dynamic soil properties involved in the assessment of dynamic slope stability, the approximation with idealised slope geometry is not considered unacceptable for practical purposes.

An engineer should exercise judgement as to which one of the two sets of idealised slope geometry is a better representation of the actual slope geometry of his problem and apply the appropriate set of results of dynamic response analysis to the pseudo-static slope stability assessment. In case of doubt, both idealised slope models should be considered in the assessment and a suitable conservative value be chosen between results from the models.

5.9 Energy Approach

The results obtained from the above analyses cannot be directly compared to those obtained from the Energy Approach (Wong & Pang, 1991), though both sets of results are similar in order. In fact, the Pseudo-static Approach and the Energy Approach are based on entirely different consideration of loading conditions and soil models. Any attempt to apply the Energy Approach to assess the stability of soil slopes under blasting vibration should be accompanied by an assessment of the possible brittle nature of the soil cohesion and generation of dynamic pore water pressure. This is beyond the scope of this report.

5.10 Further Studies

It would be useful to collect field data on the performance of soil slopes subjected to blasting vibration for calibration with the analytical results. Attention needs to be given to not only the short term but also the long term stability of the slopes, as distresses induced by blasting vibration may not necessarily be evident in the short term. When sufficient reliable field data are available, it is possible that empirical correlations may be developed for further improvement in the method of dynamic soil slope stability analysis.

The possible use of advanced time-history dynamic analysis by computer programs like "UDEC" and "FLAC" should also be explored. Though at present not convenient for routine use, advanced dynamic analysis could serve as a useful check against the results of the pseudo-static method of analysis, particularly for more complicated problems. It could also be employed to verify some of the simplified assumptions adopted in the pseudo-static method and to assess any further refinements to the method so that less conservative solutions may be obtained.

6. APPLICATION OF THE PROPOSED APPROACH TO BLAST CONTROL

A procedure of applying the pseudo-static method described in this report to blast control to safeguard the stability of soil slopes subjected to blasting vibration is outlined in Figure 13.

If the PPV at the bedrock induced by blasting is less than the PPV_c calculated from the proposed pseudo-static method, the dynamic slope stability will be acceptable.

If 'degrading' soils is present, or if the slope stability or serviceability condition is sensitive to slope movement, the need for regular slope inspection or movement monitoring should be considered. The presence of 'degrading' soil can seriously affect the slope resistance against vibration. Also, the rigid plastic soil model being adopted in the pseudo-static analysis is unable to assess the 'pre-failure' slope displacement if any.

It should be noted that as the PPV_c calculated from the proposed pseudo-static method is conservative, having PPV higher than PPV_c does not necessarily imply imminent slope failure. The need for revising the blast design or for carrying out precautionary/stabilisation work in such occasions should be considered in the light of the possible consequence of failure and the reliability of the on-site monitoring and control work.

The proposed method is relatively simple to apply. It involves only routine techniques for blast control in Hong Kong, including the measurement of PPV and the use of the available attenuation laws relating PPV with scaled distance and site factor. Sophisticated analysis is not required. Although the PPV_c so calculated are considered conservative, they are not overly so for practical application.

7. CONCLUSIONS

A simple method for assessing the stability of soil slopes subjected to blasting vibration using the Pseudo-static Approach taking dynamic slope response into consideration has been outlined in this report. Worked examples were given to illustrate the use of the method. Guidelines for applying the values of PPV_c assessed by the method to blast control were described.

The proposed method offers a valid analytical means for assessing the stability of soil slopes subjected to blasting vibration. Though the method is conservative, the estimated PPV_c values lie within achievable limits and the method can therefore be applied to blast control.

8. REFERENCES

Ambraseys, N.N. (1960). The seismic stability of earth dams. Proceedings of the Second World Conference on Earthquake Engineering, vol. 2, pp 1345-1363.

Ambraseys, N.N. & Sarma, S.K. (1967). The response of earth dams to strong motion. Geotechnique, vol. 17, pp 181-213.

Bauer, A. & Calder, P.N. (1971). The influence and evaluation of blasting on stability. Proceedings of the First International Conference on Stability in Open Pit Mining, Vancouver, pp 83-94.

Ishihara, K. (1985). Stability of natural deposits during earthquakes. Proceedings of the Eleventh International Conference on Soil Mechanics and Foundation Engineering, San Francisco, vol. 1, pp 321-376.

Jacobsen, L.S. (1930). Motion of a soil subjected to a simple harmonic ground vibration. Bulletin of the Seismological Society of America, vol. 20, no. 3, pp 160-195.

Kobayashi, Y. (1984). Back-analysis of several earthquake-induced slope failures on the Isu Peninsula, Japan. Proceedings of the Eighth World Conference on Earthquake Engineering, vol. 3, pp 405-412.

Matasovic, N. (1991). Selection of method for seismic slope stability analysis. Proceedings of the Second International Conference on Recent Advances in Geotechnical Earthquake Engineering and Soil Dynamics, St. Louis, pp 1057-1062.

Newmark, N.M. & Rosenblueth, E. (1971). Fundamentals of Earthquake Engineering, 640 p.

Sarma, S.K. (1973). Stability analysis of embankments and slopes. Geotechnique, vol. 23, no. 3, pp 423-433.

Sarma, S.K. (1974). User's Manual for Computer Program "EQS" : Stability Analysis of Embankments and Slopes by Sarma's Method, 56 p.

Sarma, S.K. (1975). Seismic stability of earth dams and embankments. Geotechnique, vol. 25, no. 4, pp 743-761.

Sarma, S.K. (1979). Response and Stability of Earth Dams during Strong Earthquake. Miscellaneous Paper GL-79-13, Geotechnical Laboratory, U.S. Army Engineer Waterways Experiment Station, 82 p.

Sarma, S.K. & Jennings, D. (1980). A dynamic pore water pressure parameter A_n. Proceedings of the International Symposium on Soil Under Cyclic and Transient Loading, Swansea, pp 295-298.

Seed, H.B. (1966). A method for earthquake resistant design of earth dams.

Journal of Soil Mechanics and Foundation, American Society of Civil Engineers, vol. 91, no. SM1, pp 13-41.

Skempton, A.W. (1954). The pore-pressure coefficient A and B. Geotechnique, vol. 4, pp 143-147.

Wong, H.N. (1991). Evaluation of Seismic Stability of Soil Slopes in Hong Kong. MSc Dissertation, Department of Civil Engineering, Imperial College of Science, Technology & Medicine, University of London, 270 p.

Wong, H.N. (1992). Assessment of seismic stability of soil slopes in Hong Kong. Submitted for publication to the International Journal of Earthquake Engineering and Structural Dynamics.

Wong, H.N. & Pang, P.L.R. (1991). An Energy Approach for the Assessment of Stability of Rock Slopes Subjected to Blasting Vibration. Special Project Report No. SPR 7/91, Geotechnical Engineering Office, 27 p.

LIST OF FIGURES

Figure No.		Page No.
1	Slope Geometry for Dynamic Response Analysis	51
2	K_a vs S/H for Slope with Horizontal Bedrock Based on Single-degree-freedom Model	52
3	ωK_a vs S/H for Slope with Horizontal Bedrock Based on Single-degree-freedom Model	53
4	F_d vs K for c' = 0, 'Dry' (B = 0) Slopes	54
5	K_c vs A_n for c' = 0, 'Saturated' (B = 1.0) Slopes	55
6	PPV_c for c' = 0 Slope with Horizontal Bedrock Based on Single-degree-freedom Model	56
7	K_a vs y/H for Slope with Horizontal Bedrock Based on One-dimensional Shear Response Model	57
8	Comparison of K_a Values from One-dimensional Shear Response Model and Single-degree-freedom Model for Slopes with Horizontal Bedrock	58
9	PPV_c for c' = 0 Slope with Horizontal Bedrock Based on One-dimensional Shear Response Model	59
10	K_a vs S/D for Inclined Soil Layer Based on Single-degree-freedom Model	60
11	K_a vs y/D for Inclined Soil Layer Based on One-dimensional Compression-rarefaction Response Model	61
12	Comparison of K_a Values from One-dimensional Compression-rarefaction Model and Single-degree-freedom Model for Inclined Soil Layer	62
13	Application of the Pseudo-static Method to Blast Control	63

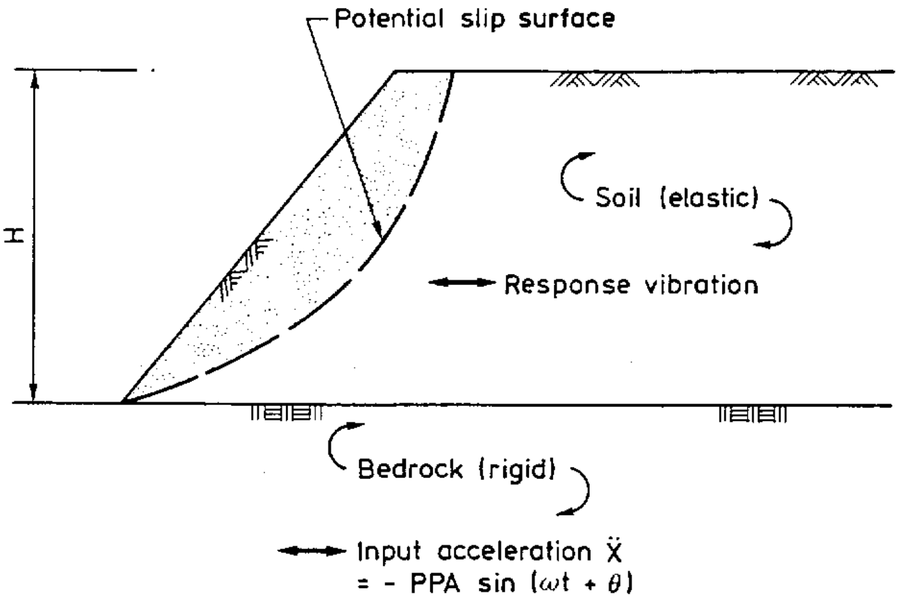
Potential slip surface
H
Soil (elastic)
Response vibration
Bedrock (rigid)
Input acceleration $\ddot{X}$
= - PPA sin (ωt + θ)

(a) Slope with Horizontal Bedrock under Shear Vibration

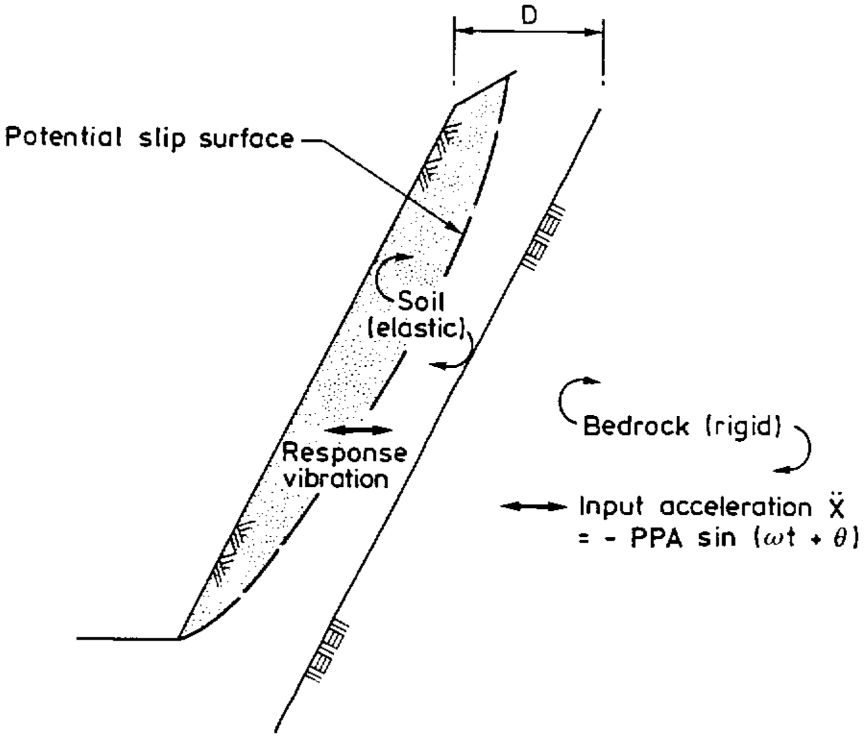
D
Potential slip surface
Soil
(elastic)
Response
vibration
Bedrock (rigid)
Input acceleration $\ddot{X}$
= - PPA sin (ωt + θ)

(b) Slope with Inclined Bedrock (i.e. Inclined Soil Layer) under Compression-rarefaction Vibration

Figure 1 - Slope Geometry for Dynamic Response Analysis

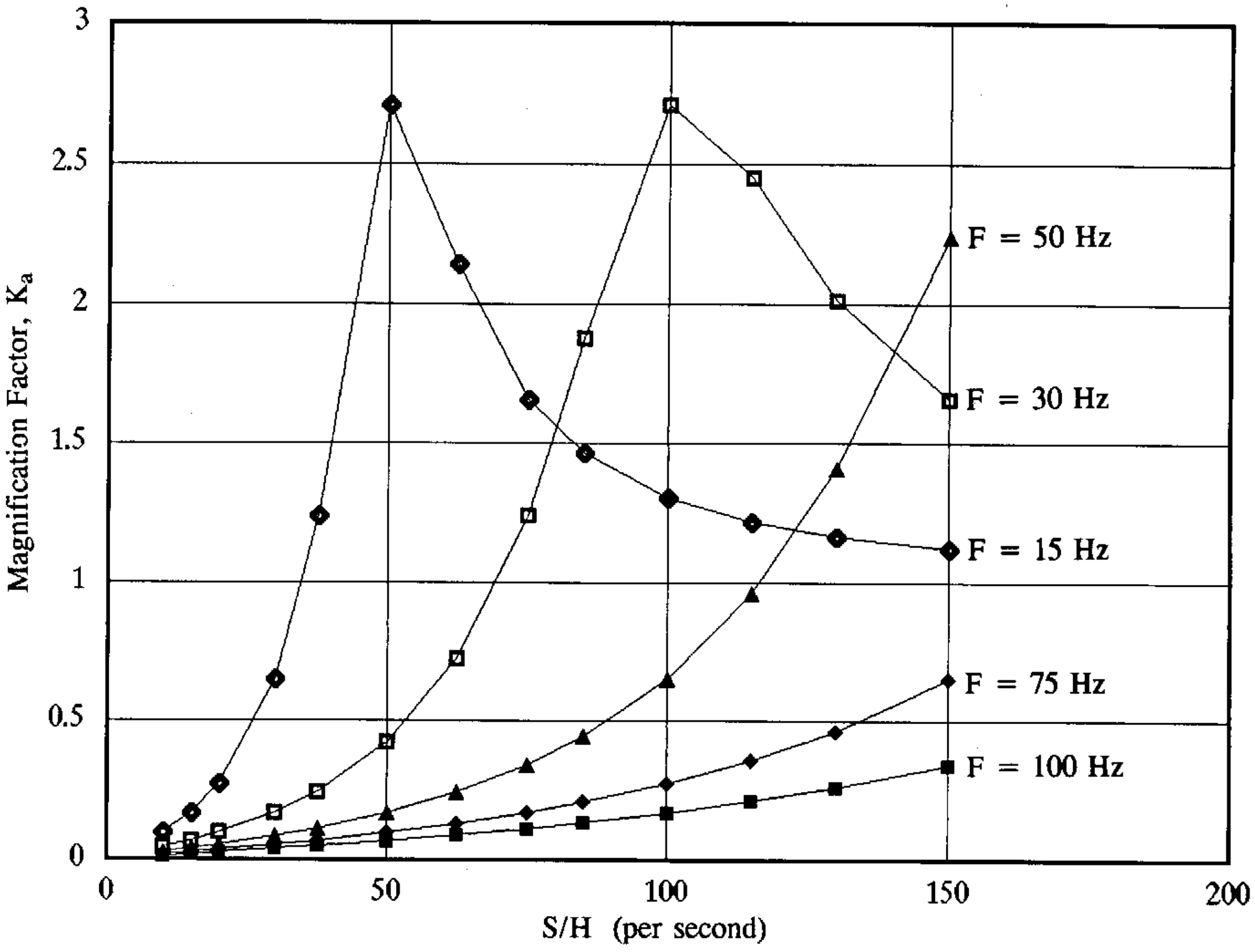

Figure 2 - K_a vs S/H for Slopes with Horizontal Bedrock Based on Single-degree-freedom Model

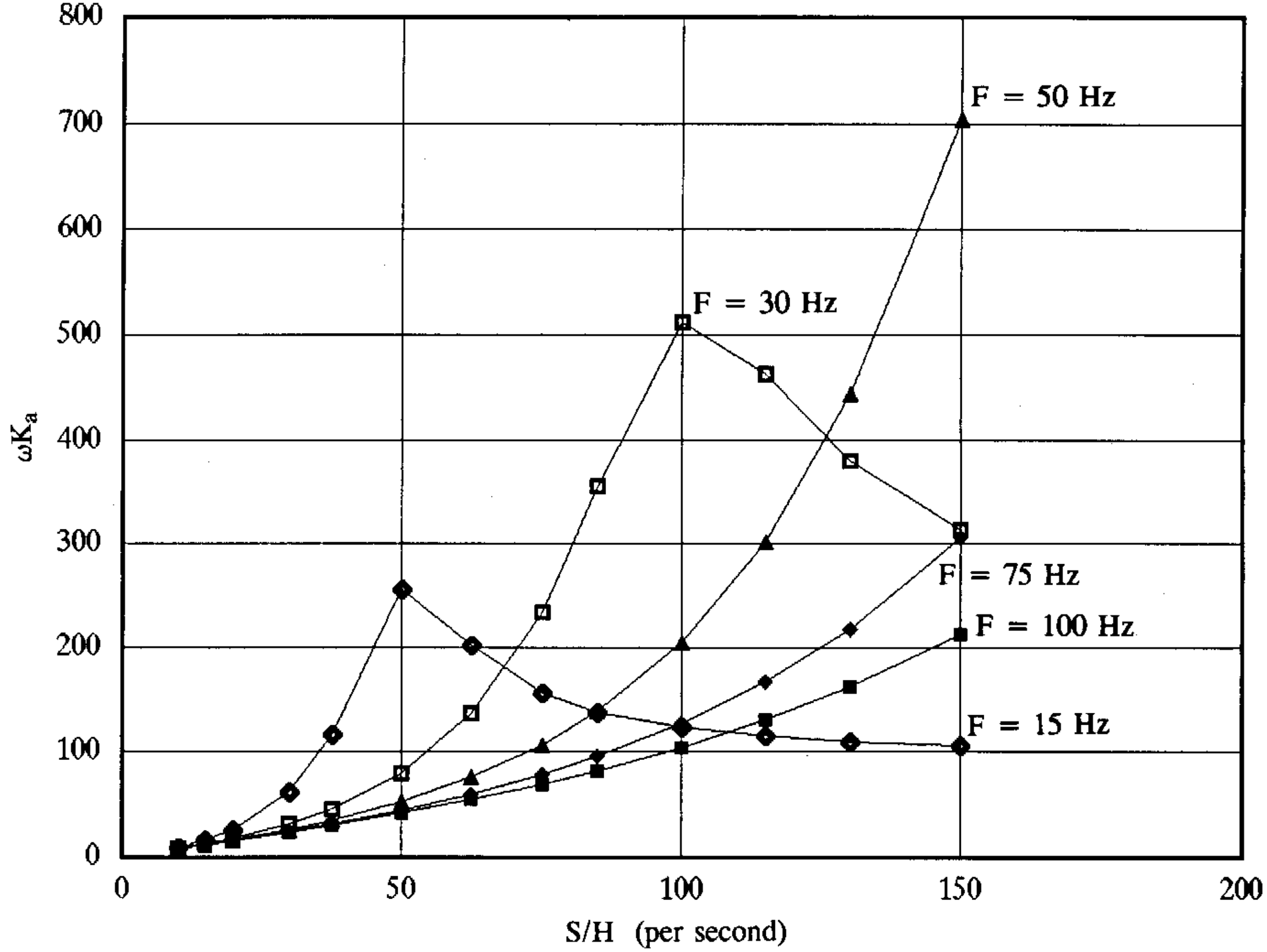

Figure 3 - ωK_a vs S/H for Slopes with Horizontal Bedrock Based on Single-degree-freedom Model

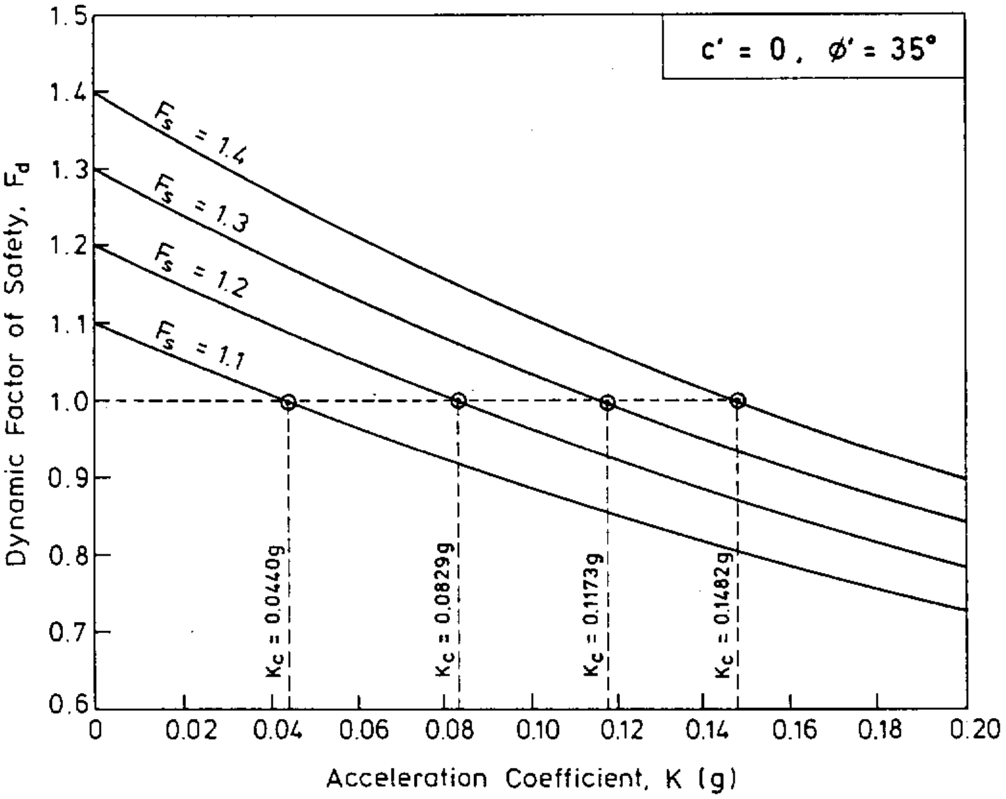

Note : K_c = critical acceleration (g)

Figure 4 - F_d vs K for c' = 0, 'Dry' (B = 0) Slopes

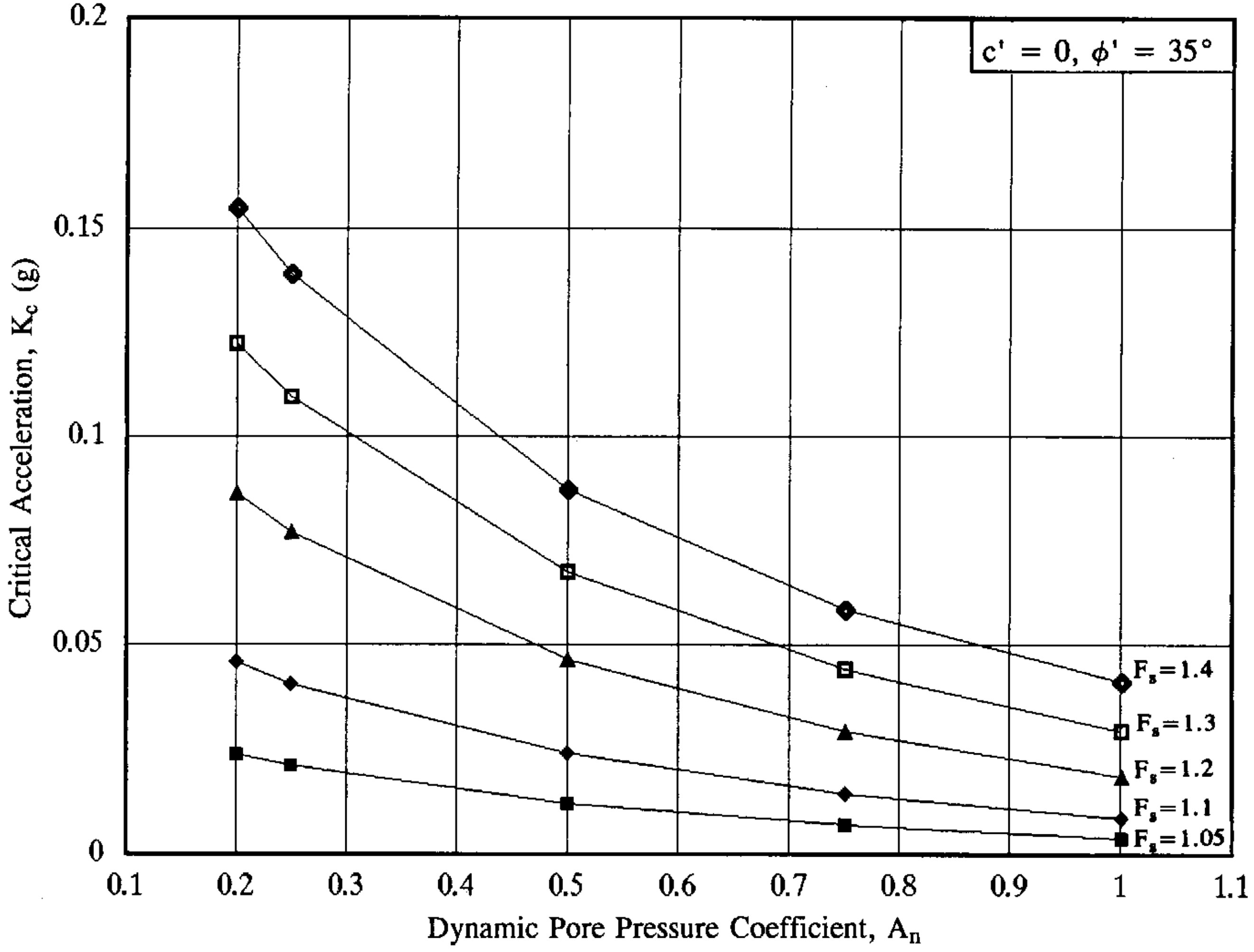

Figure 5 - K_c vs A_n for c' = 0, 'Saturated' (B = 1.0) Slopes

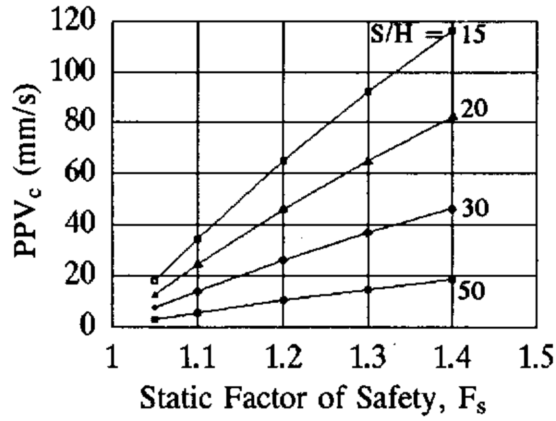

(a) 'Dry' (B = 0) Condition

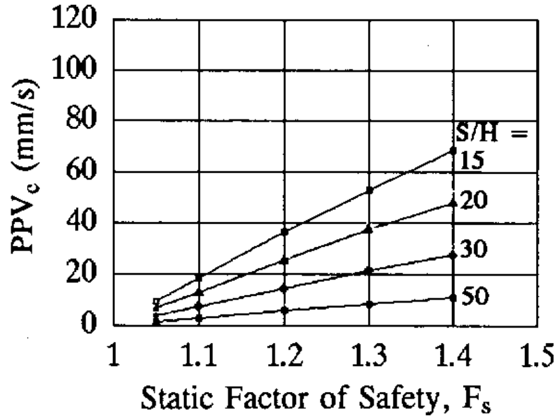

(b) 'Saturated' (B = 1.0) and A_n = 0.5 Condition

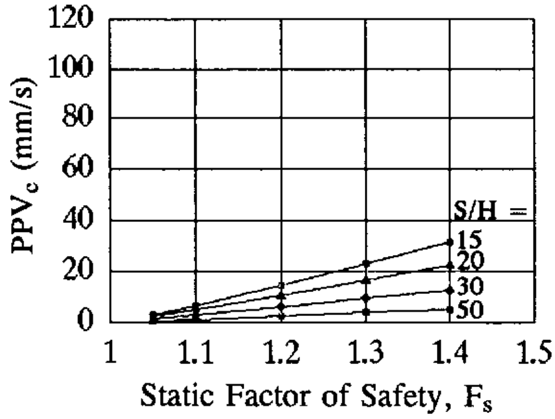

(c) 'Saturated' (B = 1.0) and A_n = 1.0 Condition

Note : F = 30 Hz, c' = 0, ϕ' = 35°, y/H = 1.0

Figure 6 - PPV$_c$ for c' = 0 Slopes with Horizontal Bedrock Based on Single-degree-freedom Model

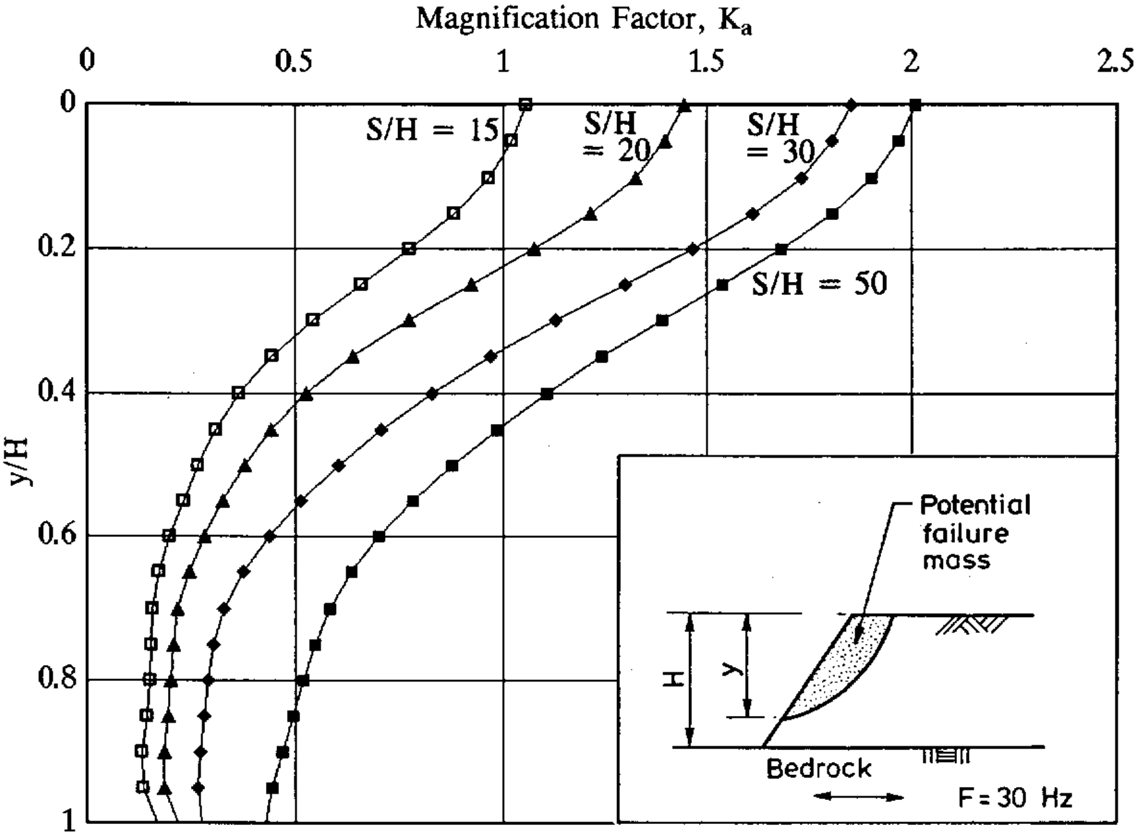

Figure 7 - K_a vs y/H for Slopes with Horizontal Bedrock Based on One-dimensional Shear Response Model

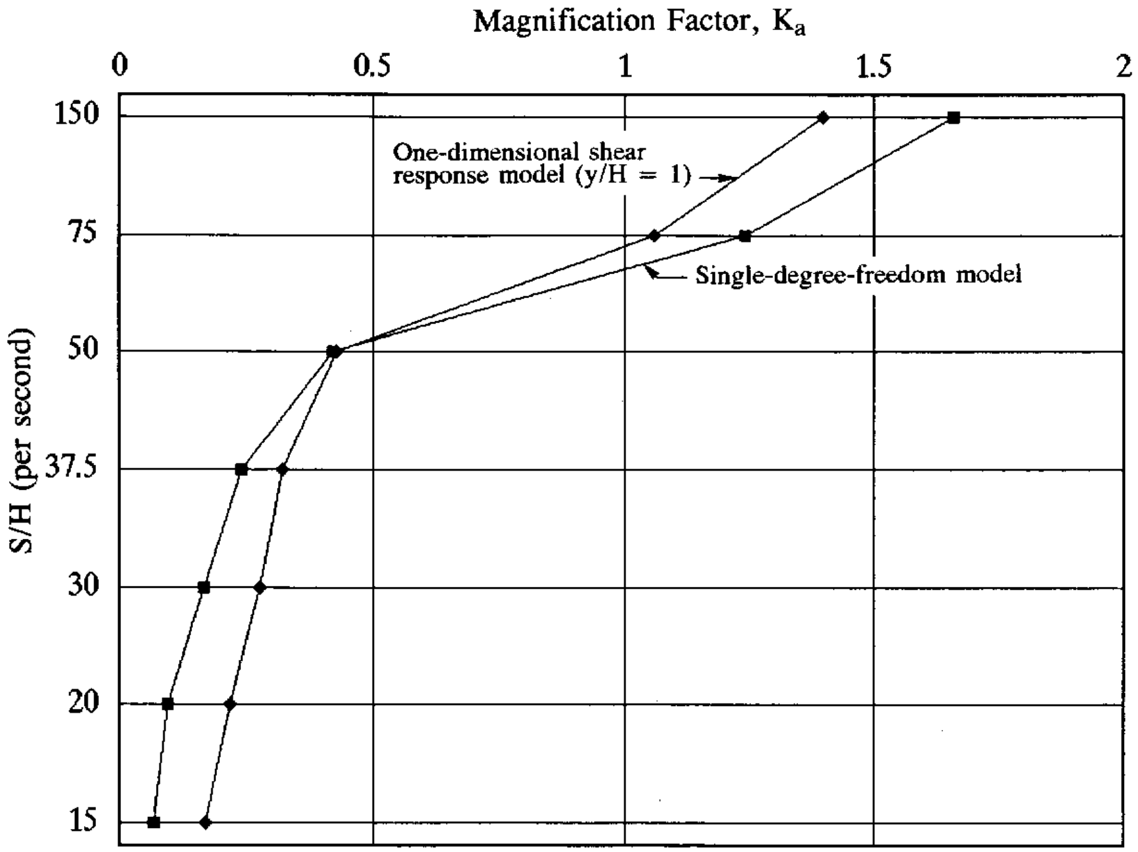

Figure 8 - Comparison of K_a Values from One-dimensional Shear Response Model and Single-degree-freedom Model for Slopes with Horizontal Bedrock

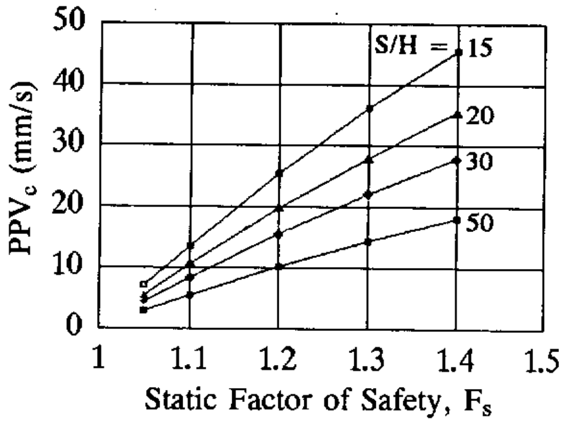

(a) 'Dry' (B = 0) Condition

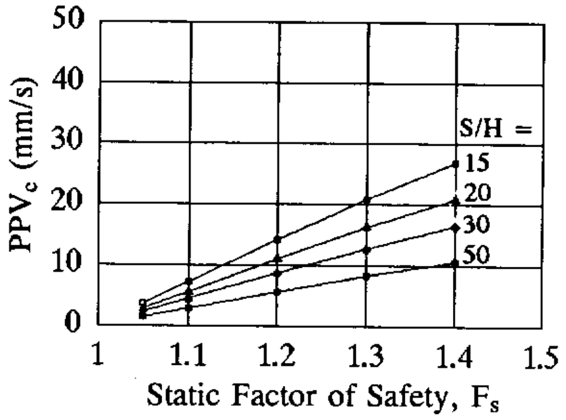

(b) 'Saturated' (B = 1.0) and A_n = 0.5 Condition

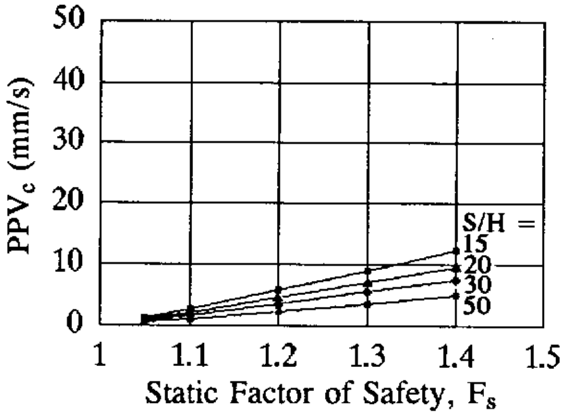

(c) 'Saturated' (B = 1.0) and A_n = 1.0 Condition

Note : F = 30 Hz, c' = 0, ϕ' = 35°, y/H = 1.0

Figure 9 - PPV$_c$ for c' = 0 Slopes with Horizontal Bedrock Based on One-dimensional Shear Response Model

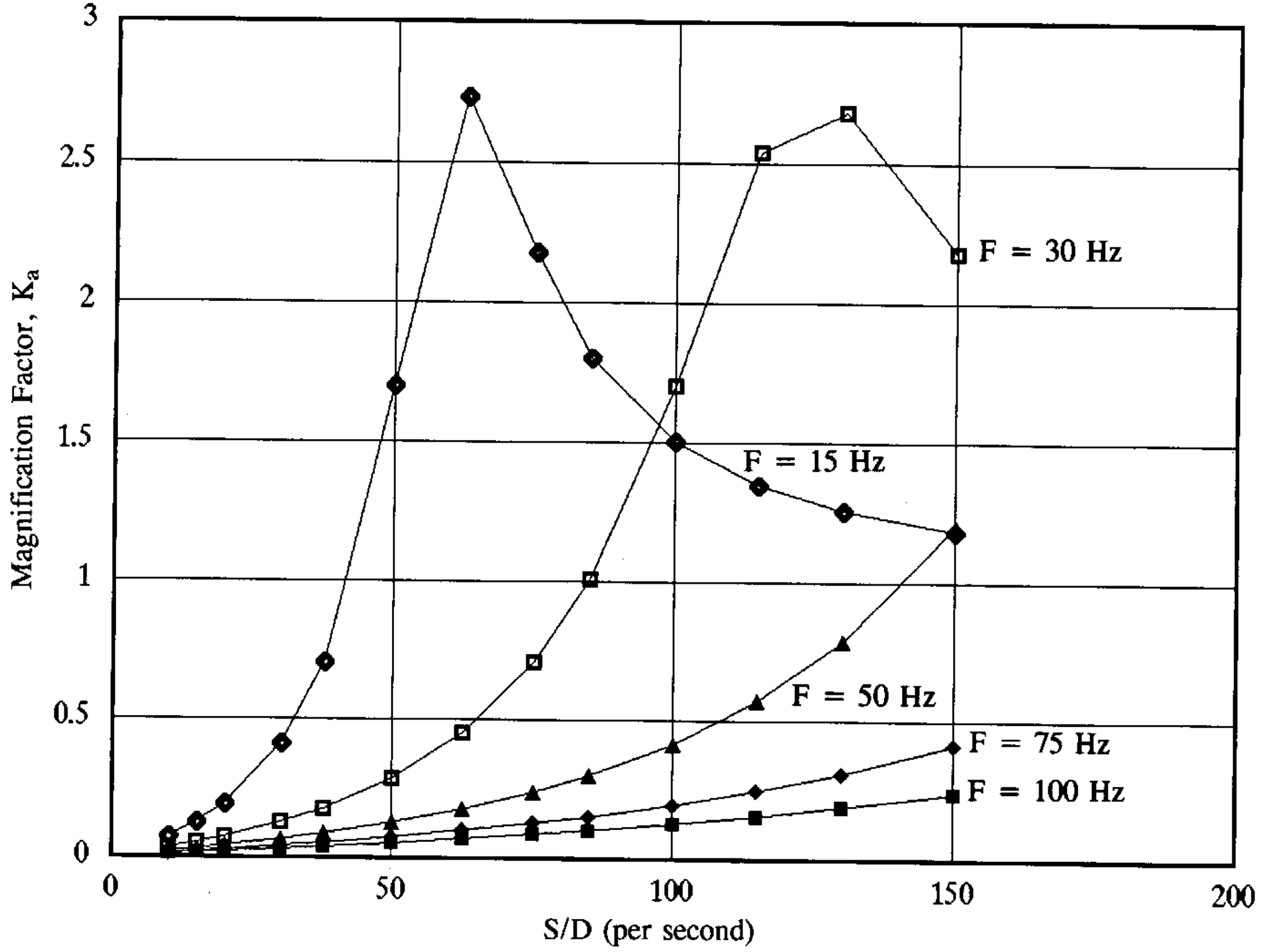

Figure 10 - K_a vs S/D for Inclined Soil Layer Based on Single-degree-freedom Model

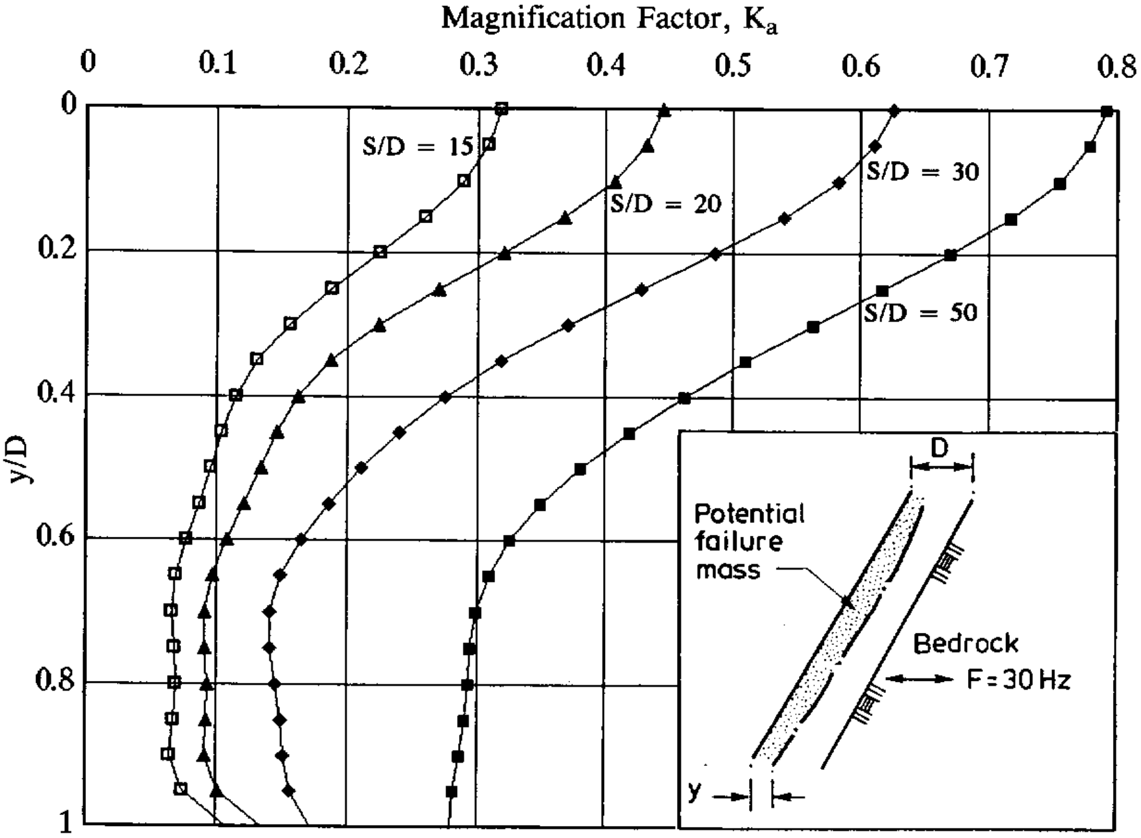

Figure 11 - K_a vs y/D for Inclined Soil Layer Based on One-dimensional Compression-rarefaction Response Model

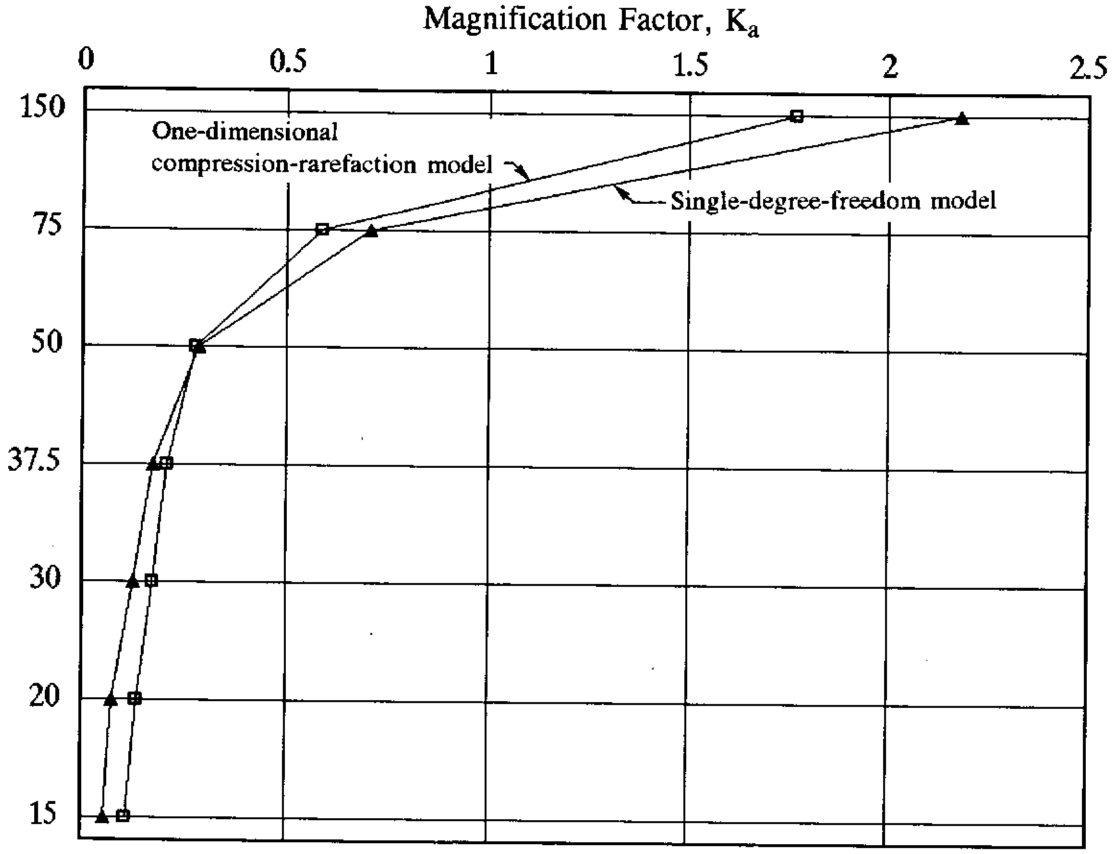

Figure 12 - Comparison of K_a Values from One-dimensional Compression-rarefaction Model and Single-degree-freedom Model for Inclined Soil Layer

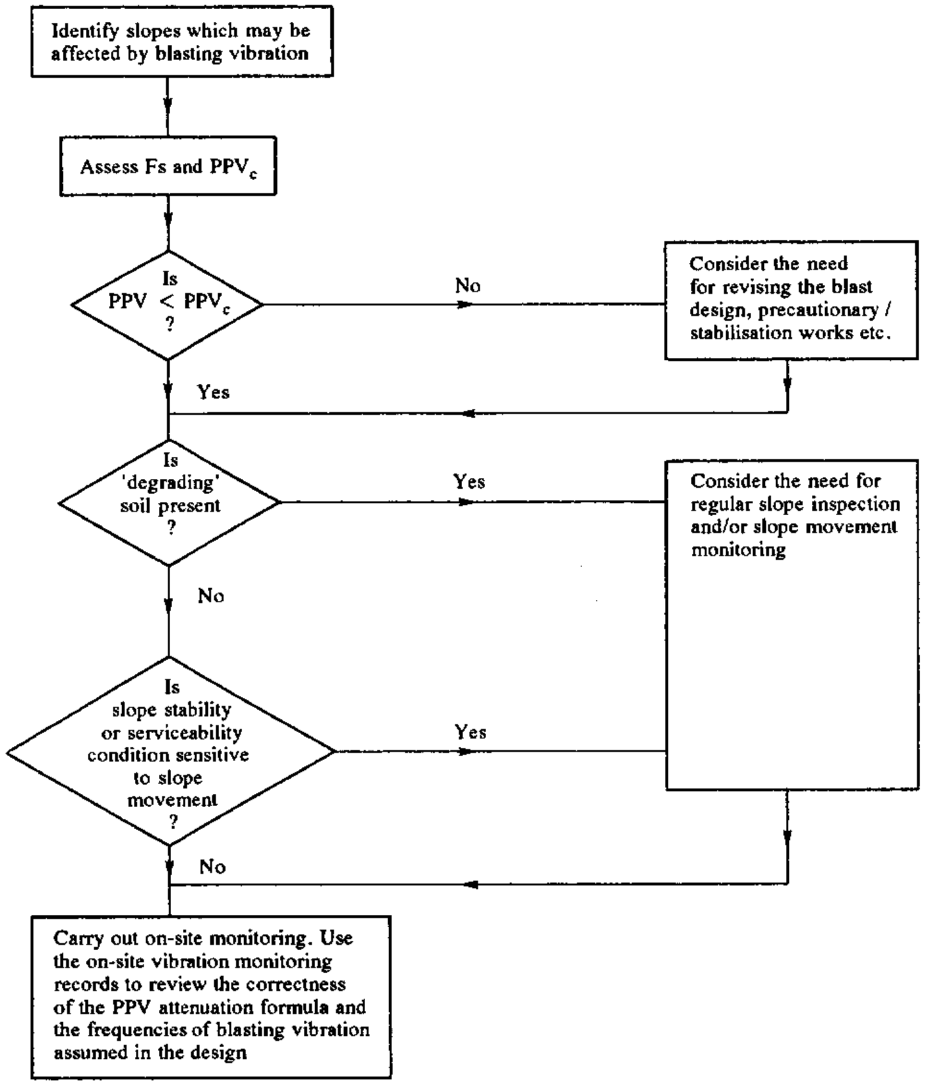
Identify slopes which may be affected by blasting vibration
Assess Fs and PPV$_c$
Is PPV < PPV$_c$?
No
Consider the need for revising the blast design, precautionary / stabilisation works etc.
Yes
Is 'degrading' soil present ?
Yes
Consider the need for regular slope inspection and/or slope movement monitoring
No
Is slope stability or serviceability condition sensitive to slope movement ?
Yes
No
Carry out on-site monitoring. Use the on-site vibration monitoring records to review the correctness of the PPV attenuation formula and the frequencies of blasting vibration assumed in the design

Legend :

F_s	Initial static factor of safety
PPV	Peak particle velocity at the bedrock underlying the slope
PPV$_c$	Critical peak particle velocity calculated from the pseudo-static method described in this report

Notes : (1) The above procedure is intended for application to sites where the consequence of soil slope instability induced by blasting vibration is of concern. Otherwise, less stringent requirements may be adopted.

(2) Near-field effects of blasting, such as the effects of delayed gas pressures, need to be considered separately.

Figure 13 - Application of the Pseudo-static Method to Blast Control

APPENDIX A

A BRIEF SUMMARY
OF THE METHOD OF
PSEUDO-STATIC ANALYSIS

1. APPROACHES OF PSEUDO-STATIC ANALYSIS

1.1 General

The method of pseudo-static analysis has been widely used for the assessment of the stability of slopes and retaining walls subjected to dynamic action. Ground vibrations are modelled as a pulse of uniform amplitude equal to or taken as a fraction of that of the peak pulse of the dynamic vibration, and hence could be represented by a constant pseudo-static inertia force (see equation 1). This force is incorporated in limit equilibrium analysis for assessing the dynamic stability.

Vibrations may induce excess pore water pressure in the ground. Depending on how the excess pore water pressure is accounted for, the pseudo-static method may be classified into three types: the Simple Pseudo-static Approach, the Modified Pseudo-static Approach and the Dynamic Parameter Approach.

1.2 Simple Pseudo-static Approach

This is the conventional pseudo-static approach in which drained shear strength parameters are adopted for routine methods of limit equilibrium analysis. Any excess pore water pressure generated by the ground vibration is not taken into account in the analysis.

This approach is suitable for analysing dry slopes or slopes that are free-draining with respect to the rate of the dynamic loading, e.g. slopes composed of coarse rock fill may be regarded as free-draining under seismic or blasting vibration. In these cases, zero or negligible excess pore water pressure is generated. Examples of use of this approach in analysing dynamic slope stability have been given in Bauer & Calder (1971), Kobayashi (1984) and Matasovic (1991).

The use of this approach for slopes comprising 'non-degrading' soils (i.e. soils in which no positive excess pore water pressure is generated under dynamic loading) will also give safe results. Further discussion on the classification of soils for the purpose of dynamic stability analysis is given in the next Section of this appendix.

It has been suggested by some authors that soil shear strength parameters c' and $\tan \phi'$ under dynamic (i.e. fast shear rate) condition may be higher than those under the static (i.e. normal shear rate) condition. Where necessary, the soil shear strength parameters corresponding to the appropriate shear rate can be incorporated in a simple pseudo-static analysis. There is however not sufficient data at present to justify the use of different shear strength parameters for the Hong Kong soils under dynamic (i.e. fast shear rate) loading.

This approach is simple to use. Solutions can be readily obtained by slightly modifying the conventional static limit equilibrium analyses to incorporate the pseudo-static inertia force. However, if significant dynamic excess pore water pressure is generated under the dynamic loading, the Simple Pseudo-static Approach will give entirely misleading results.

1.3 Modified Pseudo-static Approach

The shear rate of dynamic loading is usually so fast that soils which are saturated or near saturation will largely behave in an undrained manner. Hence, the undrained soil behaviour, i.e. the undrained strength, or the excess pore water pressure generated under the dynamic loading, should be considered in the pseudo-static stability analysis for slopes comprising such soils. This can be done by the Modified Pseudo-static Approach which is modified from the Simple Pseudo-static Approach by taking the undrained soil behaviour into consideration.

This approach is suitable for analysing slopes comprising 'degrading' soils in which positive excess pore water pressure is generated under seismic loading.

Either effective stress analysis or total stress analysis may be used:

(a) Total Stress Analysis

Undrained shear strength Su is adopted in the analysis. It should be noted that the value of Su is dependent on the initial stress state of the soil and the stress path applied. To model correctly the soil behaviour under the applied dynamic load, the appropriate stress state and stress path need to be used in laboratory testing for the determination of Su.

(b) Effective Stress Analysis

Drained shear strength parameters are adopted and the effective stresses along the slip surface are calculated by subtracting from the total stresses the relevant static pore water pressures and the excess pore water pressures generated under the dynamic loading.

The excess pore water pressure may be assessed using Skempton (1954) 's formula:

$$\Delta u = B \{ \Delta\sigma_3 + A (\Delta\sigma_1 - \Delta\sigma_3) \} \quad . . . (A1)$$

where: A, B = Skempton (1954)'s pore pressure parameters. B = 1 for saturated condition, and 0 for dry condition.
$\Delta\sigma_1$ = change in major principal stress
$\Delta\sigma_3$ = change in minor principle stress

A simple model to calculate $\Delta\sigma_1$ and $\Delta\sigma_3$, and hence the dynamic excess pore water pressure generated by the pseudo-static loading using equation (A1) has been proposed by Sarma (1975). In Sarma (1975), the term A in equation (A1) was called the dynamic pore pressure parameter to indicate that this is the A value corresponding to pseudo-static analysis.

In this appendix, the term A_f is used to denote the A value at failure induced by monotonic loading. The term A_n refers specifically to the dynamic pore pressure parameter in the rigorous sense described below.

Sarma (1979) and Sarma & Jennings (1980) proposed a method to determine the values of a 'rigorous' dynamic pore pressure coefficient (i.e. A_n) from cyclic soil tests results. Modified pseudo-static analysis using such A_n values is effectively a Dynamic Parameter Approach.

1.4 Dynamic Parameter Approach

In this approach, dynamic soil shear strength parameters are adopted in limit equilibrium stability analysis, e.g. Seed (1966) and Ishihara (1985). The dynamic soil shear strength parameters are determined from cyclic soil tests which resemble the actual time history of the dynamic loading.

At present, there is no data on the dynamic soil parameters nor is there any experience on laboratory cyclic shear testing in Hong Kong. The Dynamic Parameter Approach is hence not suitable for routine use in Hong Kong at this stage.

2. Effective Stress Analysis in Modified Pseudo-static Approach

2.1 A Model for Modified Pseudo-static Analysis

Sarma (1975) considered the undrained change of the stress states at a c′ = 0 sliding plane (at the base of a sliding block or one of the slices of a soil mass above a potential slip surface) from the initial to the failure condition brought by a pseudo-static loading. He adopted the form of Skempton (1954)'s formula (equation (A1)) and related the dynamic excess pore water pressure Δu with the pore pressure parameter A.

Closed form solutions were derived and charts showing the relationship among B, A, the input acceleration K and the dynamic factor of safety F_d were given in Sarma (1975). From these, the value of the critical acceleration K_c (corresponding to F_d = 1.0) can be determined using A (i.e. A_f or more rigorously A_n) to account for the effect of the dynamic excess pore water pressure.

By expanding Sarma's solution to cover the general c′- ϕ' condition, Wong (1991) obtained the following equations for a sliding plane. The relevant parameters are as defined in Figure A1.

From a consideration of force equilibrium:

$$F_d = \frac{[\cos\beta - K\sin(\beta-\theta) - (u_o)(a/W) - (\Delta u)(a/W)]\tan\phi' + (c')(a/W)}{\sin\beta + K\cos(\beta-\theta)} \quad . \; . \; (A2)$$

From a consideration of the geometry of Mohr circles:

$$\Delta u(a/W) = B\{ -K\sin(\beta-\theta) - \sin\beta[\tan\psi_o - (1-2A)\sec\psi_o] + [\sin\beta + K\cos(\beta-\theta)][\tan\psi_d - (1-2A)\sec\psi_d] \} \quad . \; . \; (A3)$$

The data shown in Figure 5 of this report was derived from equations (A2) and (A3). When the value of B is zero, equation (A2) gives solutions identical to those shown in Figure 4 for dry slopes. The inertia force has been assumed to be acting in the horizontal direction (i.e. θ = 0). As discussed by Wong (1991), for typical slopes in Hong Kong, horizontal inertia forces almost give the lowest value of K_c.

Such model has been incorporated in the computer program "EQS" developed by Sarma (1974) using Sarma (1973)'s method of limit equilibrium analysis. The program "EQS" is capable of performing modified pseudo-static analysis of the dynamic stability of slopes along general non-planar slip surfaces. This computer program is available in the GEO.

2.2 Threshold Pore Pressure Parameter

The threshold pore pressure parameter A_t is defined as the value of the pore pressure parameter A, above which positive dynamic excess pore water pressure is generated under the dynamic loading. Its physical meaning is illustrated in Figure A2, i.e. when A is equal to A_t, the effective stress path coincides with the total stress path and both the simple pseudo-static analysis and the modified pseudo-static analysis will give the same results.

The value of A_t for a single sliding block can be assessed by solving equations (A2) and (A3) adopting $F_d = 1.0$. By this, Wong (1991) has shown that over the typical range of values of c', tan ϕ', β etc. in Hong Kong, values of A_t lie in a small range between 0.2 to 0.3. This was also confirmed by the findings of the modified pseudo-static slope stability analyses of non-planar slip surfaces using the program "EQS" (Wong, 1992).

Based on these, the following simple classification is proposed. As shown in Figure A2:

(a) 'Non-degrading' Soil

If the calculated A_f (or more rigorously, A_n) value of a soil is less than the A_t value (i.e. 0.2 to 0.3), the soil may be classified as 'non-degrading'. There is no degradation of soil shear strength as compared with the free-draining condition (i.e. $\Delta u = 0$). For slopes comprising 'non-degrading' soils, a conservative estimate of the K_c (or F_d) value may be obtained by using the simple pseudo-static analysis.

(b) 'Degrading' Soil

On the contrary, if the calculated A_f (or more rigorously, A_n) value is larger than the A_t value, the soil is considered 'degrading'. The K_c (or F_d) value for a saturated slope comprising 'degrading' soils under dynamic loading may be drastically less than that corresponding to the dry or free-draining condition because of the generation of excess pore water pressure Δu.

It should also be noted that the total stress path of the pseudo-static loading follows the effective stress path corresponding to A_f of 0.2 to 0.3 (i.e. the A_t value). The total stress path of the conventional triaxial compression follows the effective stress path of $A_f = 0$, and is hence not far from the total stress path of the pseudo-static loading.

3. Determination of Pore Pressure Coefficient of Hong Kong Soils

The basis of the Modified Pseudo-static Approach using effective stress analysis and a method of classification of 'degrading' and 'non-degrading' soils have been briefly outlined above. It can be seen that the approach is able to model the undrained response of a slope to dynamic loading and is relatively simple to use. The pore pressure parameter (A_f or A_n) is the only 'unconventional' input parameter required.

The pore pressure parameter is not an intrinsic soil parameter. Instead, its value depends on the initial stress state of the soil element as well as its stress path to failure. Since the stress path of conventional triaxial compression is close to that of the pseudo-static loading, the values of A_f derived from conventional undrained triaxial tests may be taken as a reasonable approximation of the A_f values corresponding to the pseudo-static loading, provided that the soil test samples have been consolidated to the appropriate stress level. As undrained triaxial compression test is more or less a routine test for geotechnical investigation in Hong Kong, deriving the A_f values from the results of such test for use in modified pseudo-static analysis would require minimum additional site investigation and laboratory testing work.

An assessment of the results of conventional undrained triaxial compression tests on a number of Hong Kong soils has been carried out by Wong (1991). An example of the typical soil data is shown in Figures A3 (a) to (c). It was observed that while the effective stress failure envelope is usually reasonably well defined, the A_f values are widely scattered. However, when the values of A_f corresponding to the correct stress level (in this case, the initial isotropic consolidation pressure equals the field vertical effective stress) are considered, the scatter is significantly reduced. This shows the effects of stress level on the soil dilatancy/undrained behaviour.

A summary the soil data studied by Wong (1991) is given in Table A1. Safe estimates of the A_f values of the soils at the appropriate stress level have been taken as the design A_f values. The medium dense to dense saprolites examined are found to be 'non-degrading', whereas the loose colluvium and residual soil studied are 'degrading' for the typical slope problems considered. In view of the variability of soils derived from insitu rock weathering in Hong Kong, it is recommended that site-specific data should be studied in order to determine whether a soil will likely exhibit 'degrading' behaviour or not when the slope is subjected to the dynamic loading.

Since there is currently no data on the dynamic properties of Hong Kong soils, the approach of Sarma (1979) and Sarma & Jennings (1980) of assessing the "rigorous" A_n values for used in modified pseudo-static analysis cannot be applied.

4. Discussion

In theory, the "rigorous" A_n values would model more closely the soil behaviour under time-history dynamic loading. Their use in soil classification and in the modified pseudo-static analysis (which gives virtually the same results as using the Dynamic Parameter Approach) is preferred. This is however not practical until reliable data on the A_n values of Hong Kong soils is available.

The use of A_f values in soil classification and in the modified pseudo-static analysis, though consistent with the pseudo-static assumption, should be considered as an approximation.

The A_f values are diagnostic of the soil behaviour under the dynamic loading. Using A_f for the purpose of classifying whether a soil in Hong Kong is 'degrading' or not is considered acceptable in view that:

(a) The A_f value of a soil reflects its behaviour in undrained monotonic loading and denotes whether the soil is dense or loose. A soil with A_f less than 0.2 (i.e. A_t) is rather dense (note that for an elastic isotropic material, A_f under triaxial compression is 0.33), it is reasonable that significant amount of positive excess pore water pressure would not be generated in such a dense soil in cyclic loading of, say within 30 cycles.

(b) Soils in Hong Kong such as saprolites normally have a fair amount of fines content (10% or more is not uncommon). The presence of fines would make the soil less vulnerable to generation of excess pore water pressure during cycle loading (see e.g., Ishihara, 1985).

(c) Wong (1991) has shown from analytic results using equations (A2) and (A3) that for A_f within $A_t \pm 0.2$, the excess pore water pressure generation is not significant. Hence, some inaccuracies in the determination of the value of the dynamic pore pressure parameter is tolerable.

It is therefore proposed that A_f may be used for soil classification for routine dynamic stability analysis. If the A_f value of a soil is less than about 0.2, the soil may be considered as 'non-degrading' and the Simple Pseudo-static Approach may be adopted. It is probable that majority of the Hong Kong soils would belong to this category.

In case a soil is found to be 'degrading' from the above method of soil classification and if the slope concerned may be at a state of high degree of saturation during the dynamic loading, using A_f in modified pseudo-static analysis can give indicative results of the dynamic slope stability. Such results should be regarded as approximations as the possible difference between the values of A_f and A_n of Hong Kong soils are yet to be calibrated. Before such calibration or other advanced approaches of dynamic stability analysis using dynamic soil parameters and sophisticated computer programs are at hand, the Modified Pseudo-static Approach using conservative A_f values estimated from triaxial compression tests results appears to be a practical though not rigorous method for assessing the dynamic stability of slopes comprising' degrading' soils. Where necessary, such assessment should be backed up by on-site monitoring during blasting to verify that the actual slope performance.

LIST OF TABLES

Table No.		Page No.
A1	Summary of Soil Data	72

Table A1 - Summary of Soil Data

Site Location	Soil Type	SPT N Value	Dry Density (kg/m^3)	A_n
Nim Wan	CDG	< 50	1.3 - 1.7	0.2
	C/HDG	> 50	1.6 - 1.9	0.1
Blue Pool Road	CDG	< 50	1.3 - 1.6	0.2
	C/HDG	> 50	1.5 - 1.7	0.15
Blue Pool Road & Ventris Road	RS	< 10	1.45 - 1.65	0.4
Au Tau	CDV	< 50	1.6 - 1.85	0.1
	C/HDV	> 50	1.7 - 2.0	0.1
Tai Hang Road	Coll	< 25	1.6 - 1.65	0.4
		> 25	1.7 - 1.9	0.1

Legend :

CDG	Completely decomposed granite
C/HDG	Completely to highly decomposed granite
CDV	Completely decomposed volcanics
C/HDV	Completely to highly decomposed volcanics
RS	Residual soil
Coll	Colluvium

LIST OF FIGURES

Figure No.		Page No.
A1	Stress States	74
A2	Stress Paths and Soil Classification	75
A3	Example of Soil Data (Decomposed Granite from Nim Wan, Hong Kong)	76

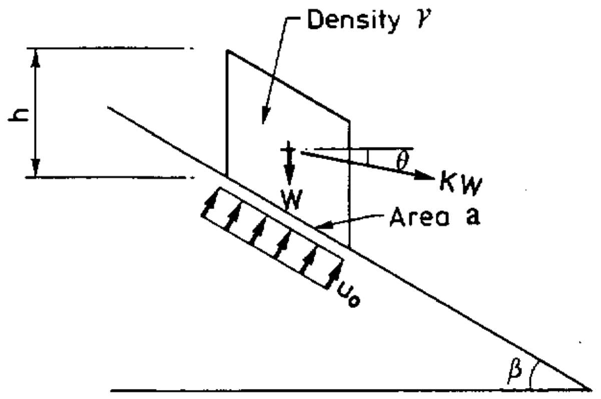
Density γ
h
W
θ
KW
Area a
u₀
β

(a) Sliding Block

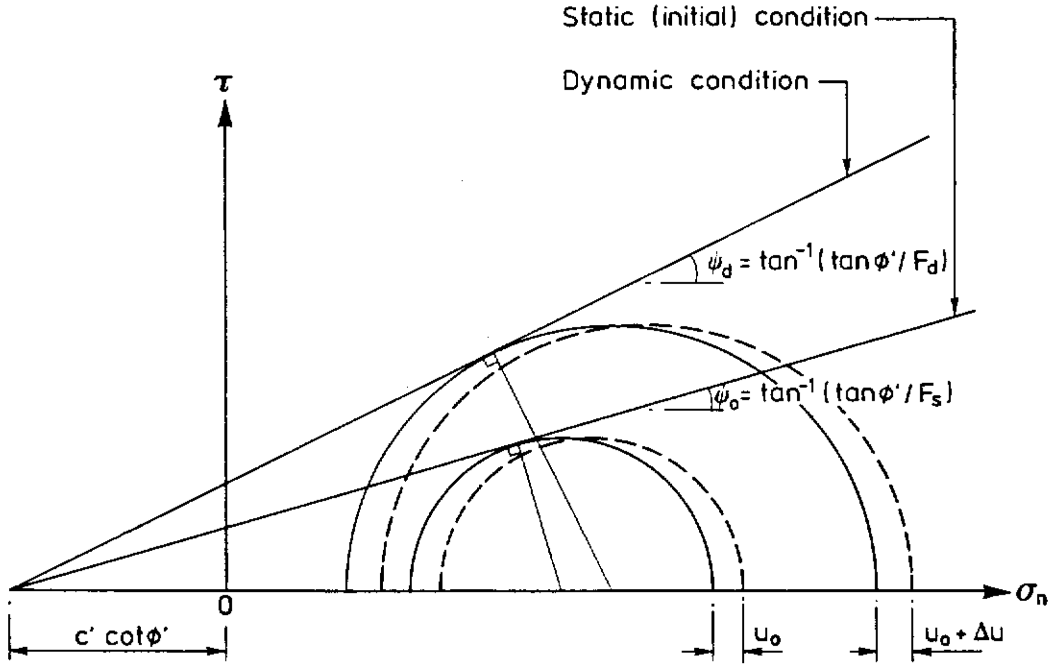
Static (initial) condition
Dynamic condition
τ
ψd = tan⁻¹ (tanφ'/ Fd)
ψo = tan⁻¹ (tanφ'/ Fs)
0
σn
c' cotφ'
u₀
u₀ + Δu

(b) Mohr Circle of Stresses

Legend :

β	Inclination of failure plane	c'	Effective cohesion
θ	Downward inclination of inertia force	ϕ'	Effective angle of shearing resistance
a	Base area of the element	F_d	Dynamic factor of safety
γ	Density	F_s	Static factor of safety
u_o	Initial pore water pressure	———	Effective stress Mohr circle
W	Weight of element	– – – –	Total stress Mohr circle
K	Acceleration coefficient (g)		

Figure A1 - Stress States

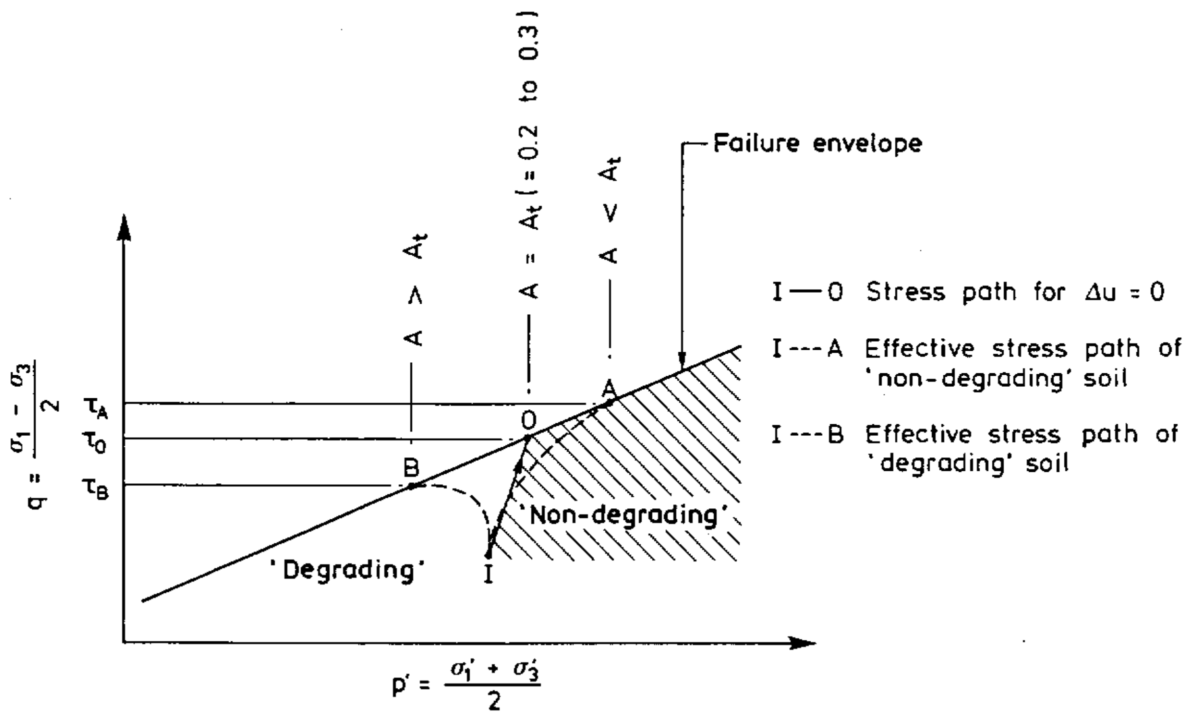
A > A_t
A = A_t (= 0.2 to 0.3)
A < A_t
Failure envelope
I — O Stress path for Δu = 0
I --- A Effective stress path of 'non-degrading' soil
I --- B Effective stress path of 'degrading' soil
q = (σ1 - σ3)/2
τA
τO
τB
A
O
B
I
'Non-degrading'
'Degrading'
p' = (σ1' + σ3')/2

(a) Schematic Diagram Showing Stress Paths of 'Non-degrading' and 'degrading' Soils

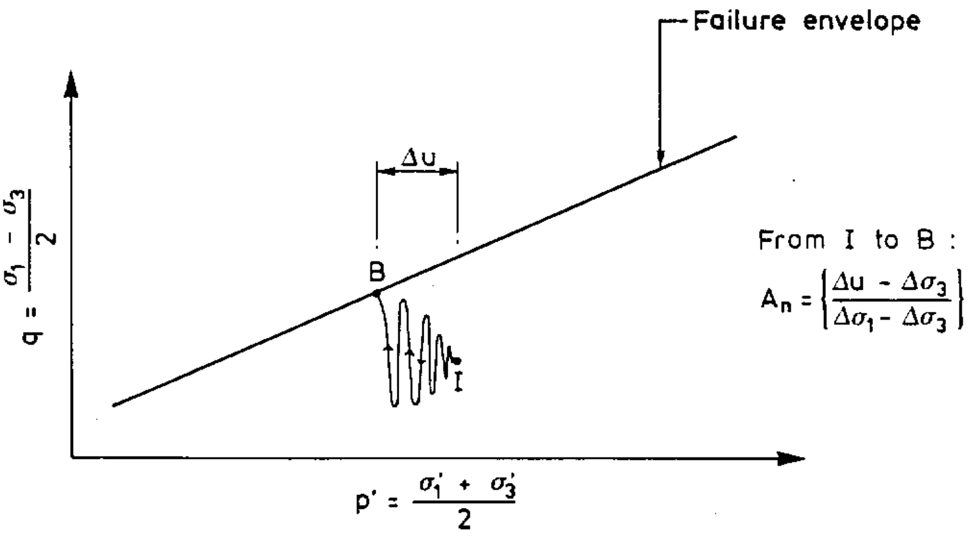
Failure envelope
Δu
B
I
q = (σ1 - σ3)/2
p' = (σ1' + σ3')/2
From I to B :
A_n = {(Δu - Δσ3)/(Δσ1 - Δσ3)}

(b) Stress Path IB under Dynamic Load

Figure A2 - Stress Paths and Soil Classification

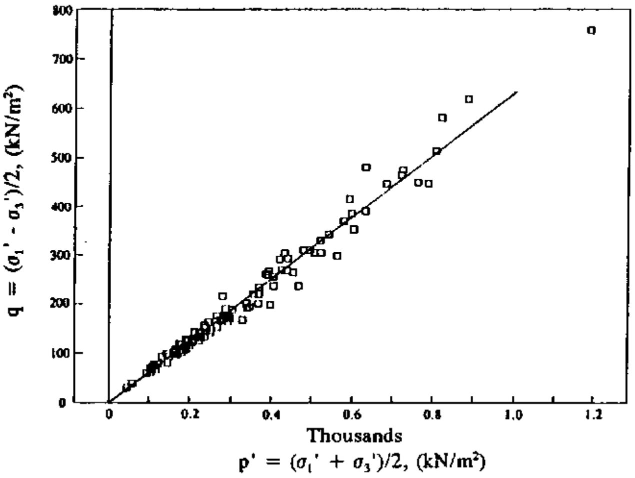

(a) p' vs q

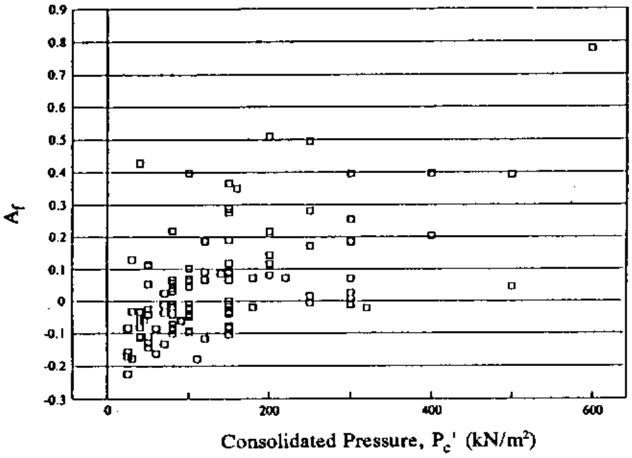

(b) A_f vs P'_c

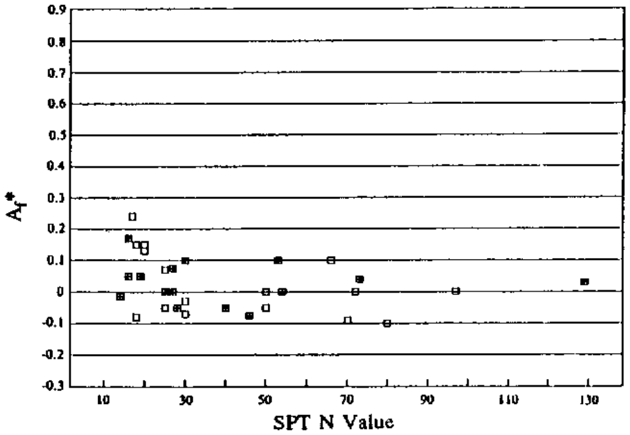

(c) A_f^* vs N

Note : A_f^* = interpolated value of A_f corresponding to P'_c equal to the field vertical stress

Figure A3 - Example of Soil Data (Decomposed Granite from Nim Wan, Hong Kong)

APPENDIX B

THE MAGNIFICATION FACTOR FOR A SINGLE-DEGREE-FREEDOM DAMPED FORCED VIBRATION SYSTEM

1. The equation of motion of a single-degree-freedom system as shown in Figure B1 under damped forced vibration is :

$$\ddot{u} + 2\lambda\omega_o\dot{u} + \omega_o^2 u = -\ddot{x}(t) \qquad \text{.................. (B1)}$$

where $\omega_o = \sqrt{\dfrac{k}{m}}$

2. The solution to equation (B1) is in the form :

$$u = u_{TR} + u_{SS} \qquad \text{.................. (B2)}$$

where u_{TR} = transient solution (i.e. tends to zero as t increases)

$= e^{-\lambda\omega_o t}\,[A \sin \omega_d t + B \cos \omega_d t]$

$\omega_d = \omega_o \sqrt{1-\lambda^2}$

A, B = constants which depend on initial conditions

u_{SS} = steady state solution

3. Consider a simple harmonic input motion $\ddot{x}(t) = p \sin(\omega t + \Theta)$. As given in Newmark & Rosenblueth (1971),

$$u \approx u_{SS}$$

$$= \frac{p}{\omega_o^2}\left|\frac{1}{\sqrt{(1-\alpha^2)^2 + 4\lambda^2\alpha^2}}\right| \sin(\omega t - \Theta_1) \qquad \text{...... (B3)}$$

where Θ, Θ_1 = phase shifts

$$\alpha = \frac{\text{Forcing (i.e. input motion) Frequency}}{\text{Natural Frequency of Vibrating System}} = \frac{\omega}{\omega_o}$$

4. The absolute acceleration $\ddot{u}_{ABS}$ is given by :

$$\ddot{u}_{ABS} = \ddot{u} + \ddot{x}(t)$$

$$= -2\lambda\omega_o\dot{u} - \omega_o^2 u$$

Substitute equation (B3) :

$$\ddot{u}_{ABS} = \frac{-p}{\omega_o^2}\left|\frac{1}{\sqrt{(1-\alpha^2)^2 + 4\lambda^2\alpha^2}}\right| \left|2\lambda\omega_o\omega \cos(\omega t-\Theta_1) + \omega_o^2 \sin(\omega t-\Theta_1)\right|$$

$$= - p \left[\frac{\sqrt{1 + 4\lambda^2\alpha^2}}{\sqrt{(1-\alpha^2)^2 + 4\lambda^2\alpha^2}} \right] \left| \sin (\omega t - \Theta_2) \right| \quad \dots\dots\dots \text{(B4)}$$

where Θ_2 = phase shift

5. Hence,

$$|\ddot{u}_{ABS}|_{max} = p \left| \sqrt{\frac{1 + 4\lambda^2\alpha^2}{(1-\alpha^2)^2 + 4\lambda^2\alpha^2}} \right|$$

$\Longrightarrow$ Magnification factor $K_a = \frac{|\ddot{u}_{ABS}|_{max}}{|\ddot{x}(t)|_{max}}$

$$= \sqrt{\frac{1 + 4\lambda^2\alpha^2}{(1-\alpha^2)^2 + 4\lambda^2\alpha^2}} \quad \dots\dots\dots\dots\dots \text{(B5)}$$

LIST OF FIGURES

Figure No.		Page No.
B1	Single-degree-freedom Model under Damped Force Vibration	81

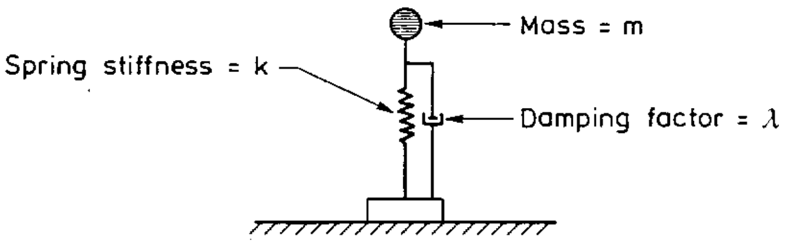
Mass = m
Spring stiffness = k
Damping factor = λ

(a) Initial Condition at time = 0

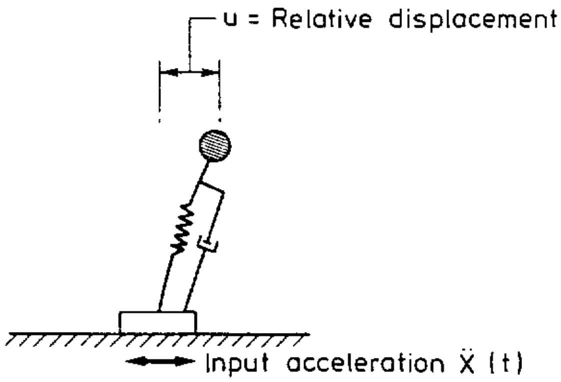
u = Relative displacement
Input acceleration $\ddot{X}(t)$

(b) During Vibration at time = t (no sliding)

Figure B1 - Single-degree-freedom Model under Damped Forced Vibration

APPENDIX C

ONE-DIMENSIONAL SHEAR RESPONSE ANALYSIS FOR SLOPES WITH HORIZONTAL BEDROCK

1. As shown by Ambraseys (1960) and Ambraseys & Sarma (1967), the solution of an untruncated wedge (Figure C1(a) & (b)) under one-dimensional shear response vibration in the horizontal direction is given by :

$$\ddot{u}(x, t) = \sum_{n=1}^{\infty} \phi_n(y/H)\, S_{dn}(t) \qquad \text{..............} \quad \text{(C1)}$$

where $\ddot{u}(x, t)$ = the absolute response acceleration at level y

$\phi_n(y/H)$ = the nth mode shape at level y

$$= \frac{2\, J_o(a_n y/H)}{a_n\, J_1(a_n)}$$

$S_{dn}(t)$ = Duhamel Integral

a_n = the nth root of the formula $J_o(a_n) = o$

J_o = Bessel function of the first kind, zero order

J_1 = Bessel function of the first kind, first order

Values of J_o and J_1 are shown in Table C1.

2. An approximate solution to equation (C1) is given by :

(a) For a point at $y = y_1$ (Figure C1(c))

$$|\ddot{u}|_{max} = \sqrt{\sum_{1}^{4} [\phi_n(y_1/H)]^2\, [S_a * PPA]^2} \qquad \text{...............} \quad \text{(C2)}$$

where PPA = peak acceleration of input bedrock motion

S_a = Maximum acceleration response factor corresponding to the mode of vibration concerned

(b) For a mass from $y = 0$ to $y = y_1$ (Figure C1(d))

$$|\bar{\ddot{u}}|_{max} = \sqrt{\sum_{1}^{4} [K_n(y_1/H)]^2\, [S_a * PPA]^2} \qquad \text{.............} \quad \text{(C3)}$$

$$\text{where } K_n(y_1/H) = \frac{\int_0^{y_1} \phi_n(y/H)\, dW}{\int_0^{y_1} dW}, \quad \text{for n = 1, 2 and 3} \qquad \text{..........} \quad \text{(C4)}$$

$$K_4(y_1/H) = 1 - K_1(y_1/H) - K_2(y_1/H) - K_3(y_1/H) \qquad \text{.............} \quad \text{(C5)}$$

$\bar{\ddot{u}}$ = the net absolute response acceleration for the mass

3. By definition, the magnification factor K_a for a given potential failure mass is given by :

$$K_a = \frac{\text{max. of the net response acceleration at the mass}}{\text{max. of input acceleration at bedrock}}$$

$$= \frac{|\ddot{u}|_{max}}{PPA}$$

$$\Rightarrow \quad K_a(y_1/H) = \sqrt{\sum_{1}^{4} [K_n(y_1/H)]^2 \, [S_a]^2} \qquad \ldots\ldots\ldots\ldots\ldots \text{(C6)}$$

4. To solve equation (C4) and hence equations (C5) and (C6), the following 2 types of geometry of the potential failure mass are considered :

   (a) Slip Surface with Uniform Soil thickness (Uniform Slip)

   Referring to Figure C1(e), dw = ρ b dy (where ρ = density of soil). Hence, for n = 1, 2 and 3 :

$$K_n(y_1/H) = \frac{\int_0^{y_1} \phi_n(y/H)\, \rho\, b\, dy}{\int_0^{y_1} \rho\, b\, dy}$$

$$= \frac{\int_0^{y_1} \phi_n(y/H)\, dy}{y_1} \qquad \ldots\ldots\ldots\ldots \text{(C7)}$$

   (b) Slip Surface with Wedge-Shaped Soil Mass (Wedge Slip)

   Referring to Figure C1(f), dw = ρ c y dy. Hence, for n = 1, 2 and 3 :

$$K_n(y_1/H) = \frac{\int_0^{y_1} \phi_n(y/H)\, \rho\, c\, y\, dy}{\int_0^{y_1} \rho\, c\, y\, dy}$$

$$= \frac{\int_0^{y_1} \phi_n(y/H)\, y\, dy}{(y_1^2/2)} \qquad \ldots\ldots\ldots\ldots\ldots \text{(C8)}$$

5. Values of $\phi_n(y/H)$ are solved using J_o and J_1 (from Table C1), and plotted in Figure C2.

   Using values of $\phi_n(y/H)$, equations (C7) and (C8) are solved by numerical integration. The calculated values of $K_n(y_1/H)$ are plotted in Figures C3 and C4.

6. Assuming the input bedrock motion as a simple harmonic motion of infinite duration with, say frequency = 30 Hz.

S_a = the magnification factor as given in Appendix B for a single-degree-freedom system of period T_n

$$= \sqrt{\frac{1 + 4\lambda^2\alpha^2}{(1-\alpha^2)^2 + 4\lambda^2\alpha^2}} \quad \text{.............. (C9)}$$

where λ = damping factor

= 0.2 for the first mode of vibration, and

= 0.5 for the 2nd, 3rd and 4th modes of vibration

$$\alpha = \frac{\text{Forcing frequency}}{\text{Slope frequency}} = 30\ T_n$$

T_n = Period of slope corresponding to the nth mode of vibration as given in Table C2

Values of S_a for S/H = 50, 30, 20 and 15 are shown in Table C2.

7. Using values of $K_n(y_1/H)$ obtained from equations (C7) and (C8) and the calculated values of S_a, values of $K_a(y/H)$ can be calculated from equation (C6).

The calculated $K_a(y/H)$ values for S/H = 50, 30, 20 and 15 are shown in Table C3 and plotted in Figures C5(a) to (d).

The mean values of $K_a(y/H)$ of the 'Uniform Slip' and the 'Wedge Slip' cases as shown in Figure 7 may be adopted in routine design.

LIST OF TABLES

Table No.		Page No.
C1	Bessel Function of the First Kind	87
C2	T_n and S_a for One-dimensional Shear Response Analysis for Slope with Horizontal Bedrock	88
C3	K_a from One-dimensional Shear Response Analysis for Slope with Horizontal Bedrock	89

Table C1 - Bessel Function of the First Kind

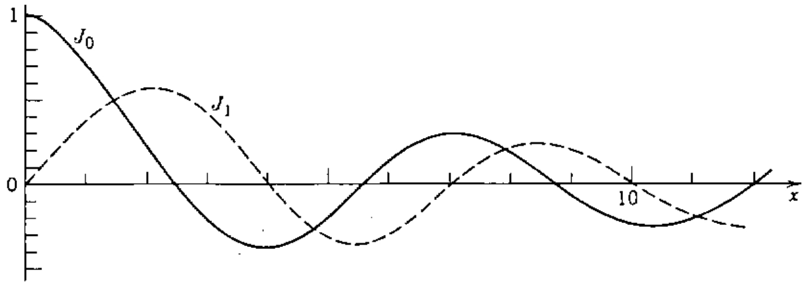

Bessel function J_o and J_1

x	$J_o(x)$	$J_1(x)$	x	$J_o(x)$	$J_1(x)$	x	$J_o(x)$	$J_1(x)$
0.0	1.0000	0.0000	3.0	−0.2601	0.3991	6.0	0.1506	−0.2767
0.1	0.9975	0.0499	3.1	−0.2921	0.3009	6.1	0.1773	−0.2559
0.2	0.9900	0.0995	3.2	−0.3202	0.2613	6.2	0.2017	−0.2329
0.3	0.9776	0.1483	3.3	−0.3443	0.2207	6.3	0.2238	−0.2081
0.4	0.9604	0.1960	3.4	−0.3643	0.1792	6.4	0.2433	−0.1816
0.5	0.9385	0.2423	3.5	−0.3801	0.1374	6.5	0.2601	−0.1538
0.6	0.9120	0.2867	3.6	−0.3918	0.0955	6.6	0.2740	−0.1250
0.7	0.8812	0.3290	3.7	−0.3992	0.0538	6.7	0.2851	−0.0953
0.8	0.8463	0.3688	3.8	−0.4026	0.0128	6.8	0.2931	−0.0652
0.9	0.8075	0.4059	3.9	−0.4018	−0.0272	6.9	0.2981	−0.0349
1.0	0.7652	0.4401	4.0	−0.3971	−0.0660	7.0	0.3001	−0.0047
1.1	0.7196	0.4709	4.1	−0.3887	−0.1033	7.1	0.2991	0.0252
1.2	0.6711	0.4983	4.2	−0.3766	−0.1386	7.2	0.2951	0.0543
1.3	0.6201	0.5220	4.3	−0.3610	−0.1719	7.3	0.2882	0.0826
1.4	0.5669	0.5419	4.4	−0.3423	−0.2028	7.4	0.2786	0.1096
1.5	0.5118	0.5579	4.5	−0.3205	−0.2311	7.5	0.2663	0.1352
1.6	0.4554	0.5699	4.6	−0.2961	−0.2566	7.6	0.2516	0.1592
1.7	0.3980	0.5778	4.7	−0.2693	−0.2791	7.7	0.2346	0.1813
1.8	0.3400	0.5815	4.8	−0.2404	−0.2985	7.8	0.2154	0.2014
1.9	0.2818	0.5812	4.9	−0.2097	−0.3147	7.9	0.1944	0.2192
2.0	0.2239	0.5767	5.0	−0.1776	−0.3276	8.0	0.1717	0.2346
2.1	0.1666	0.5683	5.1	−0.1443	−0.3371	8.1	0.1475	0.2476
2.2	0.1104	0.5560	5.2	−0.1103	−0.3432	8.2	0.1222	0.2580
2.3	0.0555	0.5399	5.3	−0.0758	−0.3460	8.3	0.0960	0.2657
2.4	0.0025	0.5202	5.4	−0.0412	−0.3453	8.4	0.0692	0.2708
2.5	−0.0484	0.4971	5.5	−0.0068	−0.3414	8.5	0.0419	0.2731
2.6	−0.0968	0.4708	5.6	0.0270	−0.3343	8.6	0.0146	0.2728
2.7	−0.1424	0.4416	5.7	0.0599	−0.3241	8.7	−0.0125	0.2697
2.8	−0.1850	0.4097	5.8	0.0917	−0.3110	8.8	−0.0392	0.2641
2.9	−0.2243	0.3754	5.9	0.1220	−0.2951	8.9	−0.0653	0.2559

$J_0(x) = 0$ for $x = 2.405, 5.520, 8.654, 11.792, 14.931, \cdots$
$J_1(x) = 0$ for $x = 0, 3.832, 7.016, 10.173, 13.324, \cdots$

Table C2 - T_n and S_a for One-dimensional Shear Response Analysis for Slope with Horizontal Bedrock

Mode No. n	1	2	3	4
T_n for layer (* H/S)	4	4/3	4/5	4/7
T_n for Dam (*H/S)	2.61	$2.61a_1/a_2$	$2.61a_2/a_3$	$2.61a_3/a_4$
T_n (Mean) for Slope (*H/S)	3.300	1.2350	0.7627	0.5519

(a) Period of n^th Mode of Vibration, T_n

S/H	S_a			
	n = 1 λ = 0.2	n = 2 λ = 0.5	n = 3 λ = 0.5	n = 4 λ = 0.5
150	1.6599	1.0609	1.0233	1.0122
75	1.2413	1.2351	1.0926	1.0487
50	0.4216	1.4349	1.2039	1.1089
37.5	0.2399	1.4224	1.3382	1.1905
30	0.1660	1.1841	1.4458	1.2865
20	0.0940	0.6886	1.2823	1.4658
15	0.0662	0.4702	0.9022	1.3237

(b) Maximum Acceleration Response Factor, S_a (for F = 30 Hz)

Table C3 - K_a from One-dimensional Shear Response Analysis for Slope with Horizontal Bedrock

y/H	Magnification Factor, K_a			
	S/H = 50	S/H = 30	S/H = 20	S/H = 15
0.00	2.0083	1.8528	1.4423	1.0580
0.05	1.9678	1.8048	1.3968	1.0226
0.10	1.9043	1.7297	1.3255	0.9673
0.15	1.8053	1.6128	1.2152	0.8821
0.20	1.6795	1.4651	1.0769	0.7757
0.25	1.5371	1.3000	0.9246	0.6596
0.30	1.3888	1.1314	0.7733	0.5457
0.35	1.2437	0.9716	0.6369	0.4454
0.40	1.1081	0.8291	0.5255	0.3663
0.45	0.9854	0.7068	0.4414	0.3089
0.50	0.8764	0.6032	0.3783	0.2661
0.55	0.7812	0.5142	0.3264	0.2299
0.60	0.7001	0.4373	0.2807	0.1972
0.65	0.6340	0.3740	0.2423	0.1707
0.70	0.5833	0.3288	0.2163	0.1557
0.75	0.5462	0.3034	0.2047	0.1520
0.80	0.5178	0.2913	0.2004	0.1506
0.85	0.4927	0.2825	0.1935	0.1429
0.90	0.4676	0.2724	0.1833	0.1304
0.95	0.4438	0.2660	0.1849	0.1331
1.00	0.4279	0.2763	0.2175	0.1691

LIST OF FIGURES

Figure No.		Page No.
C1	One-dimensional Shear Response Model for Slope with Horizontal Bedrock	91
C2	Mode Shapes from One-dimensional Shear Response Analysis	92
C3	K_n for 'Uniform Slip'	93
C4	K_n for 'Wedge Slip'	94
C5	Magnification Factor K_a from One-dimensional Shear Response Analysis for Slope with Horizontal Bedrock	95

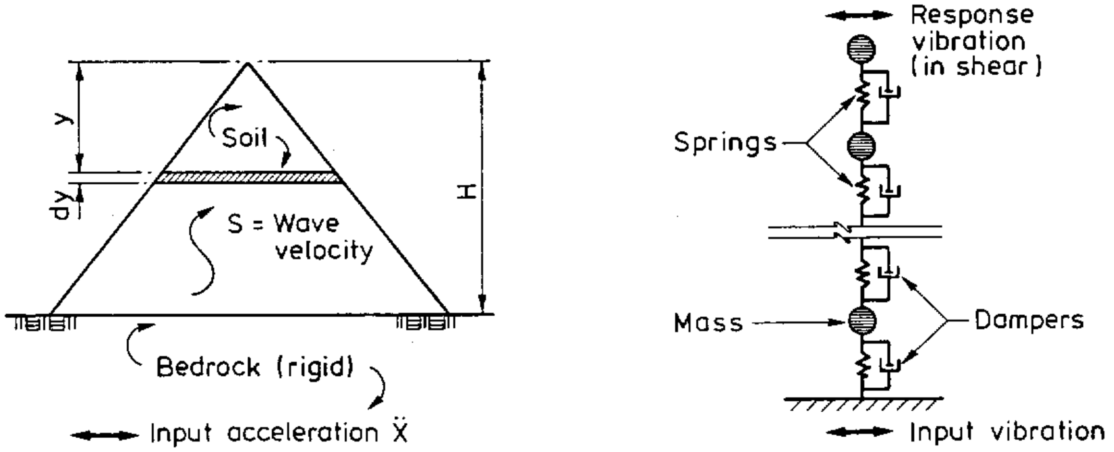
y
dy
Soil
S = Wave velocity
H
Bedrock (rigid)
Input acceleration Ẍ
Response vibration (in shear)
Springs
Mass
Dampers
Input vibration

(a) Untruncated Wedge Subjected to One-dimensional Shear Vibration

(b) Multi-degree-freedom Model

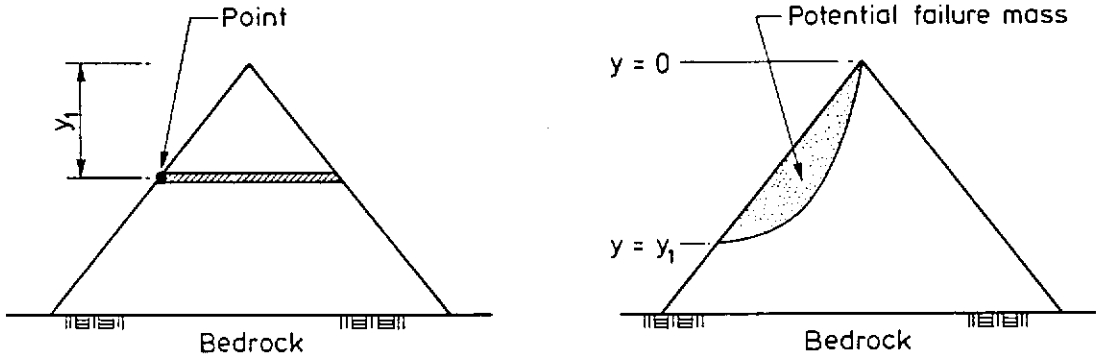
Point
y_1
Bedrock
Potential failure mass
y = 0
$y = y_1$
Bedrock

(c) A point at $y = y_1$

(d) Soil Mass Bounded by Potential Slip Surface from $y = 0$ to $y = y_1$

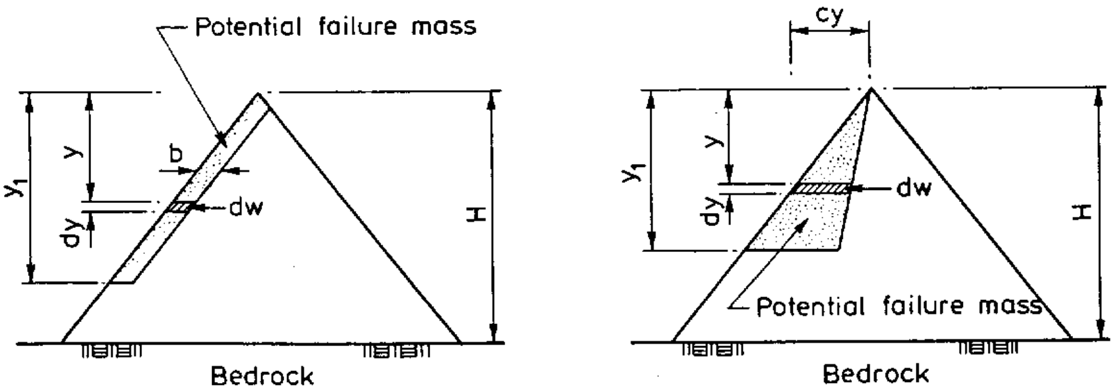
Potential failure mass
y_1
y
b
dy
dw
H
Bedrock
cy
y_1
y
dy
dw
H
Potential failure mass
Bedrock

(e) Geometry of Uniform Slip

(f) Geometry of Wedge Slip

Figure C1 - One-dimensional Shear Response Model for Slopes with Horizontal Bedrock

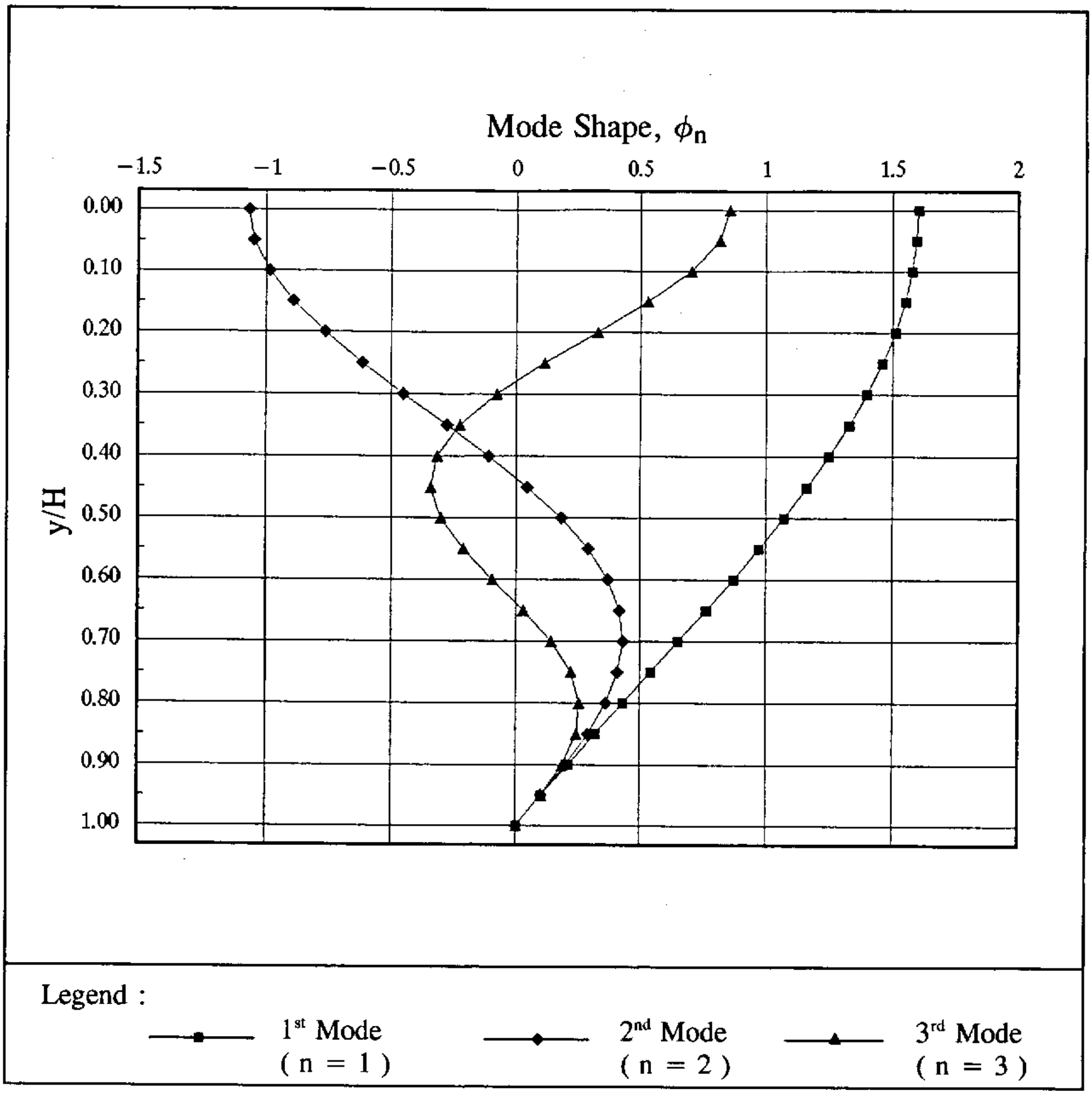

Figure C2 - Mode Shapes from One-dimensional Shear Response Analysis

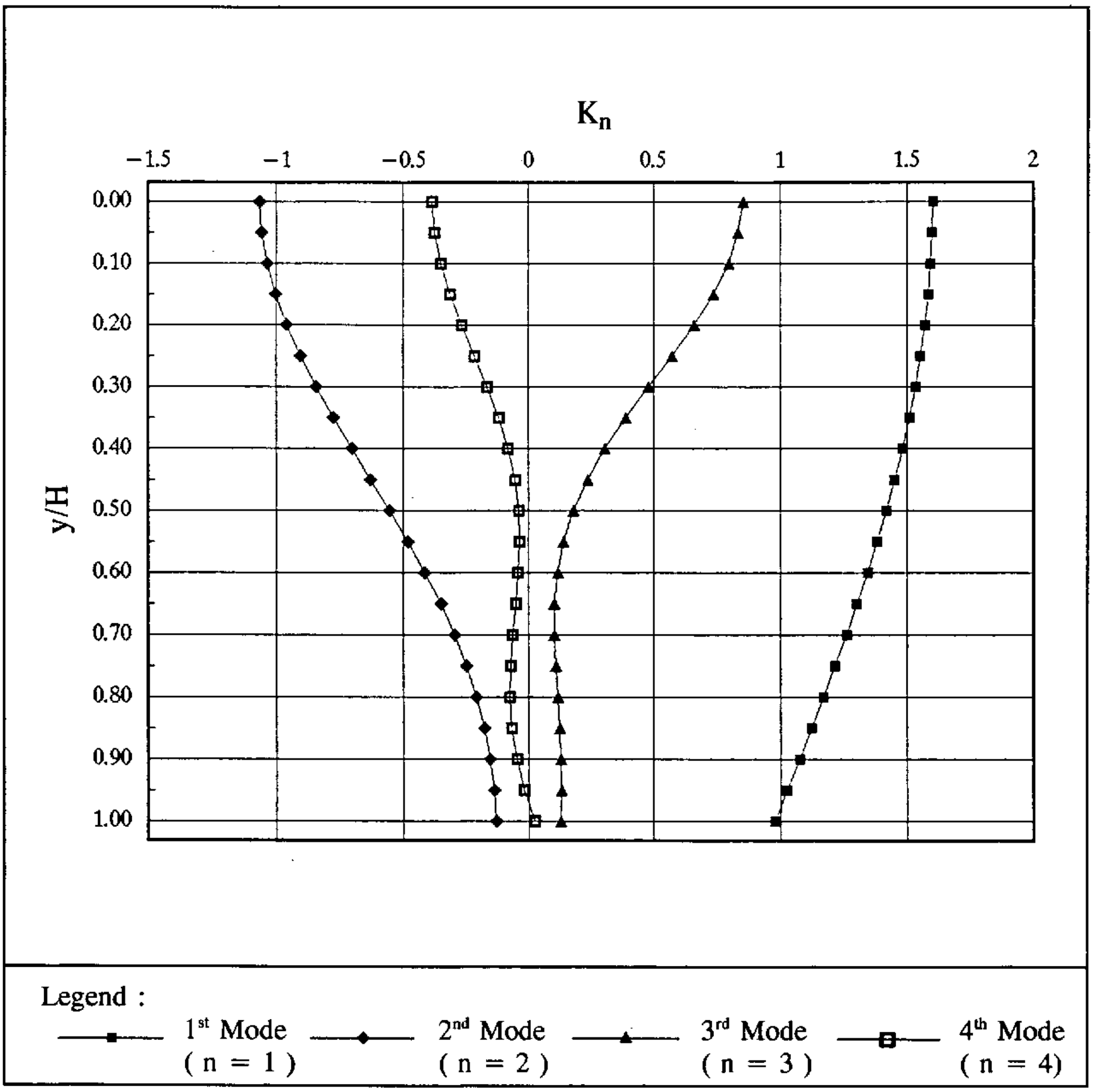

Figure C3 - K_n for 'Uniform Slip'

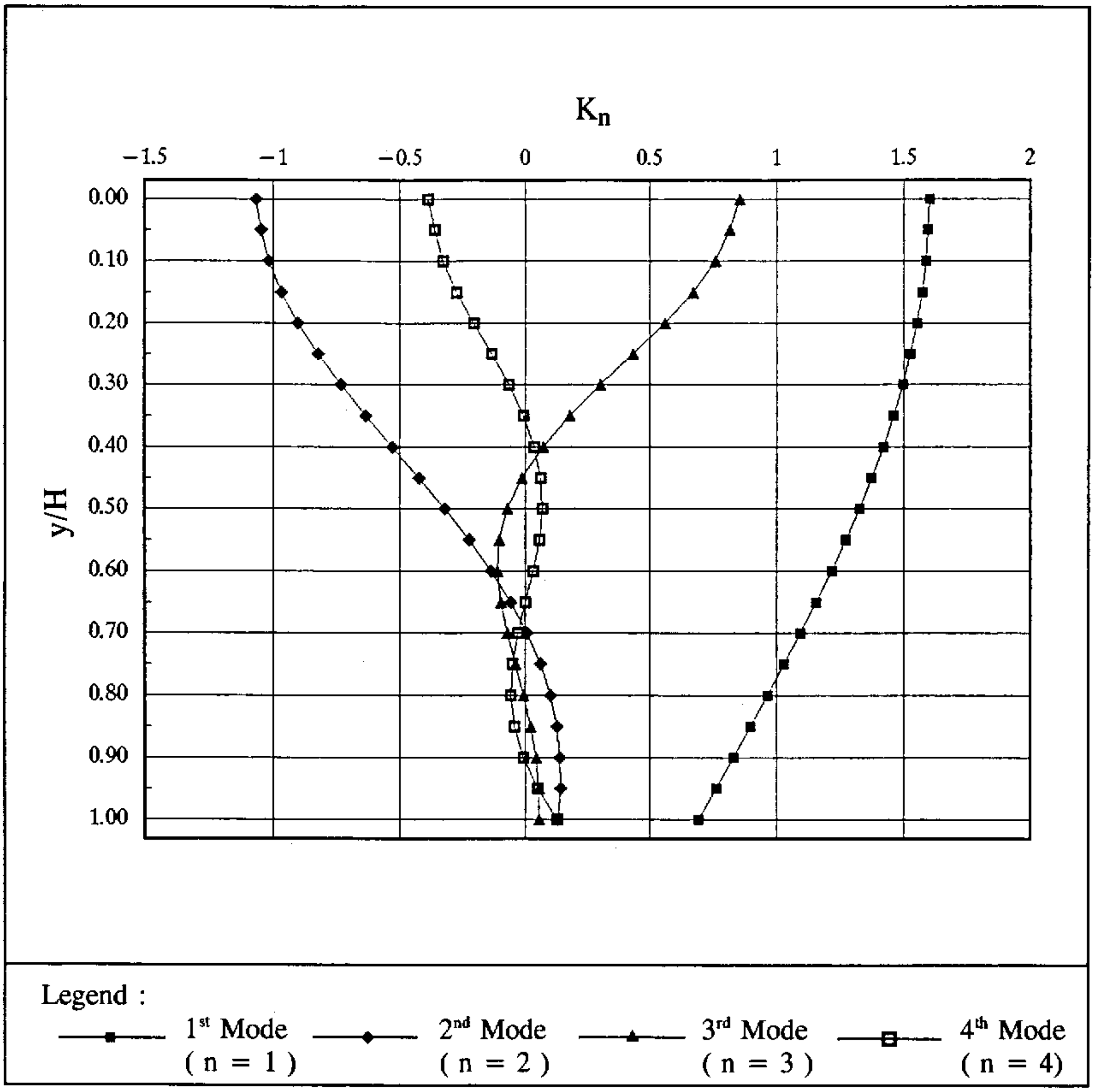

Figure C4 - K_n for 'Wedge Slip'

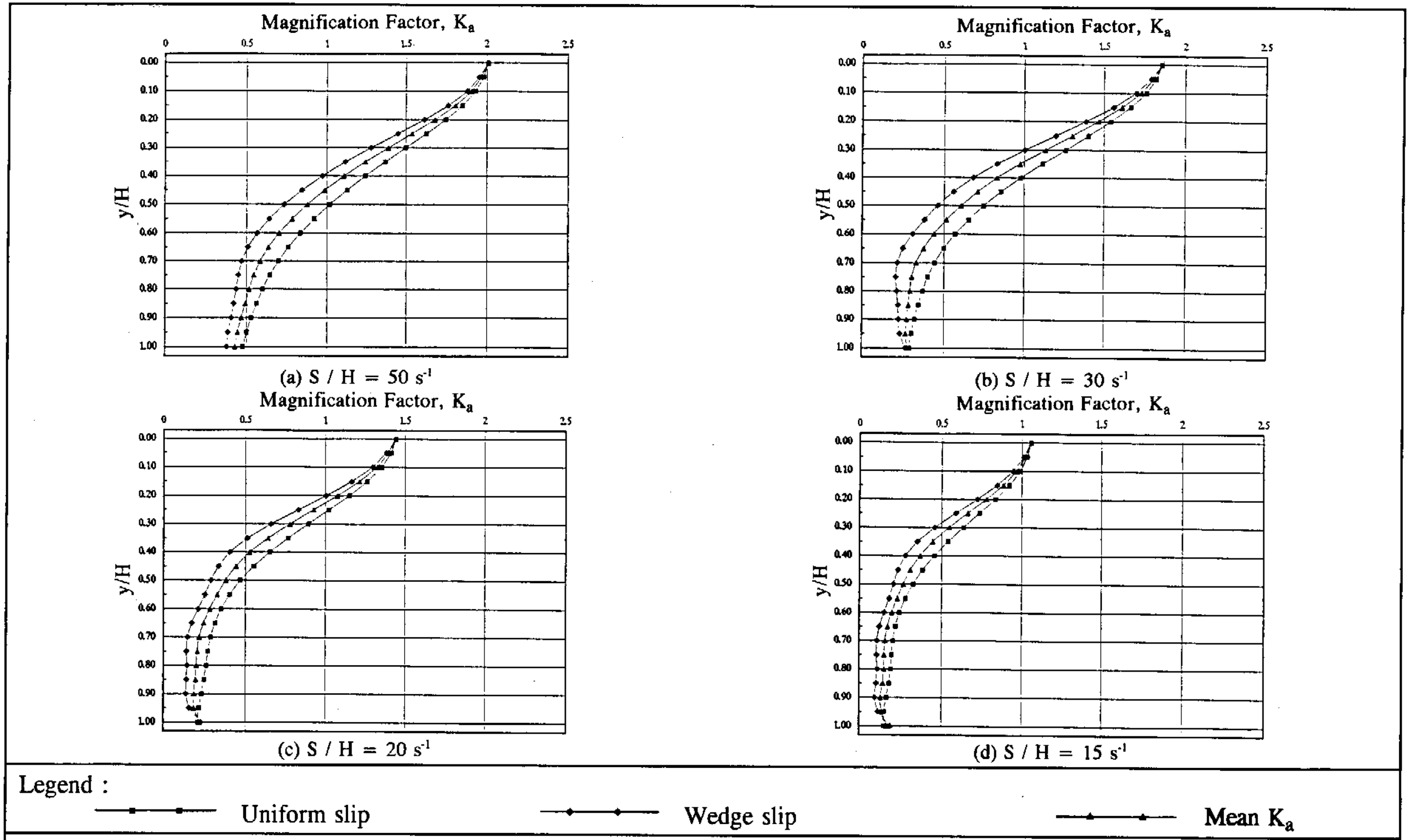

(a) S / H = 50 s^{-1}

(b) S / H = 30 s^{-1}

(c) S / H = 20 s^{-1}

(d) S / H = 15 s^{-1}

Note : F = 30 Hz

Figure C5 - Magnification Factor K_a from One-dimensional Shear Response Analysis for Slope with Horizontal Bedrock

APPENDIX D

ONE-DIMENSIONAL COMPRESSION-RAREFACTION RESPONSE ANALYSIS FOR SLOPES WITH INCLINED BEDROCK

1. For a horizontal soil layer under one dimensional shear response vibration in the horizontal direction, the solution is given by (Jacobsen, 1930):

$$\ddot{u}(y,t) = \sum_{n=1}^{\infty} \phi_n(y/D) \quad S_{dn}(t) \qquad \ldots\ldots\ldots\ldots \quad (D1)$$

where $\ddot{u}(y,t)$ = the absolute response acceleration at level y of the soil layer

$\phi_n(y/H)$ = the nth mode shape at level y

$$= \frac{(-1)^n \cos\left[(2n-1)\frac{\pi}{2}\frac{y}{D}\right]}{2n-1} * \frac{4}{\pi}$$

$S_{dn}(t)$ = Duhamel's Integral

2. It can be shown that for an infinite long soil layer of uniform thickness D as shown in Figure D1(a) under one-dimensional horizontal compression-rarefaction vibration, the equation of motion is of the same form as that of a horizontal soil layer under one-dimensional shear vibration. Hence, the solution is also given by equation (D1). Mode shapes of the inclined layer are shown in Figure D2. Now, y is measured horizontally from the slope surface.

3. Approximate solutions to equation (D1) are derived following the procedures outlined in Paragraphs 2 to 7 of Appendix C. Note that

   (a) For the soil layer, the period of the n^{th} mode of vibration is given by

$$T_n = \frac{4}{(2n-1)} \frac{D}{S} \qquad \ldots\ldots\ldots\ldots\ldots\ldots\ldots \quad (D2)$$

   where D = thickness of soil layer
   S = travelling wave velocity

   Values of the corresponding S_a are given in Table D1.

   (b) Since y is now measured horizontally from the soil surface, and an infinite slope is assumed (i.e. length of soil layer is large compared with D), the 'Uniform Slip' (i.e. slip surface with uniform soil thickness) case is considered in deriving the K_n and hence the K_a values.

4. By numerical integration, the calculated $K_a(y/D)$ values for S/D = 50, 30, 20 and 15 are shown in Table D2 and Figure 11.

LIST OF TABLES

Table No.		Page No.
D1	T_n and S_a for One-dimensional Compression-rarefaction Response Analysis for Inclined Soil Layer	99
D2	K_a from One-dimensional Compression-rarefaction Response Analysis for Inclined Soil Layer	100

Table D1 - T_n and S_a for One-dimensional Compression-rarefaction Response Analysis for Inclined Soil Layer

Mode No,	1	2	3	4
T_n for layer (*H/S)	4.00	1.33	0.80	0.57
alpha = F * T_n (*H/S)	120.00	40.00	24.00	17.14

(a) Period of nth Mode of Vibration, T_n

S/H	S_a			
	$n = 1$ $\lambda = 0.2$	$n = 2$ $\lambda = 0.5$	$n = 3$ $\lambda = 0.5$	$n = 4$ $\lambda = 0.5$
150	2.1798	1.0709	1.0256	1.0131
75	0.7041	1.2699	1.1018	1.0522
50	0.2855	1.4598	1.2229	1.1166
37.5	0.1741	1.3594	1.3635	1.2035
30	0.1251	1.0797	1.4598	1.3040
20	0.0741	0.6202	1.2221	1.4679
15	0.0531	0.4271	0.8443	1.2835

(b) Maximum Acceleration Response Factor, S_a (for F = 30 Hz)

Table D2 - K_a from One-dimensional Compression-rarefaction Response Analysis for Inclined Soil Layer

y/D	Magnification Factor, K_a			
	S/D = 50	S/D = 30	S/D = 20	S/D = 15
0.00	0.7914	0.6259	0.4451	0.3183
0.05	0.7789	0.6112	0.4318	0.3082
0.10	0.7549	0.5832	0.4065	0.2892
0.15	0.7175	0.5400	0.3677	0.2602
0.20	0.6703	0.4863	0.3204	0.2250
0.25	0.6173	0.4279	0.2704	0.1885
0.30	0.5628	0.3705	0.2244	0.1557
0.35	0.5100	0.3189	0.1876	0.1307
0.40	0.4615	0.2757	0.1624	0.1146
0.45	0.4183	0.2407	0.1462	0.1045
0.50	0.3810	0.2117	0.1339	0.0961
0.55	0.3500	0.1867	0.1215	0.0866
0.60	0.3258	0.1653	0.1083	0.0766
0.65	0.3090	0.1493	0.0971	0.0689
0.70	0.2992	0.1412	0.0912	0.0664
0.75	0.2949	0.1410	0.0910	0.0679
0.80	0.2931	0.1449	0.0926	0.0692
0.85	0.2909	0.1489	0.0921	0.0671
0.90	0.2867	0.1514	0.0913	0.0643
0.95	0.2814	0.1563	0.1011	0.0739
1.00	0.2792	0.1724	0.1351	0.1082

LIST OF FIGURES

Figure No.		Page No.
D1	One-dimensional Compression-rarefaction Response Model for Inclined Soil Layer	102
D2	Mode Shapes from One-dimensional Compression-rarefaction Response Analysis	103

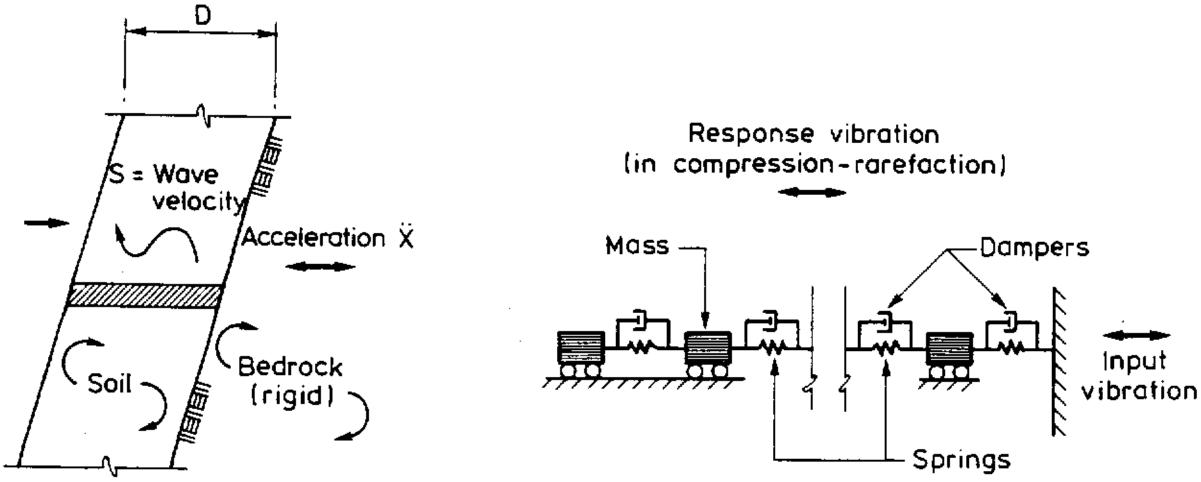
D
S = Wave velocity
Acceleration $\ddot{X}$
Soil
Bedrock (rigid)
Response vibration (in compression-rarefaction)
Mass
Dampers
Input vibration
Springs

(a) Infinite Slope Subjected to One-dimensional Compression-rarefaction Response Vibration

(b) Multi-degree-freedom Model

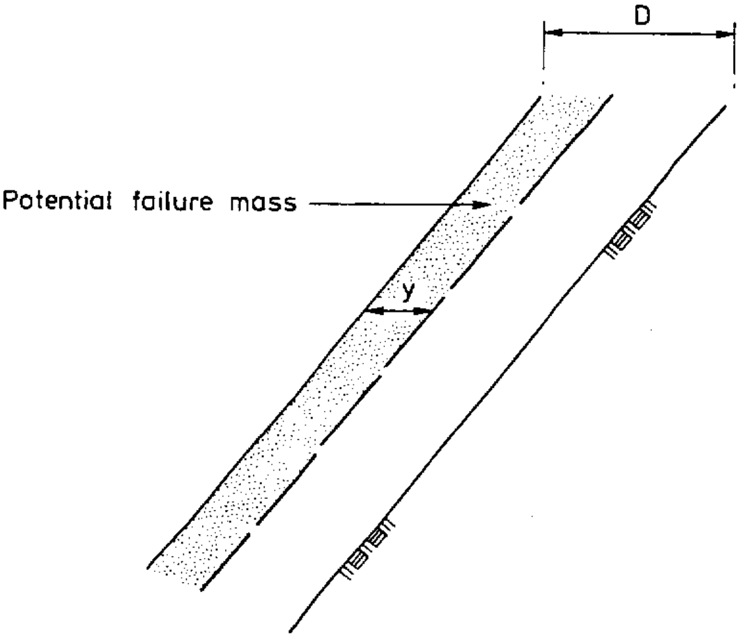
D
Potential failure mass
y

(c) Geometry of Uniform Slip

Figure D1 - One-dimensional Compression-rarefaction Response Model for Inclined Soil Layer

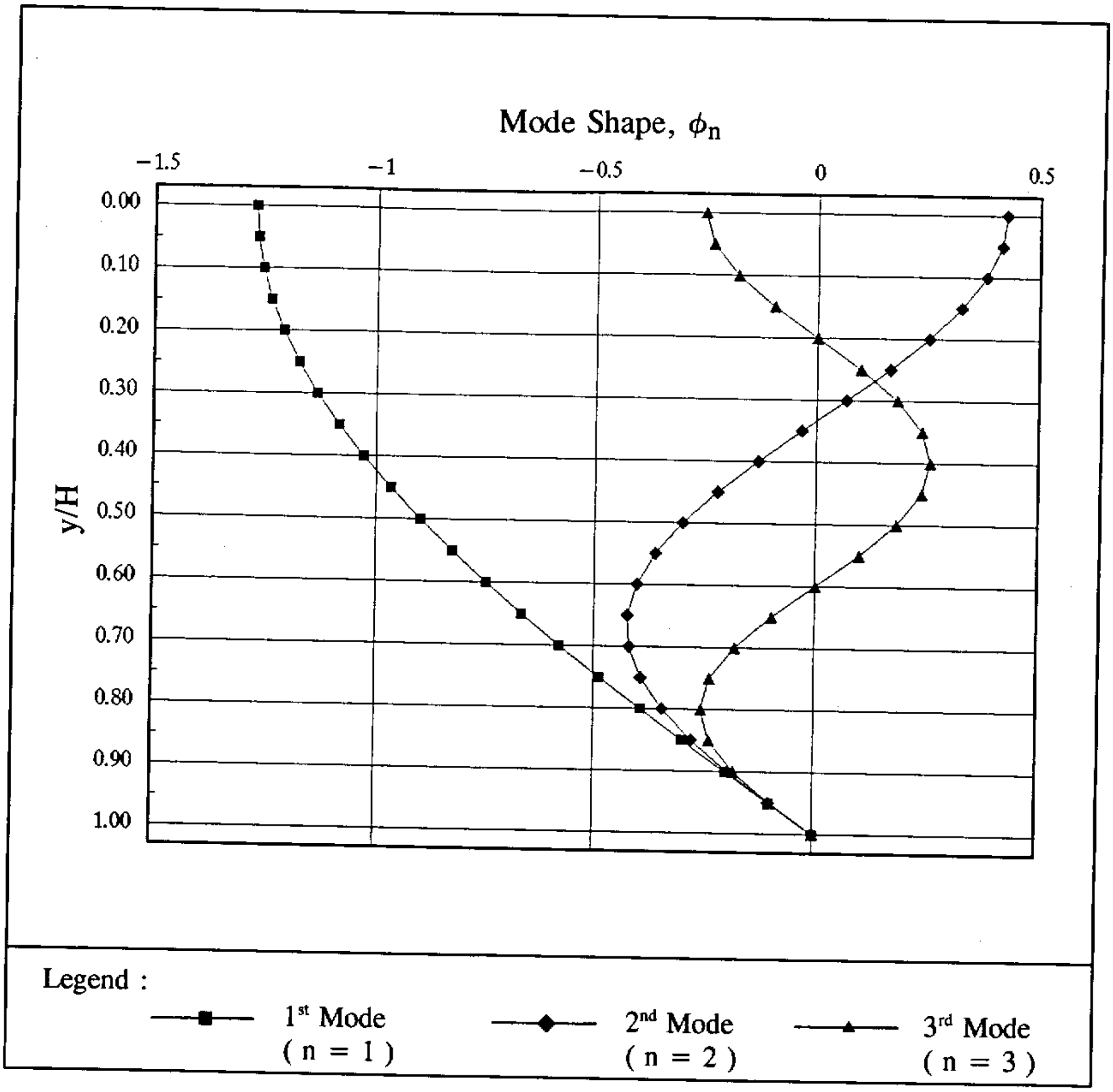

Figure D2 - Mode Shapes from One-dimensional Compression-rarefaction Response Analysis

APPENDIX E

WORKED EXAMPLES

1. WORKED EXAMPLE NO. 1 - SLOPE WITH HORIZONTAL BEDROCK UNDER SHEAR VIBRATION

1.1 Slope Condition

Figure E1 shows the slope geometry and the design soil parameters.

1.2 Dynamic Response

Based on the results of the one-dimensional shear response analysis shown in Figure 10 (or Table B3), for S/H = 20 and frequency of input motion = 30 Hz:

y/H	0.2	0.4	0.6	0.8	1.0
K_a	1.077	0.526	0.281	0.200	0.218

1.3 Pseudo-static Stability Analysis

Slope stability analyses based on the Pseudo-static Approach were carried out using the computer program "EQS" adopting Sarma (1973)'s method of limit equilibrium analysis. Both simple pseudo-static analysis (for B = 0) and modified pseudo-static analysis (for B = 1.0) were carried out.

The results are shown in Figures E2(a) to (e).

1.4 Critical Peak Particle Velocity PPVc

The PPV_c for the critical slip surfaces at various y/H are calculated (using equation (7)) and shown in Figure E3.

For the design condition of B = 0, the PPV_c for the slope is 31.2 mm/s. The PPV_c value may be adopted in blast design using, say, the available PPV vs scaled distance attenuation formulae.

1.5 Sensitivity Analysis

(a) Modified Pseudo-static Analysis

As shown in Figure E3, if the slope-forming material is 'degrading', the PPV_c will reduce considerably to 19.6 mm/s (for B = 1.0 & A_n = 0.5) and 6.7 mm/s (for B = 1.0 & A_n = 1.0). The identification of the presence of any 'degrading' soils in the slope is therefore important.

(b) Single-degree-freedom vs Multi-degree-freedom Model

If the single-degree-freedom slope model (K_a = 0.094) is adopted, the corresponding PPV_c will be 72.2 mm/s (for B = 0), 45.5 (for B = 1.0, A_n = 0.5) and 15.6 mm/s (for B = 1.0, A_n = 1.0). The single-degree-freedom model overestimates the PPV_c considerably.

(c) Local Failure

Slip surfaces corresponding to $y/H < 0.2$ have not been considered in the above analyses. As discussed in Section 5.7, as the initial F_s of the local slip surfaces corresponding to $y/H < 0.2$ are high (well above 2.0), the shear strain increment $\Delta\epsilon_s$ during blasting vibration will be small and the slope will remain in the state of elastic vibration despite the high local response acceleration.

2. WORKED EXAMPLE NO. 2 - SLOPE WITH INCLINED BEDROCK UNDER COMPRESSION-RAREFACTION VIBRATION

2.1 Slope Condition

The slope geometry is shown in Figure E4.

2.2 Dynamic Response

The slope is modelled as an infinite slope with bedrock parallel to the slope surface. Based on the results of the one-dimensional compression-rarefaction response analysis shown in Figure 11 (or Table D2), for $S/D = 50$ and frequency of input motion = 30 Hz:

y/D	0.4	0.65	1.0
K_a	0.462	0.309	0.279

2.3 Pseudo-static Stability Analysis

Slip surfaces No. a1, a2 and a3 shown in Figure E2(a) are critical.

2.4 Critical Peak Particle Velocity PPV_c

The PPV_c for the critical slip surfaces at various y/D are calculated using equation (7) and are shown in Figure E5. For the design condition of $B = 0$, the PPV_c for the slope is 22.0 mm/s. The PPV_c value may be adopted in blast design using, say, the available PPV vs scaled distance attenuation formulae.

Presence of 'degrading' soil under high degree of saturation would reduce the PPV_c to 13.8 mm/s (for $B = 1.0$ & $A_n = 0.5$) and 4.7 mm/s (for $B = 1.0$ & $A_n = 1.0$).

LIST OF FIGURES

Figure No.		Page No.
E1	Example No. 1 : Slope Geometry and Soil Properties	108
E2	Example No. 1 : Results of Pseudo-static Analysis	109
E3	Example No. 1 : K_c and PPV_c for Critical Slip Surfaces	110
E4	Example No. 2 : Slope Geometry and Soil Properties	111
E5	Example No. 2 : K_c and PPV_c for Critical Slip Surfaces	112

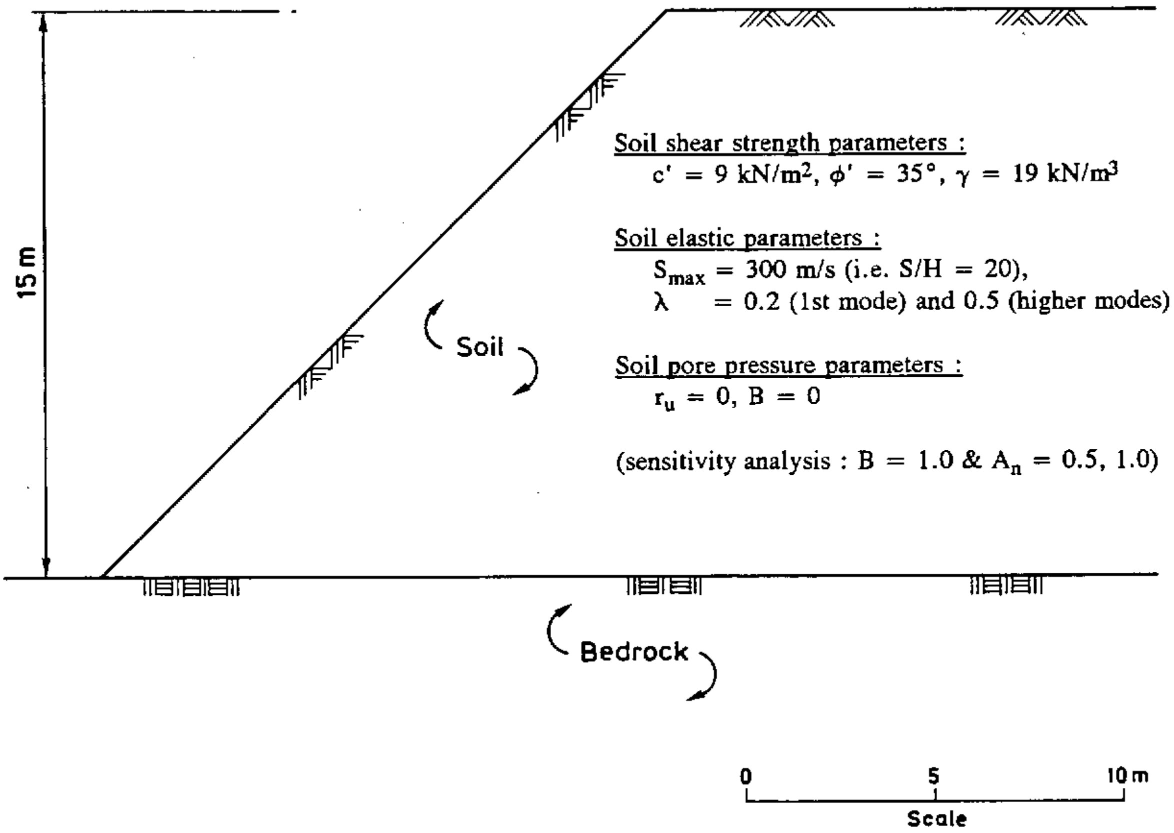

Soil shear strength parameters :

$c' = 9\ \text{kN/m}^2$, $\phi' = 35°$, $\gamma = 19\ \text{kN/m}^3$

Soil elastic parameters :

$S_{max} = 300$ m/s (i.e. $S/H = 20$),

$\lambda = 0.2$ (1st mode) and 0.5 (higher modes)

Soil pore pressure parameters :

$r_u = 0$, $B = 0$

(sensitivity analysis : $B = 1.0$ & $A_n = 0.5, 1.0$)

Figure E1 - Example No. 1 : Slope Geometry and Soil Properties

Slip No.	F_s	K_c (g) for y/H = 1.0				
		B = 0	1.0			
		A_n = -	0.2	0.4	0.5	1.0
a1	1.422	0.2480	0.3283	0.2193	0.1835	0.0822
a2	1.226	0.1304	0.1579	0.1010	0.0821	0.0281
a3	1.251	0.1370	0.1591	0.1025	0.0838	0.0308
a4	1.344	0.1745	0.1983	0.1304	0.1081	0.0452

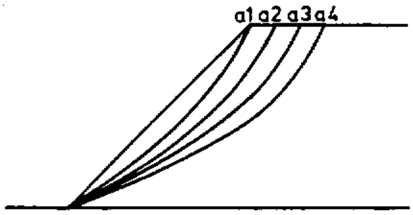

(a) y/H = 1.0

Slip No.	F_s	K_c (g) for y/H = 0.8				
		B = 0	1.0			
		A_n = -	0.2	0.4	0.5	1.0
b1	1.6099	0.3618	0.4900	0.3346	0.2836	0.1398
b2	1.3116	0.1835	0.2264	0.1483	0.1225	0.0493
b3	1.3018	0.1729	0.2023	0.1324	0.1094	0.0443
b4	1.3732	0.2068	0.2335	0.1563	0.1309	0.0597

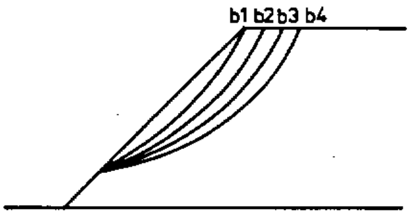

(b) y/H = 0.8

Slip No.	F_s	K_c (g) for y/H = 0.6				
		B = 0	1.0			
		A_n = -	0.2	0.4	0.5	1.0
c1	1.6577	0.3291	0.5322	0.3640	0.3087	0.1527
c2	1.4067	0.2463	0.2990	0.2007	0.1684	0.0777
c3	1.4481	0.2598	0.2969	0.2021	0.1711	0.0842
c4	1.5217	0.2787	0.3093	0.2132	0.1817	0.0930

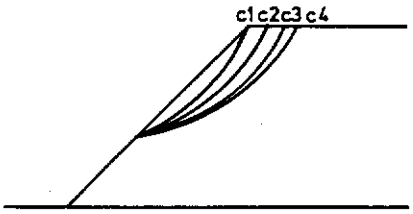

(c) y/H = 0.6

Slip No.	F_s	K_c (g) for y/H = 0.4				
		B = 0	1.0			
		A_n = -	0.2	0.4	0.5	1.0
d1	1.7082	0.4226	0.5421	0.3733	0.3179	0.1621
d2	1.6651	0.3787	0.4562	0.3146	0.2683	0.1378
d3	1.7329	0.4040	0.4596	0.3218	0.2766	0.1492
d4	1.8141	0.4088	0.4567	0.3215	0.2770	0.1513

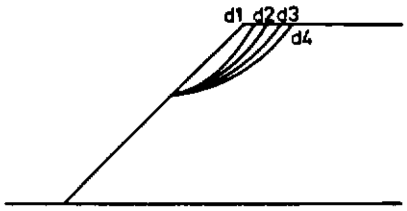

(d) y/H = 0.4

Slip No.	F_s	K_c (g) for y/H = 0.2				
		B = 0	1.0			
		A_n = -	0.2	0.4	0.5	1.0
e1	2.4805	0.8059	1.0714	0.7618	0.6603	0.3747
e2	2.4260	0.6528	0.7946	0.5663	0.4913	0.2797
e3	2.7064	0.6992	0.7949	0.5741	0.5012	0.2944
e4	2.9682	0.7853	0.8309	0.6135	0.5410	0.3323

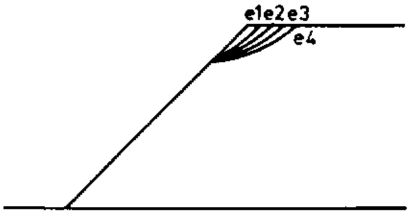

(e) y/H = 0.2

Figure E2 - Example No. 1 : Results of Pseudo-static Analysis

y/H	K_a	Critical Slip No.	F_s	B = 0		B = 1.0, A_n = 0.5		B = 1.0, A_n = 1.0	
				K_c (g)	PPV_c (mm/s)	K_c (g)	PPV_c (mm/s)	K_c (g)	PPV_c (mm/s)
0.2	1.077	e2	2.43	0.6528	31.5	0.4913	23.7	0.2797	13.5
0.4	0.526	d2	1.67	0.3787	37.5	0.2683	26.5	0.1378	13.6
0.6	0.281	c2	1.41	0.2463	45.7	0.1684	31.2	0.0777	14.4
0.8	0.200	b3	1.30	0.1729	44.9	0.1094	28.4	0.0443	11.5
1.0	0.218	a2	1.23	0.1304	31.2	0.0821	19.6	0.0281	6.7

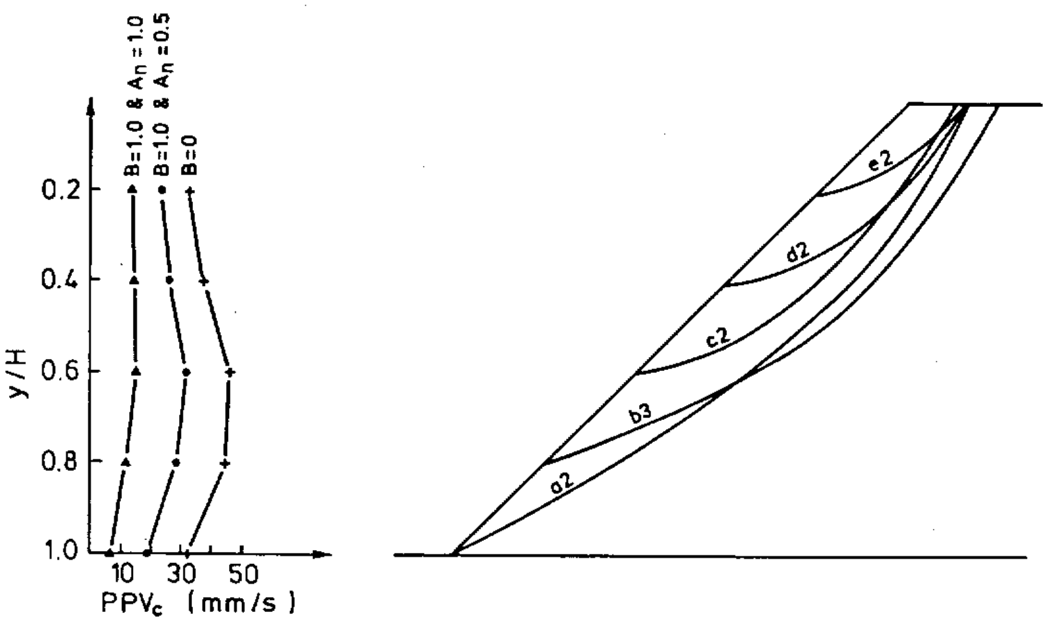

Figure E3 - Example No. 1 : K_c and PPV_c for Critical Slip Surfaces

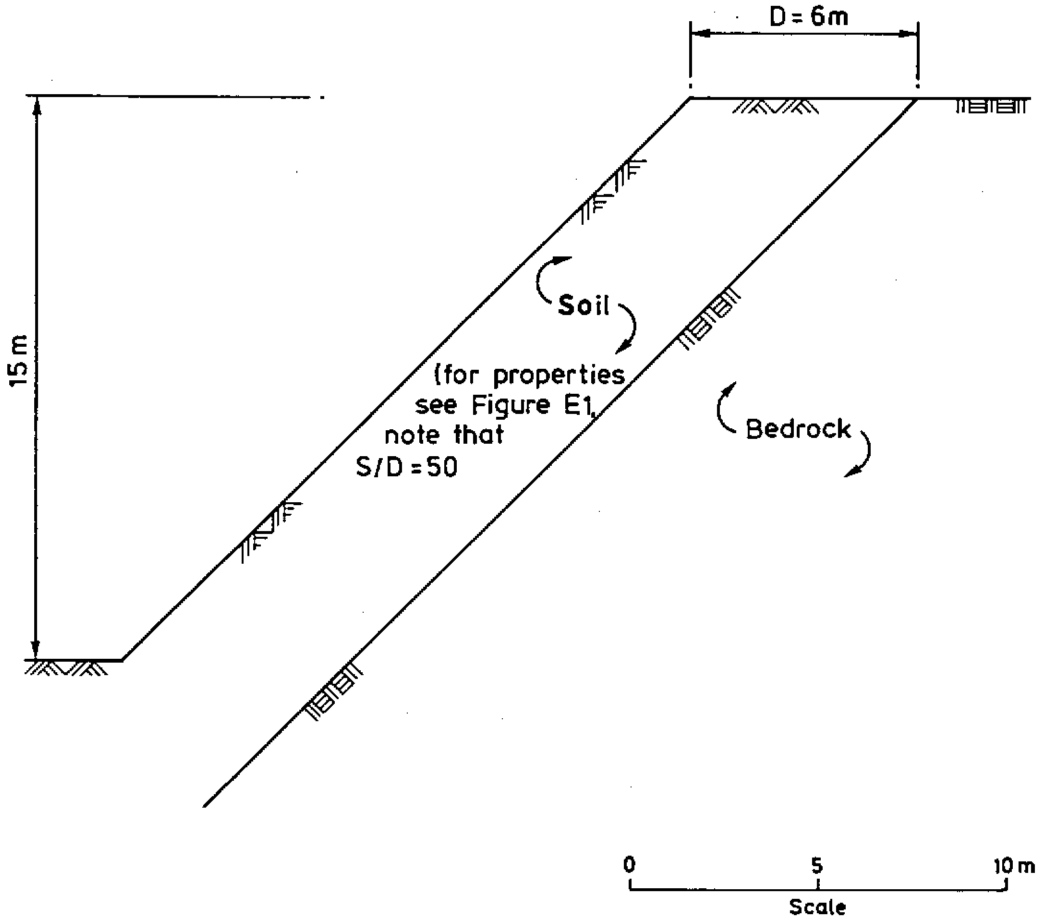
D = 6m
15 m
Soil
(for properties
see Figure E1,
note that
S/D = 50
Bedrock
0
5
10 m
Scale

Figure E4 - Example No. 2 : Slope Geometry and Soil Properties

y/D	K_a	Critical Slip No.	F_s	B = 0		B = 1.0, A_n = 0.5		B = 1.0, A_n = 1.0	
				K_c (g)	PPV_c (mm/s)	K_c (g)	PPV_c (mm/s)	K_c (g)	PPV_c (mm/s)
0.4	0.462	a1	1.42	0.2480	27.9	0.1835	20.7	0.0822	9.3
0.65	0.309	a2	1.23	0.1304	22.0	0.0821	13.8	0.0281	4.7
1.0	0.279	a3	1.25	0.1370	25.6	0.0838	15.6	0.0308	5.7

Note : F_s and K_c refer to Figure D2 (a).

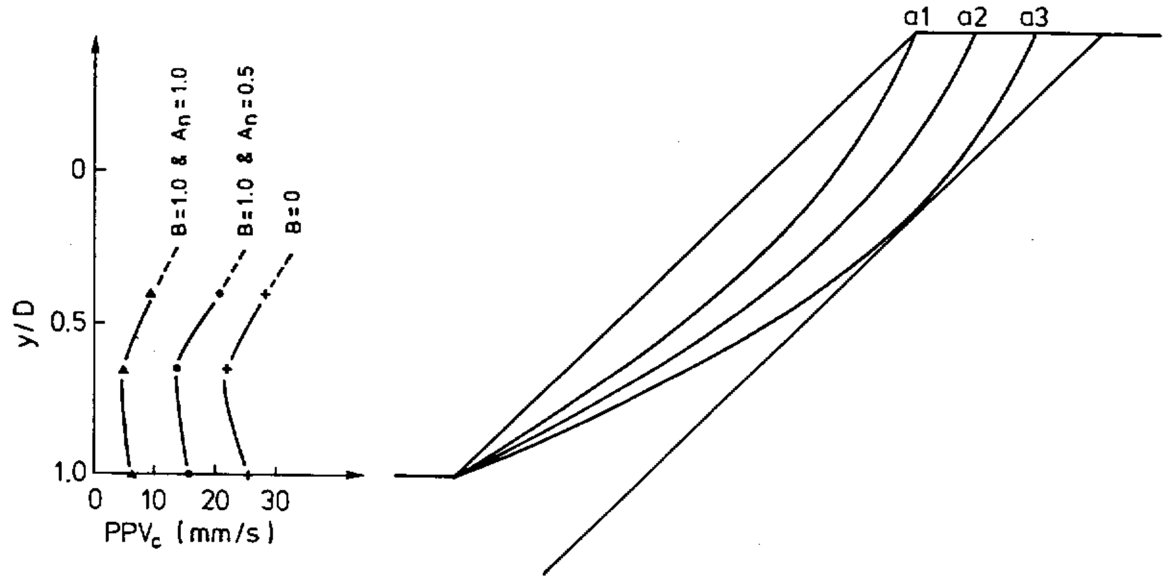

Figure E5 - Example No. 2 : K_c and PPV_c for Critical Slip Surfaces